



Calhoun: The NPS Institutional Archive

Theses and Dissertations

Thesis Collection

1990-12

An investigation of two broadband HF shipboard communication antennas

Fragoulis, Ioannis

Monterey, California: Naval Postgraduate School

<http://hdl.handle.net/10945/27585>



Calhoun is a project of the Dudley Knox Library at NPS, furthering the precepts and goals of open government and government transparency. All information contained herein has been approved for release by the NPS Public Affairs Officer.

Dudley Knox Library / Naval Postgraduate School
411 Dyer Road / 1 University Circle
Monterey, California USA 93943

<http://www.nps.edu/library>

AD-A245 608



NAVAL POSTGRADUATE SCHOOL

Monterey, California



THESIS



AN INVESTIGATION OF TWO BROADBAND HF
SHIPBOARD COMMUNICATION ANTENNAS

by

Ioannis Fragoulis

December 1990

Thesis Advisor:

Richard W. Adler

Approved for public release; distribution is unlimited.

92-03122



UNCLASSIFIED

SECURITY CLASSIFICATION OF THIS PAGE

REPORT DOCUMENTATION PAGE				Form Approved OMB No. 0704-0188	
1a REPORT SECURITY CLASSIFICATION UNCLASSIFIED			1b RESTRICTIVE MARKINGS		
2a SECURITY CLASSIFICATION AUTHORITY			3 DISTRIBUTION/AVAILABILITY OF REPORT Approved for public release; distribution is unlimited		
2b. DECLASSIFICATION/DOWNGRADING SCHEDULE					
4. PERFORMING ORGANIZATION REPORT NUMBER(S)			5 MONITORING ORGANIZATION REPORT NUMBER(S)		
6a NAME OF PERFORMING ORGANIZATION Naval Postgraduate School		6b OFFICE SYMBOL (If applicable) EC	7a. NAME OF MONITORING ORGANIZATION Naval Postgraduate School		
6c. ADDRESS (City, State, and ZIP Code) Monterey, CA 93943-5000			7b ADDRESS (City, State, and ZIP Code) Monterey, CA 93943-5000		
8a NAME OF FUNDING/SPONSORING ORGANIZATION		8b OFFICE SYMBOL (If applicable)	9 PROCUREMENT INSTRUMENT IDENTIFICATION NUMBER		
8c. ADDRESS (City, State, and ZIP Code)			10 SOURCE OF FUNDING NUMBERS		
			PROGRAM ELEMENT NO	PROJECT NO	TASK NO
			WORK UNIT ACCESSION NO.		
11 TITLE (Include Security Classification) AN INVESTIGATION OF TWO BROADBAND HF SHIPBOARD COMMUNICATION ANTENNAS					
12 PERSONAL AUTHOR(S) FRAGOULIS, Ioannis					
13a TYPE OF REPORT Master's Thesis		13b TIME COVERED FROM _____ TO _____		14 DATE OF REPORT (Year, Month, Day) 1990 December	
15 PAGE COUNT 109					
16 SUPPLEMENTARY NOTATION The views expressed in this thesis are those of the author and do not reflect the official policy or position of the Department of the Navy or the US Government.					
17 COSATI CODES			18 SUBJECT TERMS (Continue on reverse if necessary and identify by block number)		
FIELD	GROUP	SUB-GROUP	inverted cone antenna; computer antenna modeling; NEC; HF antennas; shipboard antennas		
19 ABSTRACT (Continue on reverse if necessary and identify by block number) The capability of an electromagnetic radiating system depends on its ability to operate effectively in a complex environment, where its pattern performance can be limited by pattern distortion effects. On a modern military ship, this task is complicated by the large number of systems that are competing for prime locations. It is recommended, therefore, that a given situation be studied systematically, looking at individual pieces of the problem separately and developing intermediate conclusions. This thesis investigates computer antenna models to improve shipboard antenna systems performance for HF, VHF, and UHF bands. Possible improvements for present ships might lead to the reduction of the number of existing antennas. Two different computer models are investigated for various geometry: (1) a "multi-wire" whip antenna and					
20 DISTRIBUTION/AVAILABILITY OF ABSTRACT <input checked="" type="checkbox"/> UNCLASSIFIED/UNLIMITED <input type="checkbox"/> SAME AS RPT <input type="checkbox"/> DTIC USERS			21 ABSTRACT SECURITY CLASSIFICATION UNCLASSIFIED		
22a NAME OF RESPONSIBLE INDIVIDUAL ADLER, Richard W.			22b TELEPHONE (Include Area Code) 408-646-2352		22c OFFICE SYMBOL EC/Ab

19. cont.

(2) an inverted cone antenna. Both are modeled by using wire grids, in the Numerical Electromagnetics Code (NEC). Average power gain, input impedance and radiation patterns of most of the models are presented, in the frequency range of 4-300 MHz. It is seen that good performance occurs for the inverted cone antenna over perfect ground in the frequency range 4-152 MHz and over a wire grid box (approximately a ship's shape), for 8-48 MHz.

Approved for public release; distribution is unlimited

An Investigation of Two Broadband HF Shipboard
Communication Antennas

by

Ioannis Fragoulis
Lieutenant, Hellenic Navy
B.S., Hellenic Naval Academy, 1981

Submitted in partial fulfillment of the
requirements of degree of

MASTER OF SCIENCE IN ELECTRICAL ENGINEERING

from the

NAVAL POSTGRADUATE SCHOOL
December 1990

Author:

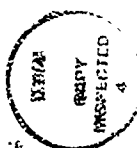
Ioannis Fragoulis

Approved by:

Richard W. Adler, Thesis Advisor

Wilbur R. Vincent, Second Reader

Michael A. Morgan, Chairman
Department of Electrical and Computer Engineering



Accession For	
NTIS GRA&I	<input checked="checked" type="checkbox"/>
DTIC TAB	<input type="checkbox"/>
Unannounced	<input type="checkbox"/>
Justification	
By _____	
Distribution/	
Availability Codes	
Dist.	Avail and/or Special

ABSTRACT

The capability of an electromagnetic radiating system depends on its ability to operate effectively in a complex environment, where its pattern performance can be limited by pattern distortion effects. On a modern military ship, this task is complicated by the large number of systems that are competing for prime locations. It is recommended, therefore, that a given situation be studied systematically, looking at individual pieces of the problem separately and developing intermediate conclusions. This thesis investigates computer antenna models to improve shipboard antenna systems performance for HF, VHF and UHF bands. Possible improvements for present ships might lead to the reduction of the number of existing antennas. Two different computer models are investigated for various geometry: (1) a "multi-wire" whip antenna and (2) an inverted cone antenna. Both are modeled by using wire grids, in the Numerical Electromagnetics Code (NEC). Average power gain, input impedance and radiation patterns of most of the models are presented, in the frequency range of 4-300 MHz. It is seen that good performance occurs for the inverted cone antenna over perfect ground in the frequency range 4-152 MHz and over a wire grid box (approximating a ship's shape), for 8-48 MHz.

TABLE OF CONTENTS

I. INTRODUCTION	1
A. NEED FOR THE STUDY.....	1
B. STATEMENT OF THE PROBLEM.....	2
C. SCOPE AND LIMITATIONS	2
II. "MULTI-WIRE" WHIP ANTENNA COMPUTER MODELS AND RESULTS	4
A. "MULTI-WIRE" WHIP ANTENNA COMPUTER MODEL.....	4
B. COMPUTER MODEL RESULTS	7
1. Average Power Gain.....	7
III. INVERTED CONE COMPUTER MODELS AND RESULTS.....	14
A. INVERTED CONE COMPUTER MODEL.....	14
B. COMPUTER MODEL RESULTS.....	16
1. Average Power Gain.....	16
2. Input Impedance.....	19
IV. INVERTED CONE ON A WIRE GRID BOX COMPUTER MODEL AND RESULTS	26
A. INVERTED CONE ON A WIRE GRID BOX COMPUTER MODEL.....	26
B. COMPUTER MODEL RESULTS	28
1. Average Power Gain.....	28
2. Input Impedance.....	30
3. Radiation Patterns.....	34
V. CONCLUSIONS AND RECOMMENDATIONS.....	40
A. CONCLUSIONS.....	40
B. RECOMMENDATIONS.....	41
APPENDIX A	43
NEC INPUT DATA.....	43

APPENDIX B.....	47
AVERAGE POWER GAIN FOR "MULTI-WIRE"	
WHIP ANTENNAS.....	47
APPENDIX C.....	61
ELEVATION PATTERNS FOR "MULTI-WIRE"	
WHIP ANTENNAS.....	61
APPENDIX D	66
AVERAGE POWER GAIN FOR INVERTED CONE ANTENNAS.	66
APPENDIX E.....	70
INPUT IMPEDANCE FOR INVERTED CONE ANTENNAS.....	70
APPENDIX F.....	73
ELEVATION PATTERNS FOR INVERTED CONE ANTENNAS	73
APPENDIX G	81
AZIMUTH PATTERNS FOR INVERTED CONE.....	81
LIST OF REFERENCES.....	92
BIBLIOGRAPHY	93
INITIAL DISTRIBUTION LIST.....	94

LIST OF FIGURES

Figure 2.1	Two "multi-wire" Whip Antennas in a row.....	6
Figure 2.2	Three "multi-wire" Whip Antennas in triangular form.	7
Figure 2.3	Average Power Gain for two and four "multi-wire" whip antennas, 10 meters height, in-line configuration.....	9
Figure 2.4	Average Power Gain for three "multi-wire" whip antennas in triangular configuration, 5 m and 10 m height.	11
Figure 2.5	Average Power Gain for two "multi-wire" whip antennas with 5 m spacing between them.....	12
Figure 3.1	Inverted cone computer model mounied on the ground, upper ring and vertical wires, only.	15
Figure 3.2	Inverted cone computer model connected to ground by four vertical wires.....	16
Figure 3.3	Average Power Gain for inverted cone antenna models mounted on the ground.....	17
Figure 3.4	Average Power Gain for inverted cone antenna models connected to the ground by vertical wires.....	18
Figure 3.5.	Input Impedance for inverted cone antenna mounted on the ground, with 12 feed points and wire radius 0.01 m.....	20
Figure 3.6	Smith Chart plot for inverted cone antenna mounted on the ground, with 12 feed points and wire radius 0.01 m, in frequency range 12-156 MHz.	21
Figure 3.7	Input Impedance for an inverted cone antenna 0.4 m above the ground, with 4 feed points and wire radius 0.01 m.....	22
Figure 3.8	Input Impedance for an inverted cone antenna 0.4 m above the ground, with 4 feed points and wire radius 0.10 m.....	23
Figure 3.9	Smith Chart plot for an inverted cone antenna 0.4 m above the ground with 4 feed points and wire radius 0.01 m, in the frequency range 12-120 MHz.	24
Figure 3.10	Smith Chart plot for an inverted cone antenna 0.4 m above the ground, with 4 feed points and wire radius 0.10 m, in the frequency range 12-120 MHz.	25
Figure 4.1	Wire grid box representing a ship's shape.....	26
Figure 4.2	Inverted cone 0.4 m above the wire grid box, connected to it by four vertical wires.	27

Figure 4.3	Inverted cone mounted on the wire grid box with one connection point.....	28
Figure 4.4	Average Power Gain for inverted cone mounted on the wire grid box, with 12 feed points, one connection point and wire radius 0.01 m.....	29
Figure 4.5	Average Power Gain for inverted cone 0.4 m above the wire grid box connected to it with four vertical wires, and wire radius 0.01 m.....	30
Figure 4.6	Input Impedance for inverted cone mounted on the wire grid box, with 12 feed points, one connection point and wire radius 0.01 m....	31
Figure 4.7	Input Impedance for inverted cone 0.4 m above the wire grid box connected to it by four vertical wires, and wire radius 0.01 m.....	32
Figure 4.8	Smith Chart plot for an inverted cone antenna mounted on the wire grid box with 12 feed points, one connection point and wire radius 0.01 m, in the frequency range 8-48 MHz.....	33
Figure 4.9	Smith Chart plot for inverted cone antenna 0.4 m above the wire grid box connected to it by four vertical wires and wire radius 0.01 m, in the frequency range 8-44 MHz.....	34
Figure 4.10	E-Field Elevation Pattern for an inverted cone antenna mounted on the wire grid box with 12 feed points, one connection point and wire radius 0.01 m, at 20 MHz, $f = 0$ degrees.....	35
Figure 4.11	E-Field Elevation Pattern for an inverted cone antenna mounted on the wire grid box with 12 feed points, one connection point and wire radius 0.01 m, at 20 MHz, $f = 63.47$ degrees.....	36
Figure 4.12	E-Field Elevation Pattern for an inverted cone antenna with 12 feed points, one connection point and wire radius 0.01 m, at 20 MHz, $f = 90$ degrees.....	37
Figure 4.13	E-Field Elevation Pattern for an inverted cone antenna 0.4 m above the wire grid box connected to it by four vertical wires and wire radius 0.01 m, at 20 MHz, $f = 0$ degrees.....	37
Figure 4.14	E-Field Elevation Pattern for an inverted cone antenna 0.4 m above the wire grid box connected to it by four vertical wires and wire radius 0.01 m, at 20 MHz, $f = 63.47$ degrees.....	38
Figure 4.15	E-Field Elevation Pattern for an inverted cone antenna 0.4 m above the wire grid box connected to it by four vertical wires and wire radius 0.01 m, at 20 MHz, $f = 90$ degrees.....	38
Figure C.1	E-Field Elevation Pattern for two "multi-wire" whip antennas, with a 5 m spacing between them, base width 0.10 m, antenna height 10 m, at 4 MHz, $f = 0$ degrees.....	61

Figure C.2	E-Field Elevation Pattern for two "multi-wire" whip antennas, with a 5 m spacing between them, wire radius 0.10 m, antenna height 10 m, at 12 MHz, $f = 0$ degrees.....	62
Figure C.3	E-Field Elevation Pattern for two "multi-wire" whip antennas, with a 5 m spacing between them, wire radius 0.10 m, antenna height 10 m, at 20 MHz, $f = 0$ degrees.....	62
Figure C.4	E-Field Elevation Pattern for two "multi-wire" whip antennas, with a 5 m spacing between them, wire radius 0.10 m, antenna height 10 m, at 30 MHz, $f = 0$ degrees.....	63
Figure C.5	E-Field Elevation Pattern for two "multi-wire" whip antennas, with a 5 m spacing between them, wire radius 0.10 m, antenna height 10 m, at 40 MHz, $f = 0$ degrees.....	63
Figure C.6	E-Field Elevation Pattern for two "multi-wire" whip antennas, with a 5 m spacing between them, wire radius 0.10 m, antenna height 10 m, at 60 MHz, $f = 0$ degrees.....	64
Figure C.7	E-Field Elevation Pattern for two "multi-wire" whip antennas, with a 5 m spacing between them, wire radius 0.10 m, antenna height 10 m, at 80 MHz, $f = 0$ degrees.....	64
Figure C.8	E-Field Elevation Pattern for two "multi-wire" whip antennas, with a 5 m spacing between them, wire radius 0.10 m, antenna height 10 m, at 100 MHz, $f = 0$ degrees.....	65
Figure F.1	E-Field Elevation Pattern for inverted cone mounted on the ground with 12 feed points, wire radius 0.01 m, at 8 MHz, $f = 0$ degrees.	73
Figure F.2	E-Field Elevation Pattern for inverted cone mounted on the ground with 12 feed points, wire radius 0.01 m, at 60 MHz, $f = 0$ degrees.	74
Figure F.3	E-Field Elevation Pattern for inverted cone mounted on the ground with 12 feed points, wire radius 0.01 m, at 80 MHz, $f = 0$ degrees.	74
Figure F.4	E-Field Elevation Pattern for inverted cone mounted on the ground with 12 feed points, wire radius 0.01 m, at 100 MHz, $f = 0$ degrees.	75
Figure F.5	E-Field Elevation Pattern for inverted cone mounted on the ground with 12 feed points, wire radius 0.01 m, at 120 MHz, $f = 0$ degrees.	75
Figure F.6	E-Field Elevation Pattern for inverted cone mounted on the ground with 12 feed points, wire radius 0.01 m, at 140 MHz, $f = 0$ degrees.	76

Figure F.7	E-Field Elevation Pattern for inverted cone 0.4 m above the ground with 4 feed points, wire radius 0.01 m, at 8 MHz, $f = 0$ degrees.	76
Figure F.8	E-Field Elevation Pattern for inverted cone 0.4 m, above the ground with 4 feed points, wire radius 0.01 m, at 60 MHz, $f = 0$ degrees.	77
Figure F.9	E-Field Elevation Pattern for inverted cone 0.4 m above the wire grid box with 4 feed points, wire radius 0.01 m, at 70 MHz, $f = 0$ degrees.	77
Figure F.10	E-Field Elevation Pattern for inverted cone 0.4 m above the wire grid box with 4 feed points, wire radius 0.01 m, at 80 MHz, $f = 0$ degrees.	78
Figure F.11	E-Field Elevation Pattern for inverted cone 0.4 m above the wire grid box with 4 feed points, wire radius 0.01 m, at 90 MHz, $f = 0$ degrees.	78
Figure F.12	E-Field Elevation Pattern for inverted cone 0.4 m above the wire grid box with 4 feed points, wire radius 0.01 m, at 100 MHz, $f = 0$ degrees.	79
Figure F.13	E-Field Elevation Pattern for inverted cone 0.4 m above the wire grid box with 4 feed points, wire radius 0.01 m, at 120 MHz, $f = 0$ degrees.	79
Figure F.14	E-Field Elevation Pattern for inverted cone 0.4 m above the wire grid box with 4 feed points, wire radius 0.01 m, at 140 MHz, $f = 0$ degrees.	80
Figure G.1.	E-Field Azimuth Pattern for inverted cone mounted on the wire grid box with 12 feed points and one connection point, at 20 MHz, $q = 30$ degrees.	82
Figure G.2	E-Field Azimuth Pattern for inverted cone mounted on the wire grid box with 12 feed points, one connection point, at 20 MHz, $q = 40$ degrees.	83
Figure G.3	E-Field Azimuth Pattern for inverted cone mounted on the wire grid box with 12 feed points, one connection point, at 20 MHz, $q = 50$ degrees.	84
Figure G.4	E-Field Azimuth Pattern for inverted cone mounted on the wire grid box with 12 feed points, one connection point, at 20 MHz, $q = 60$ degrees.	85
Figure G.5	E-Field Azimuth Pattern for inverted cone mounted on the wire grid box with 12 feed points, one connection point, at 20 MHz, $q = 70$ degrees.	86

Figure G.6 E-Field Azimuth Pattern for inverted cone 0.4 m above the wire grid box connected to it by four vertical wires, at 20 MHz, $q = 30$ degrees.	87
Figure G.7 E-Field Azimuth Pattern for inverted cone 0.4 m above the wire grid box connected to it by four vertical wires, at 20 MHz, $q = 40$ degrees.	88
Figure G.8 E-Field Azimuth Pattern for inverted cone 0.4 m above the wire grid box connected to it by four vertical wires, at 20 MHz, $q = 50$ degrees.	89
Figure G.9 E-Field Azimuth Pattern for inverted cone 0.4 m above the wire grid box connected to it by four vertical wires, at 20 MHz, $q = 60$ degrees.	90
Figure G.10 E-Field Azimuth Pattern for inverted cone 0.4 m above the wire grid box connected to it by four vertical wires, at 20 MHz, $q = 70$ degrees.	91

I. INTRODUCTION

A. NEED FOR THE STUDY

The use of multiple communication systems co-located on a military platform has increased dramatically in the past decade, especially in the Navy, where more equipment is constantly added in an already-crowded electromagnetic environment. This concentration of telecommunication systems is due to the varied operational requirements imposed on a modern Naval ship. As a result of this, undesirable electromagnetic interference can occur onboard ship, and can degrade the efficiency of onboard communication systems.

Radiation and conduction are mechanisms for coupling strong electromagnetic fields associated with antenna currents to nearby electronic equipment. Reducing the number of the antennas decreases this possibility. Interference often occurs between two systems operating on nearby frequencies. In addition, a minor modification, such as adding a new antenna, can seriously affect impedances and radiation patterns of existing nearby antennas. Again, reducing the number of antennas on a ship can reduce these antenna-to-antenna coupling problems. Frequency independent antennas can be used to accomplish the reduction, but their actual size and the element spacing required make this type unrealistic aboard a ship. Another alternative is the use of multiband antennas, which operate in two or more frequency bands. These antennas often have a common physical structure and either a single RF connector or separate RF connectors for each frequency band.

B. STATEMENT OF THE PROBLEM

In this thesis, two, three, and four "multi-wire" whip antennas are clustered closely together and mounted over a perfect ground plane.

One antenna design, which uses two or more "multi-wire" whip antennas, with variable geometry and spacing, shows promise by reducing the number of radiators for optimum performance.

A second broadband design uses an inverted cone antenna. By varying the geometry and electrical feed points, performance may be optimized. This study also examines two inverted cones, first over perfect ground and then on a wire grid box, which approximates a ship's shape.

C. SCOPE AND LIMITATIONS

The purpose of this study is to investigate possible ways to reduce the number of shipboard communication antennas, which may reduce unwanted interference effects. The frequency range of this investigation is 4-300 MHz, the primary communication frequencies of interest for naval vessels.

The computer code for all models in this study is the Numerical Electromagnetics Code (NEC).

This study investigates the performance of "multi-wire" whip antennas of different geometries. Limitations and results for "multi-wire" whips led to investigating the inverted cone.

The inverted cone antenna was modeled over a perfect ground plane, and also over a wire grid box. In NEC, there are two options for surface modeling; wire grid and patches. The choice of a wire grid box with dimensions 26x13x6.5

meters is made, because it approximates a ship's shape without complex superstructures.

This thesis begins with a discussion of the "multi-wire" whip antenna in Chapter II, and presents the computed results for the models described.

Chapter III discusses the inverted cone antenna with corresponding computed results over a perfect ground plane.

Chapter IV demonstrates the inverted cone on a wire grid box and the computed results of this test.

Conclusions and recommendations based on these results are discussed in Chapter V. Finally, the Appendices contain NEC data sets, average power gain, input impedance and radiation patterns for the different models.

II. "MULTI-WIRE" WHIP ANTENNA COMPUTER MODELS AND RESULTS

This chapter presents the "multi-wire" whip antenna computer models used in this thesis. The model's geometry was varied and tested over a perfect ground plane.

A. "MULTI-WIRE" WHIP ANTENNA COMPUTER MODEL

One of the simplest ways to describe a "multi-wire" whip antenna is that of four wires, each with one end on the perfect ground plane, forming a square base, and the other ends coming together at an elevated point. Figures 2.1 and 2.2 show the configurations of two "multi-wire" whip antennas in a row and of three "multi-wire" whip antennas in triangular form, respectively. Almost all the parameters of the initial model were varied, in the following manner:

- a. The number of the wires comprising the antenna ranged from 2 to 4,
- b. The spacing between the wire ends on the perfect ground plane varied from 0.05 to 0.12 m,
- c. The wire radius varied from 0.01 to 0.4 m, and
- d. The height of the "multi-wire" whip antennas varied from 1 to 10 m.

All computer models met NEC's restrictions and limitations. The radius of the wire, a , relative to the wavelength, λ , depends on the kernel of the electric field equation; there are available two options, which are discussed in reference 1; the thin-wire kernel which models a filament current and the extended thin-wire kernel which models a uniform current distribution around the segment

surface. Both of them require $2\pi a/\lambda \ll 1$. Most of the guidelines for NEC wire antenna models concern the segment length, Δ , and the wire radius, a :

- a. Δ should be less than 0.1λ for accurate results in most cases,
- b. Δ should be less than 0.05λ in critical regions, such as feed regions and wire junctions,
- c. Δ should be less than 0.2λ on long, straight segments,
- d. Δ should be not less than $10^{-4} \lambda$,
- e. a should be less than 0.5Δ with the NEC thin wire kernel,
- f. a should be less than 2Δ with the NEC extended thin wire kernel,
- g. a should be less than 0.1λ ,
- h. avoid large radius changes especially in short segments,
- i. wires that are connected must contact at segment ends (the separation of two segment ends must be greater than 10^{-3} times the length of the shortest segment, otherwise they are considered as connected), and
- f. when a voltage source is applied on a certain segment, segments before and after should have equal length and radius.

In Appendix A, NEC data sets used for multi-wire models are listed.

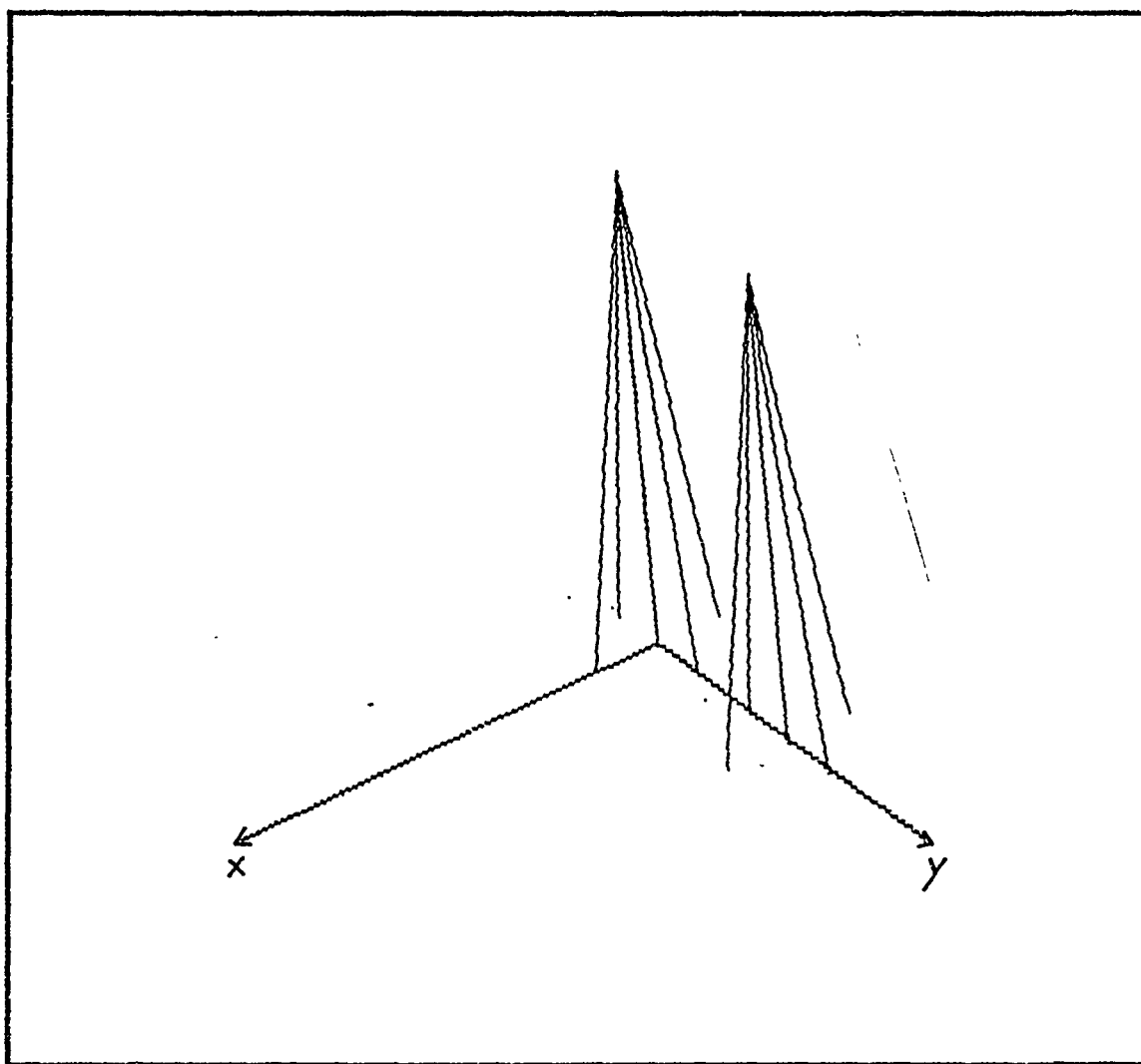


Figure 2.1 Two "multi-wire" Whip Antennas in a row.

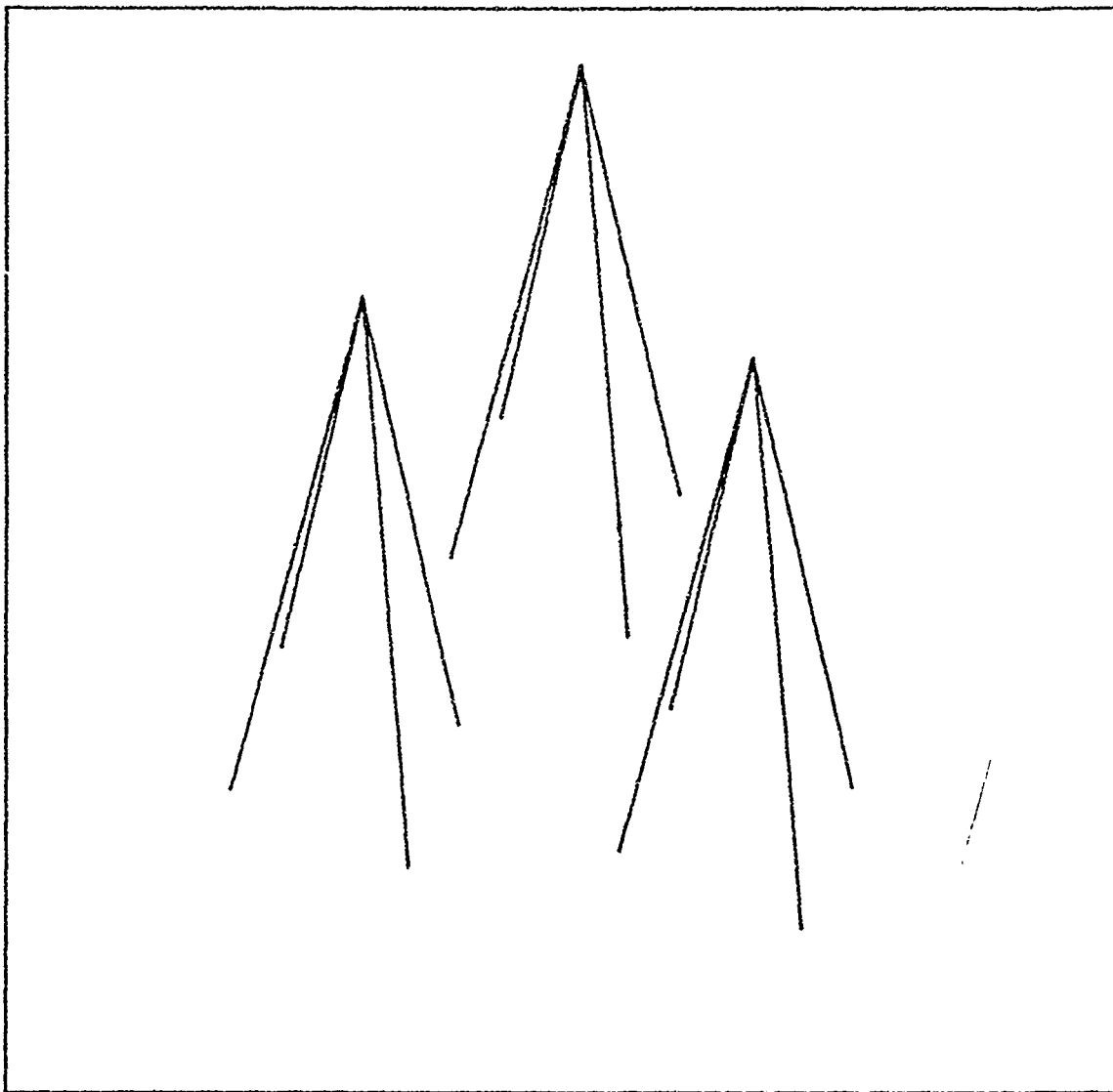


Figure 2.2 Three "multi-wire" Whip Antennas in triangular form.

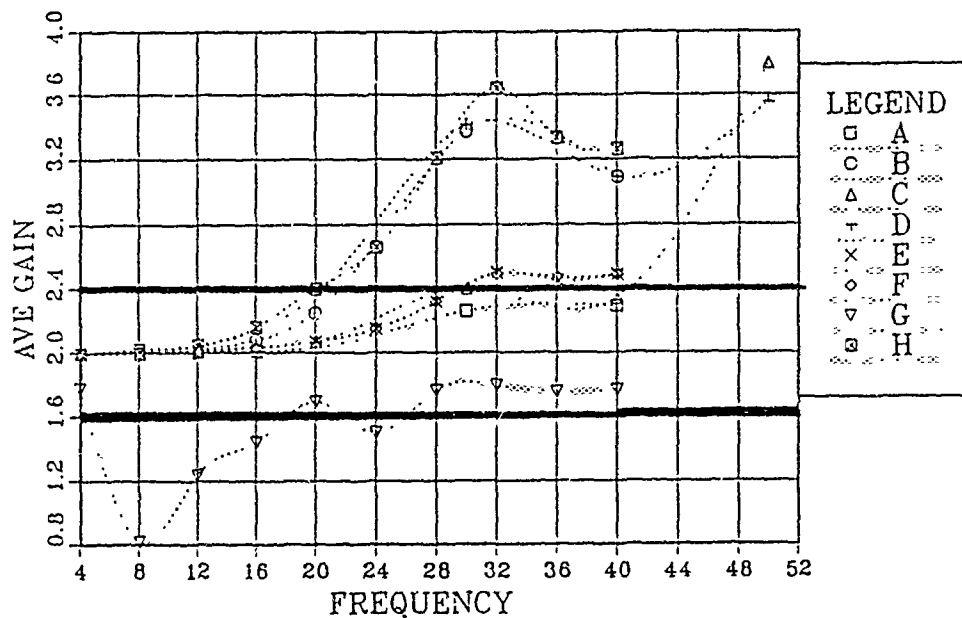
B. COMPUTER MODEL RESULTS

1. Average Power Gain

The validity of an antenna computer model is checked, using the average power gain as criterion. An average power gain of 1.0 represents an ideal, lossless antenna radiating in a free space. Average power gain is computed by integrating

the radiated power density over all space to find the total radiated power and comparing that to the total input power at the feed points. An average power gain of 2.0 represents the antenna radiating in a half space over a perfect ground plane. In this study, an average power gain value from 1.8 to 2.2 is desirable, with the range of 1.6 to 2.4 considered acceptable.

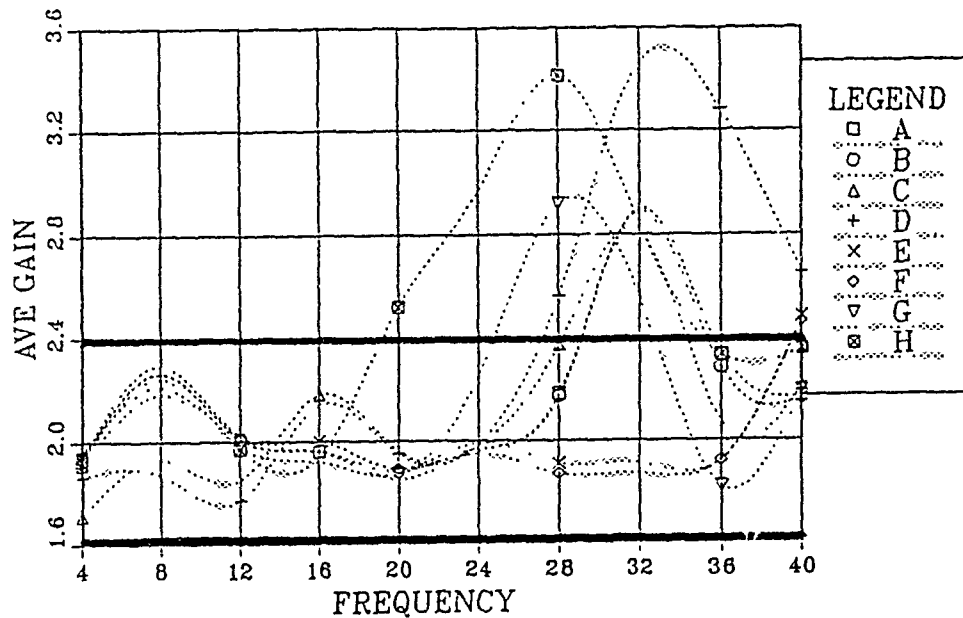
Figure 2.3 shows the calculated average power gain for "multi-wire" whip antennas, 10 meters high each, and 0.10 meter base width.



- a. Two antennas, 4 m spacing, 3 segments per wire.
- b. Two antennas, 4 m spacing, 5 segments per wire.
- c. Two antennas, 6 m spacing, 3 segments per wire.
- d. Two antennas, 6 m spacing, 5 segments per wire.
- e. Four antennas, 2 m spacing, wire radius 0.01 m.
- f. Four antennas, 2 m spacing, wire radius 0.02 m.
- g. Four antennas, 3 m spacing, wire radius 0.01 m.
- h. Four antennas, 3 m spacing, wire radius 0.02 m.

Figure 2.3 Average Power Gain for two and four "multi-wire" whip antennas, 10 meters height, in-line configuration.

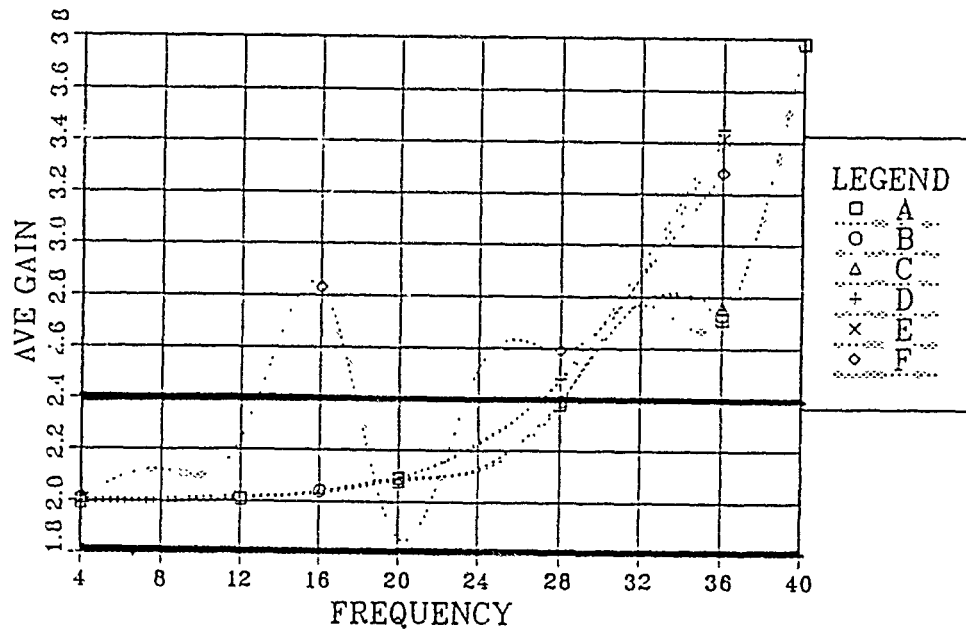
Figure 2.4 shows the calculated average power gain for three "multi-wire" whip antennas in triangular form, as in Figure 2.2, with 6 meter spacing between them.



- a. Antenna height 10 m, wire radius 0.03 m, 5 segments per wire.
- b. Antenna height 10 m, wire radius 0.02 m, 3 segments per wire.
- c. Antenna height 10 m, wire radius 0.03 m, 3 segments per wire.
- d. Antenna height 5 m, wire radius 0.02 m, 3 segments per wire.
- e. Antenna height 5 m, wire radius 0.03 m, 3 segments per wire.
- f. Antenna height 5 m, wire radius 0.03 m, 5 segments per wire.
- g. Antenna height 5 m, wire radius 0.02 m, 5 segments per wire.
- h. Antenna height 5 m, wire radius 0.04 m, 5 segments per wire.

Figure 2.4 Average Power Gain for three "multi-wire" whip antennas in triangular configuration, 5 m and 10 m height.

Figure 2.5 shows the calculated average power gain for two "multi-wire" whip antennas with 5 meter spacing between them.



- a. Antenna height 10 m, base width 0.10 m, wire radius 0.01 m.
- b. Antenna height 10 m, base width 0.16 m, wire radius 0.05 m.
- c. Antenna height 5 m, base width 0.40 m, wire radius 0.06 m.
- d. Antenna height 3 m, base width 0.14 m, wire radius 0.03 m.
- e. Antenna height 3 m, base width 0.40 m, wire radius 0.06 m.
- f. Antenna height 3 m, base width 0.80 m, wire radius 0.06 m.

Figure 2.5 Average Power Gain for two "multi-wire" whip antennas with 5 m spacing between them.

From Figures 2.3, 2.4 and 2.5, it is seen that the average gain values are not all acceptable, i.e. close to the value of two (1.6-2.4). Although a large variation of geometry parameters was used, only in the frequency range 4-28 MHz, were the values useable. This result does not satisfy the purpose of this study, which demands antenna performance over a very wide frequency range, 4-300 MHz. Further investigation of the "multi-wire" whip antenna models thus is not warranted.

III. INVERTED CONE COMPUTER MODELS AND RESULTS

This chapter presents the inverted cone computer models. Two different geometry schemes are described and exercised for a variety of feed points.

A. INVERTED CONE COMPUTER MODEL

One simple way to describe an inverted cone is that of two wire rings of unequal diameter, parallel to the ground, one above the other, the larger on top. These rings are connected to each other with equal-length wires, almost vertical to the ground. Figure 3.1 shows an inverted cone configuration with an upper ring only. Figure 3.2 shows another inverted cone, with two connected parallel rings and the lower ring connected to the ground by four vertical wires. The parameters of these two models which were varied are:

- a. The number of feed points (2 to 12),
- b. The wire radius ranged from 0.01 to 0.1 m, and
- c. The distance of the antenna from ground (0 to 0.4 m).

All of these designs were modeled using NEC. Appendix A lists the input data sets. The restrictions and limitations which were followed are listed in paragraph A of chapter II.

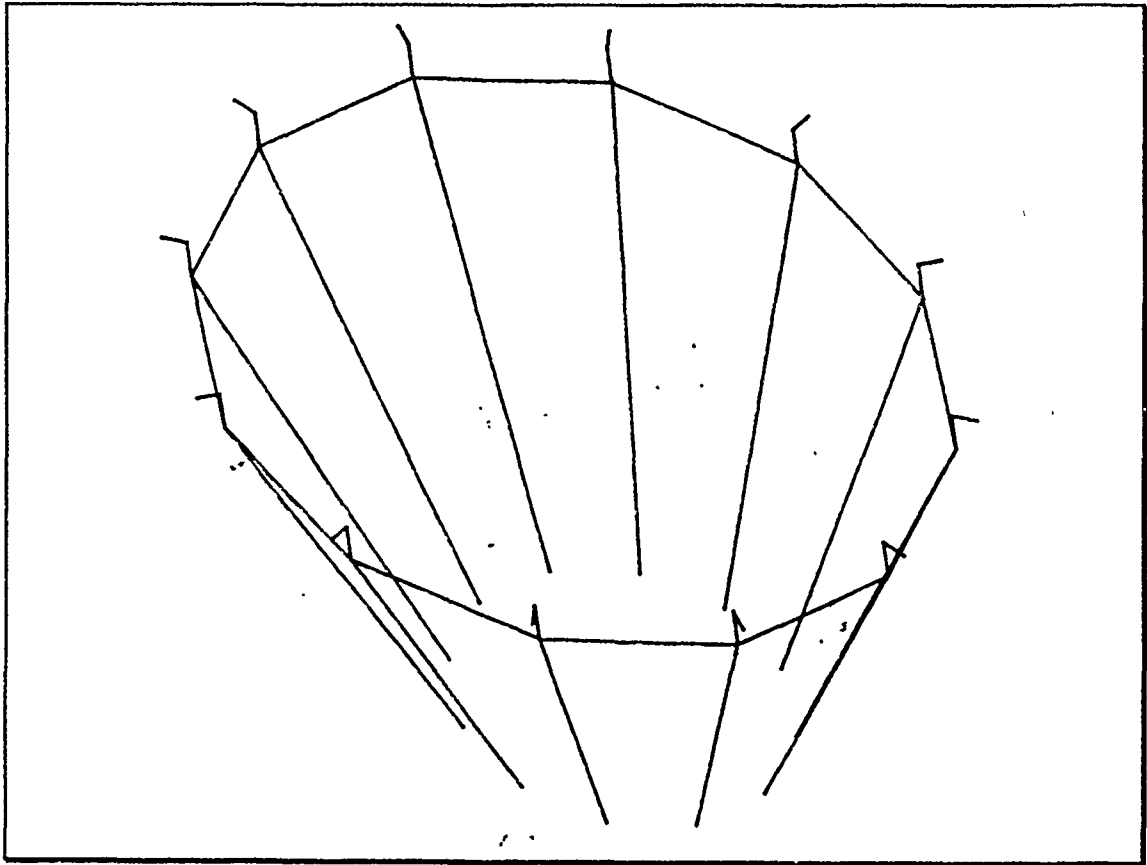


Figure 3.1 Inverted cone computer model mounted on the ground, upper ring and vertical wires, only.

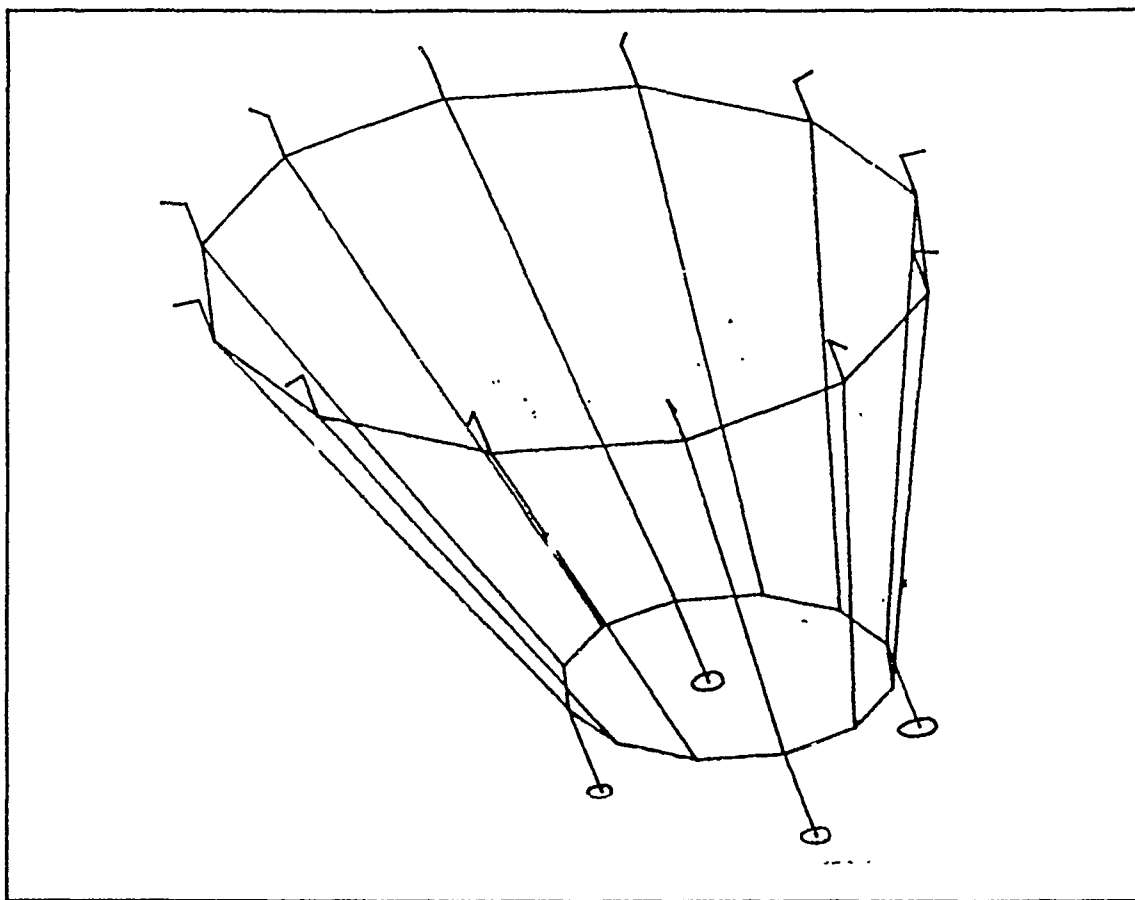


Figure 3.2 Inverted cone computer model connected to ground by four vertical wires.

B. COMPUTER MODEL RESULTS

1. Average Power Gain

Figure 3.3 shows the calculated average power gain for inverted cone antenna models mounted on the ground, (Figure 3.1), for the following configurations :

- a. Antenna mounted on the ground with 12 feed points
- b. Antenna mounted on the ground with 4 feed points
- c. Antenna mounted on the ground with 2 feed points

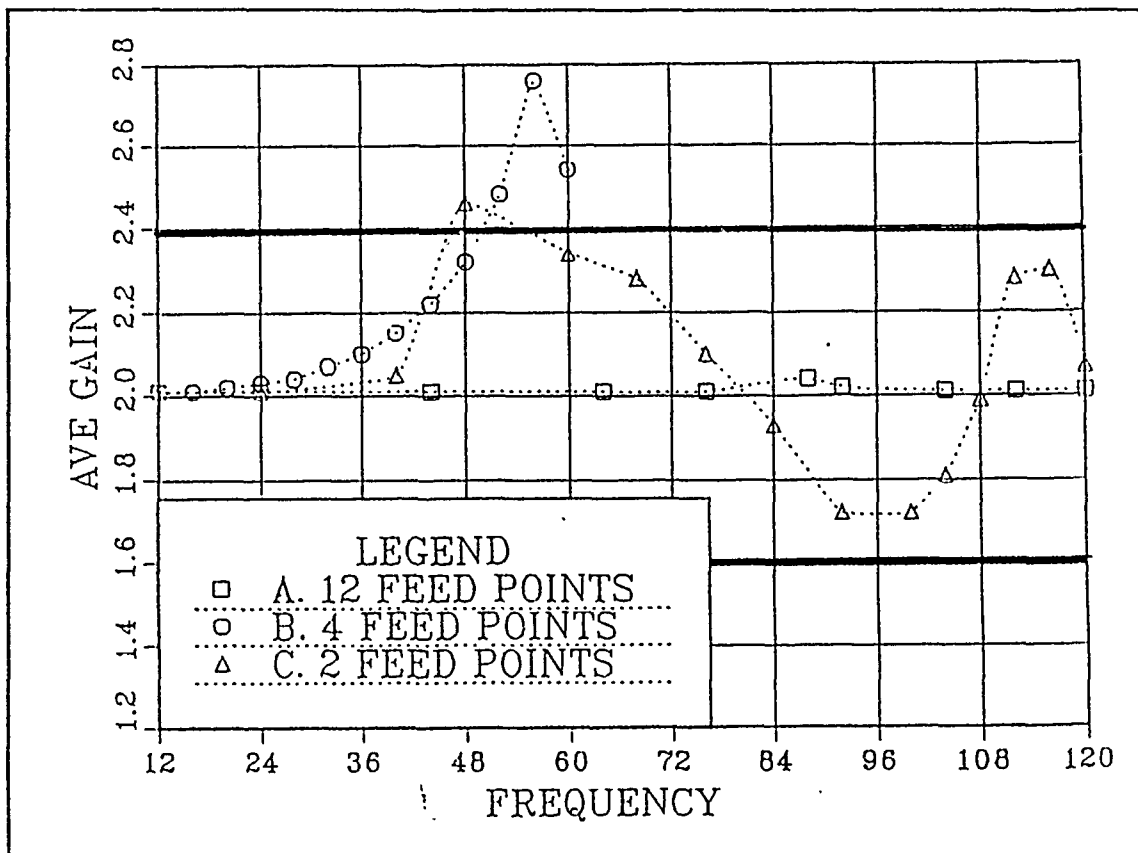


Figure 3.3 Average Power Gain for inverted cone antenna models mounted on the ground.

Figure 3.4 shows the calculated average power gain for inverted cone antenna models of Figure 3.2 connected to the ground by vertical wires, for the following configurations:

- a. Antenna 0.4 m above ground with 4 feed points
- b. Antenna 0.4 m above ground with 2 feed points
- c. Antenna 0.2 m above ground with 2 feed points

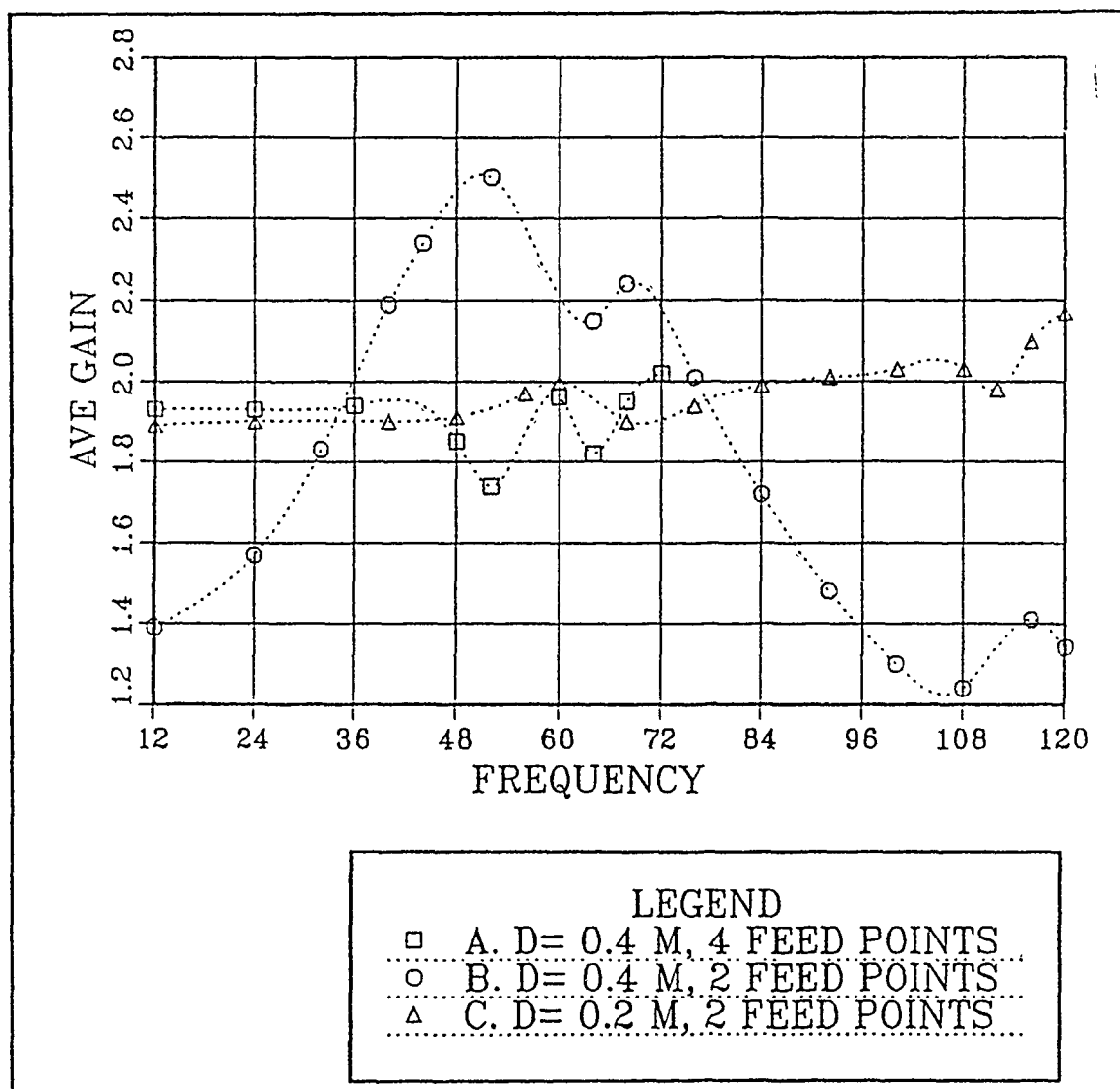


Figure 3.4 Average Power Gain for inverted cone antenna models connected to the ground by vertical wires.

From Figures 3.3 and 3.4, it is seen that the average power gain values are mostly acceptable, i.e. in the range 1.6-2.4. This is required for the validity of the antenna computer model, and further investigation is needed to examine antenna performance.

2. Input Impedance

The two different inverted cone antenna models were run to evaluate the variation of input impedance of each model as a function of frequency. The two specific configurations of these models were chosen because their average gain values were acceptable (1.6-2.4) over the frequency range. The results are indicated on two different curves, one for resistance (R), the other for reactance (jX)

Figure 3.5 shows the results for an inverted cone antenna mounted on the ground. These values are easy to match, as can be seen from the plot of the Smith Chart of Figure 3.6, considering a 3:1 VSWR as a reasonable criterion for broadband shipboard antenna operation (only point 1, for frequency value 156 MHz, is outside the 3:1 VSWR circle). A characteristic impedance of 400 Ohms was chosen to optimize the matchable region in this case. Typical shipboard systems use 50 Ohm feedlines, which will require broadband impedance transformers to be installed at the antenna base.

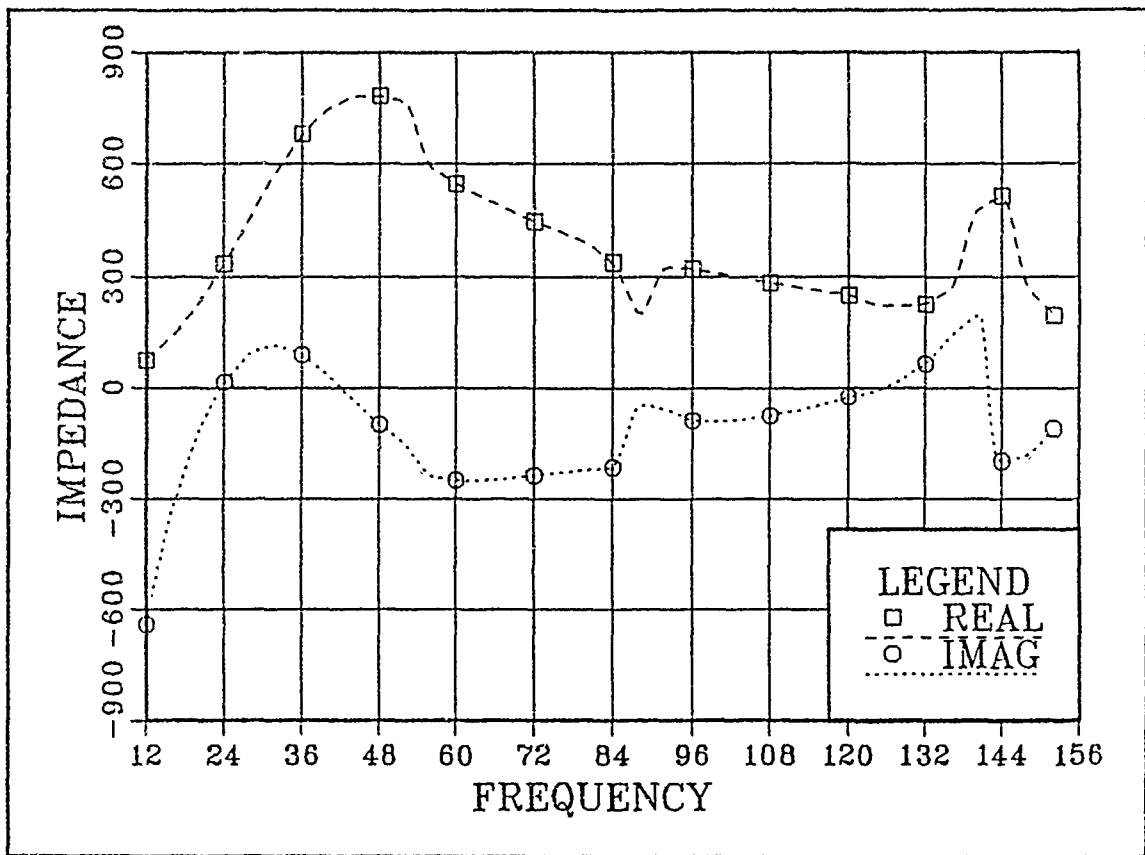


Figure 3.5 Input Impedance for inverted cone antenna mounted on the ground, with 12 feed points and wire radius 0.01 m.

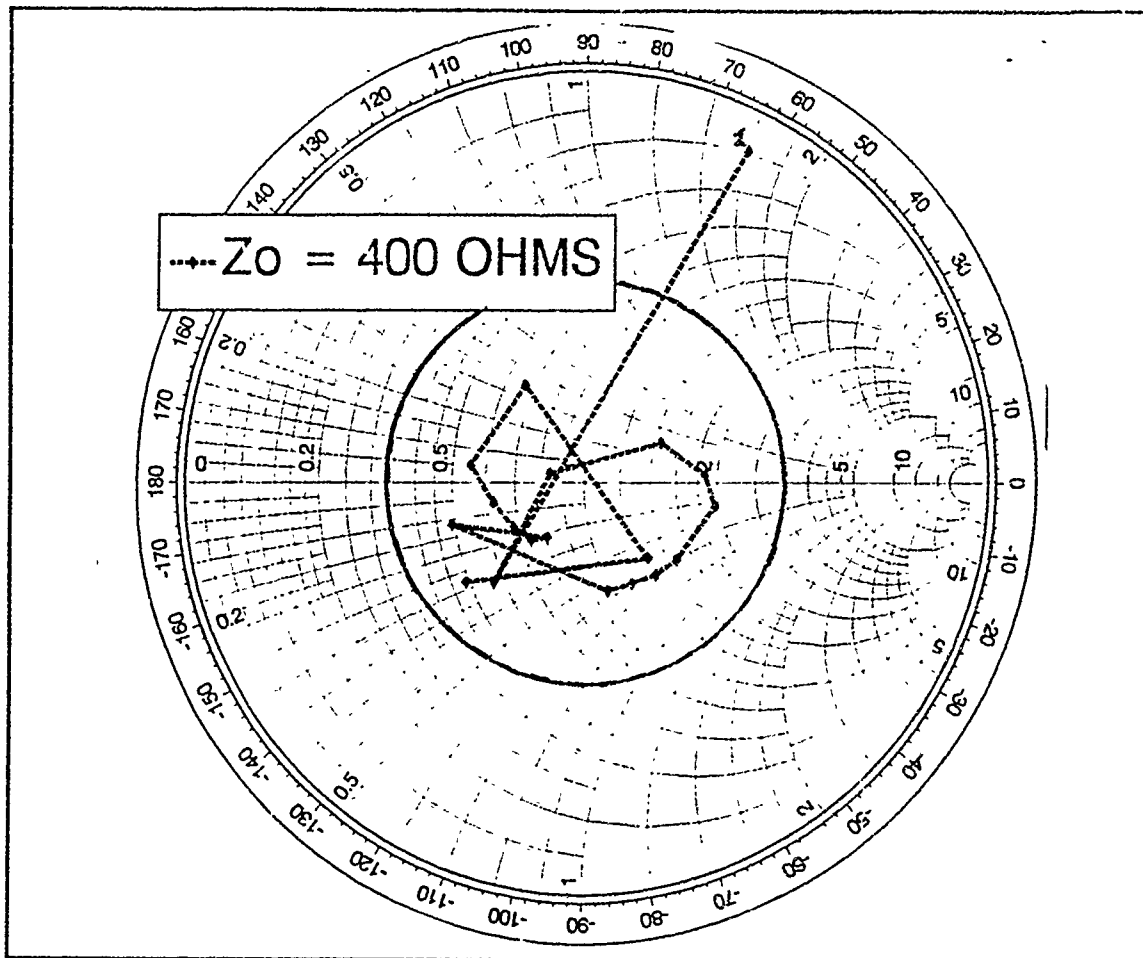


Figure 3.6 Smith Chart plot for inverted cone antenna mounted on the ground, with 12 feed points and wire radius 0.01 m, in frequency range 12-156 MHz.

Figures 3.7 and 3.8 show the results for inverted cone antennas 0.4 meters above the ground, for different wire radii. For the results of Figure 3.7, a characteristic impedance of 150 Ohms was chosen to broaden the 3:1 VSWR as it is shown in Figure 3.9 (points 1 and 2, for frequency values 12 and 156 MHz respectively, are outside the 3:1 VSWR circle). Figure 3.10 shows the Smith Chart plot for the results of Figure 3.8, using 100 Ohms as characteristic impedance, which matches almost perfectly, since only point 1 is just outside the 3:1 VSWR circle.

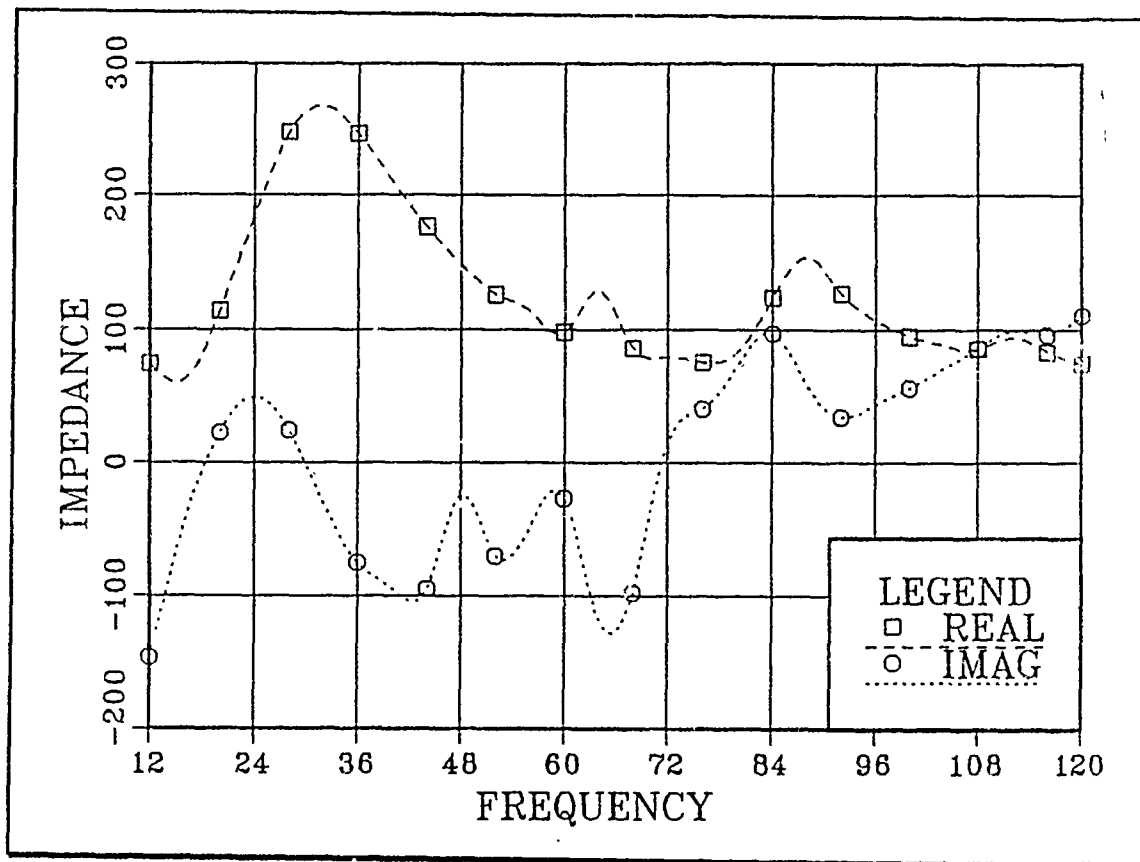


Figure 3.7 Input Impedance for an inverted cone antenna 0.4 m above the ground, with 4 feed points and wire radius 0.01 m.

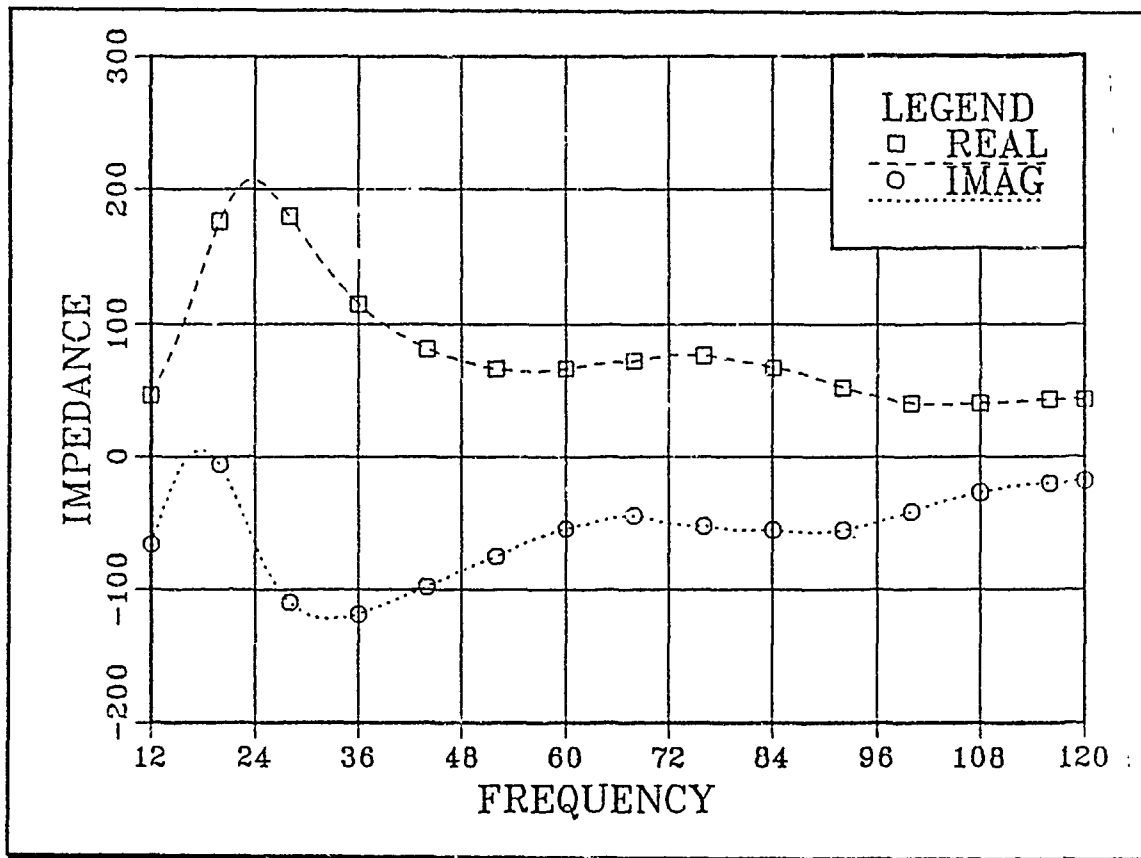


Figure 3.8 Input Impedance for an inverted cone antenna 0.4 m above the ground, with 4 feed points and wire rad 0.10 m.

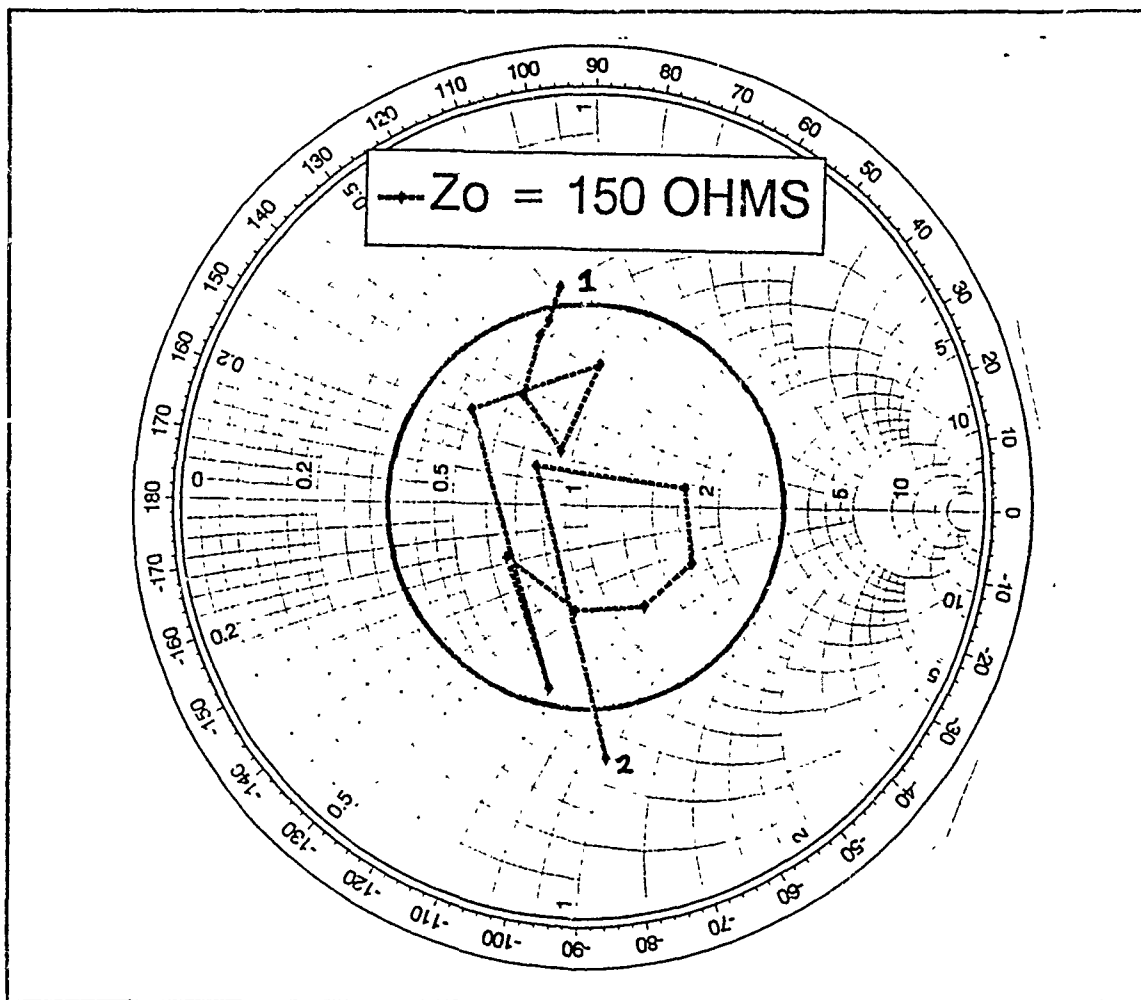


Figure 3.9 Smith Chart plot for an inverted cone antenna 0.4 m above the ground with 4 feed points and wire radius 0.01 m, in the frequency range 12-120 MHz.

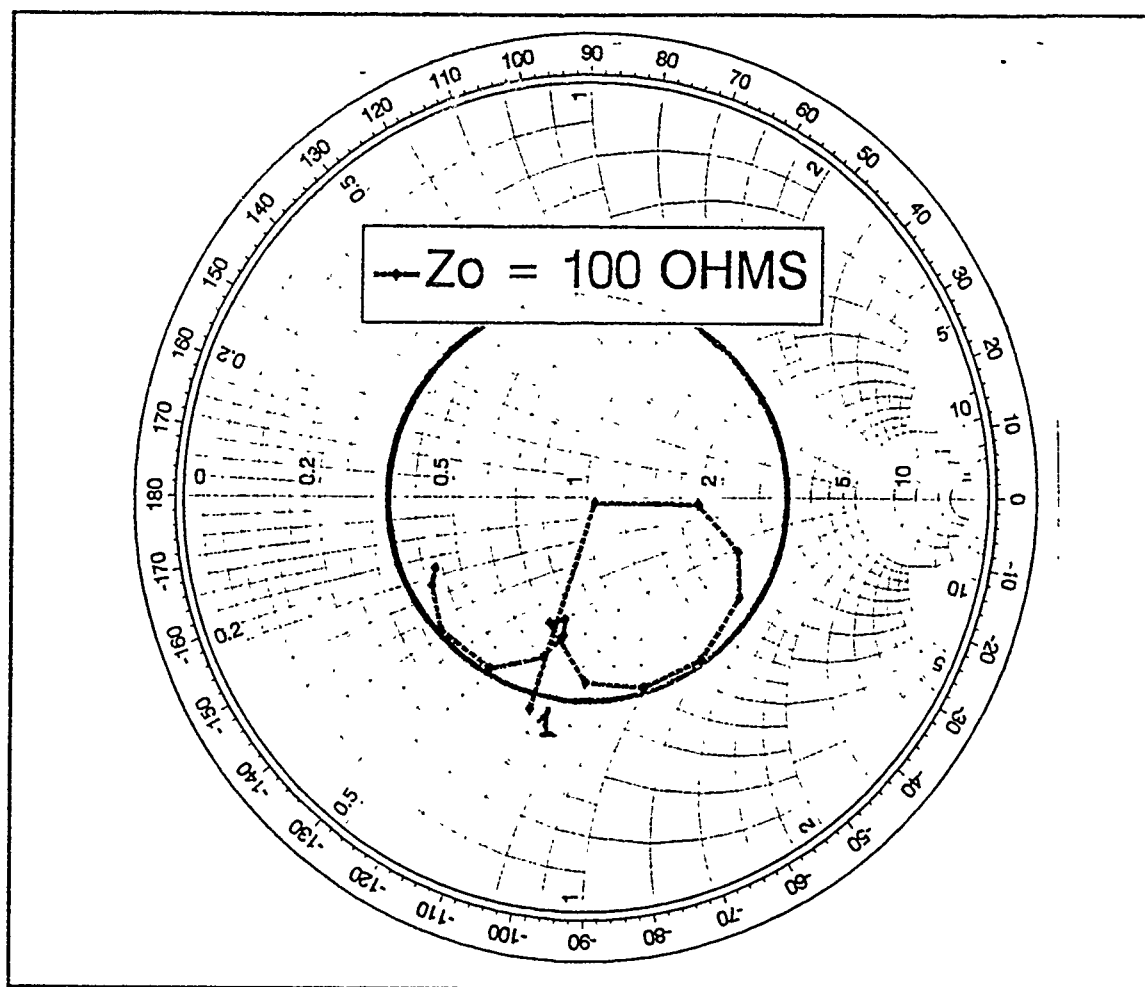


Figure 3.10 Smith Chart plot for an inverted cone antenna 0.4 m above the ground, with 4 feed points and wire radius 0.10 m, in the frequency range 12-120 MHz.

IV. INVERTED CONE ON A WIRE GRID BOX COMPUTER MODEL AND RESULTS

This chapter presents inverted cone computer antennas mounted on a wire grid box, as modeled in NEC.

A. INVERTED CONE ON A WIRE GRID BOX COMPUTER MODEL

Figure 4.1 shows a wire grid box with dimensions 26 x 13 x 6.5 meters, which crudely approximates a ship's shape.

Figure 4.2 shows the inverted cone of Figure 3.2, 0.4 m above the wire grid box, connected to it by four vertical wires.

Figure 4.3 shows the inverted cone of Figure 3.1, mounted on the wire grid box with 12 feed points and one connection point.

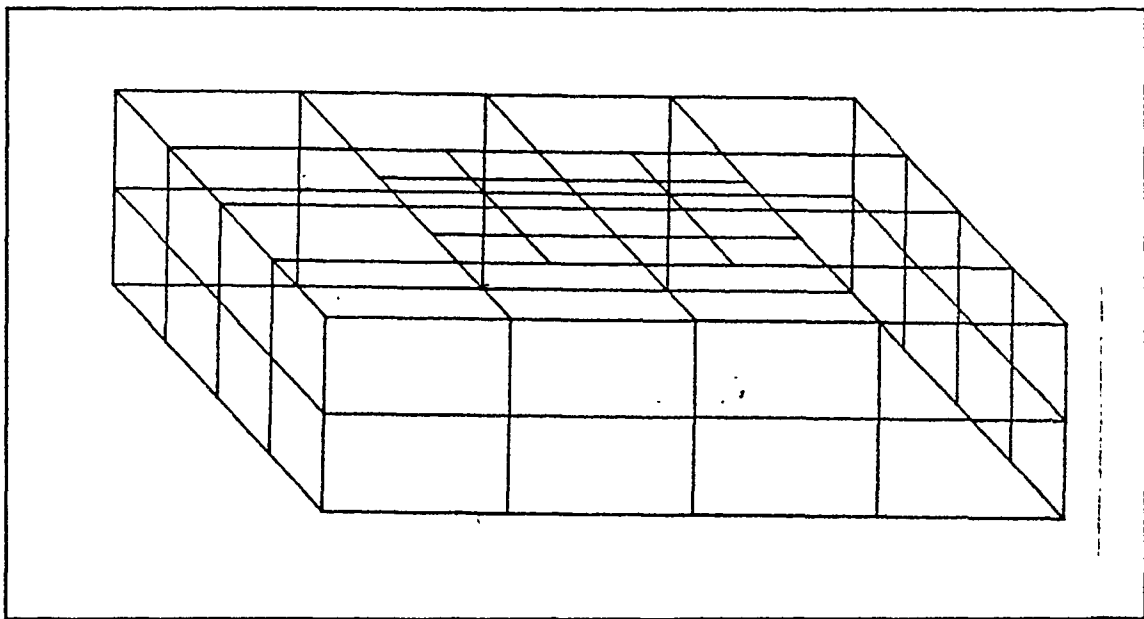


Figure 4.1 Wire grid box representing a ship's shape.

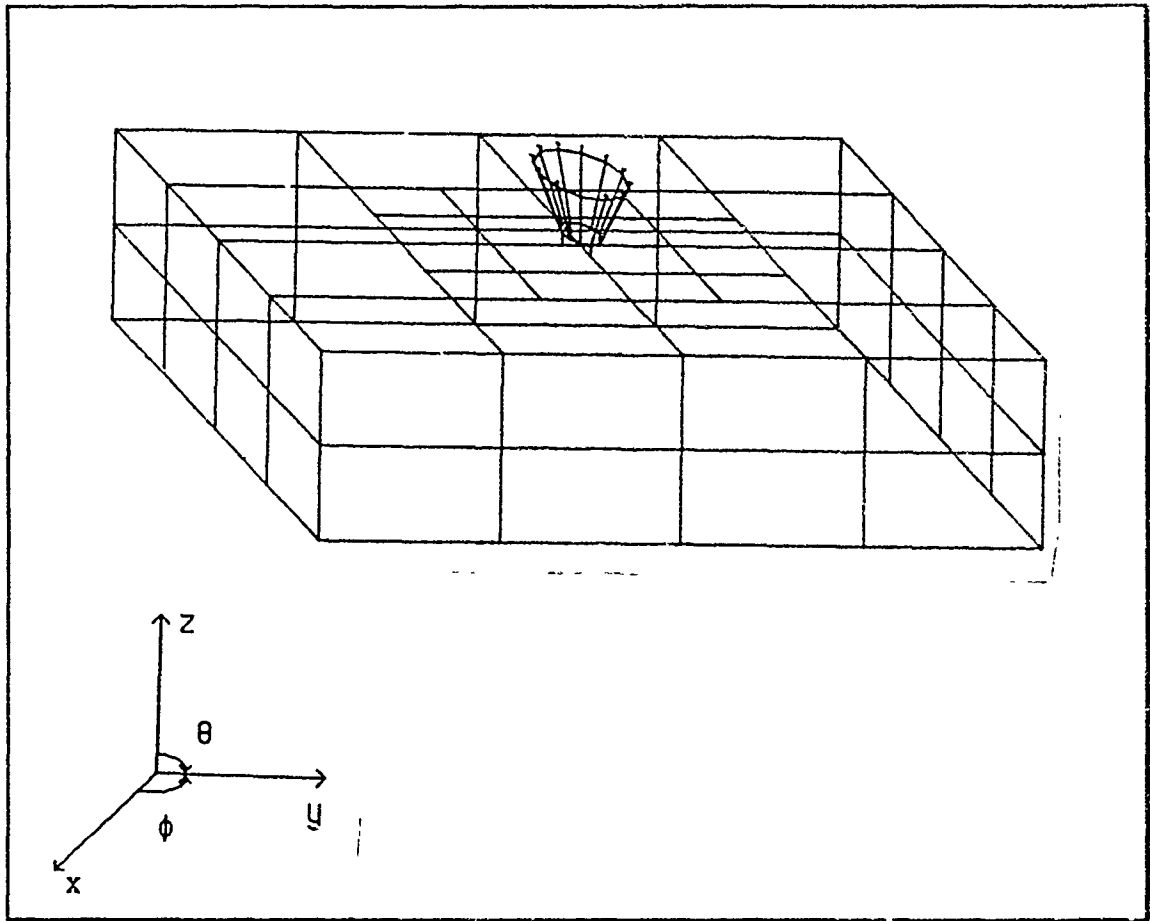


Figure 4.2 Inverted cone 0.4 m above the wire grid box, connected to it by four vertical wires.

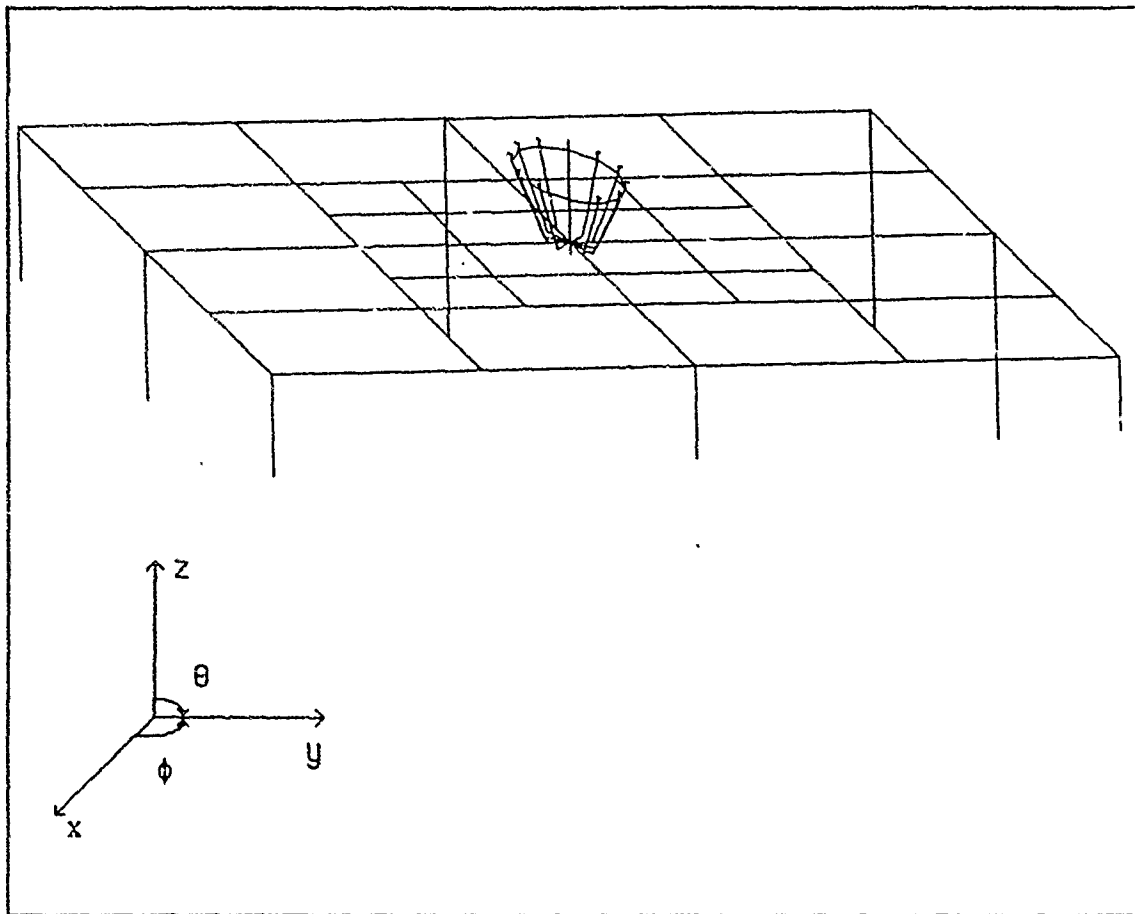


Figure 4.3 Inverted cone mounted on the wire grid box with one connection point.

B. COMPUTER MODEL RESULTS

1. Average Power Gain

Figures 4.4 and 4.5 show the calculated average power gain for the models of Figures 4.2 and 4.3.

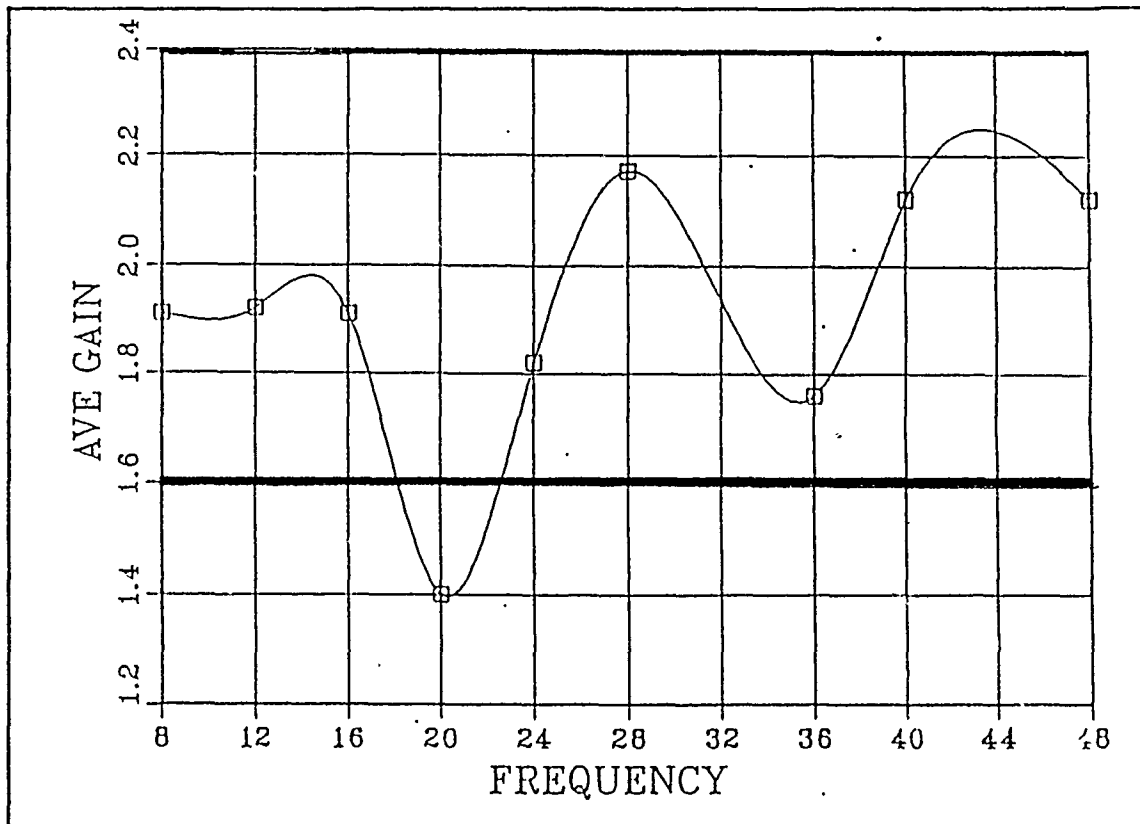


Figure 4.4 Average Power Gain for inverted cone mounted on the wire grid box, with 12 feed points, one connection point and wire radius 0.01 m.

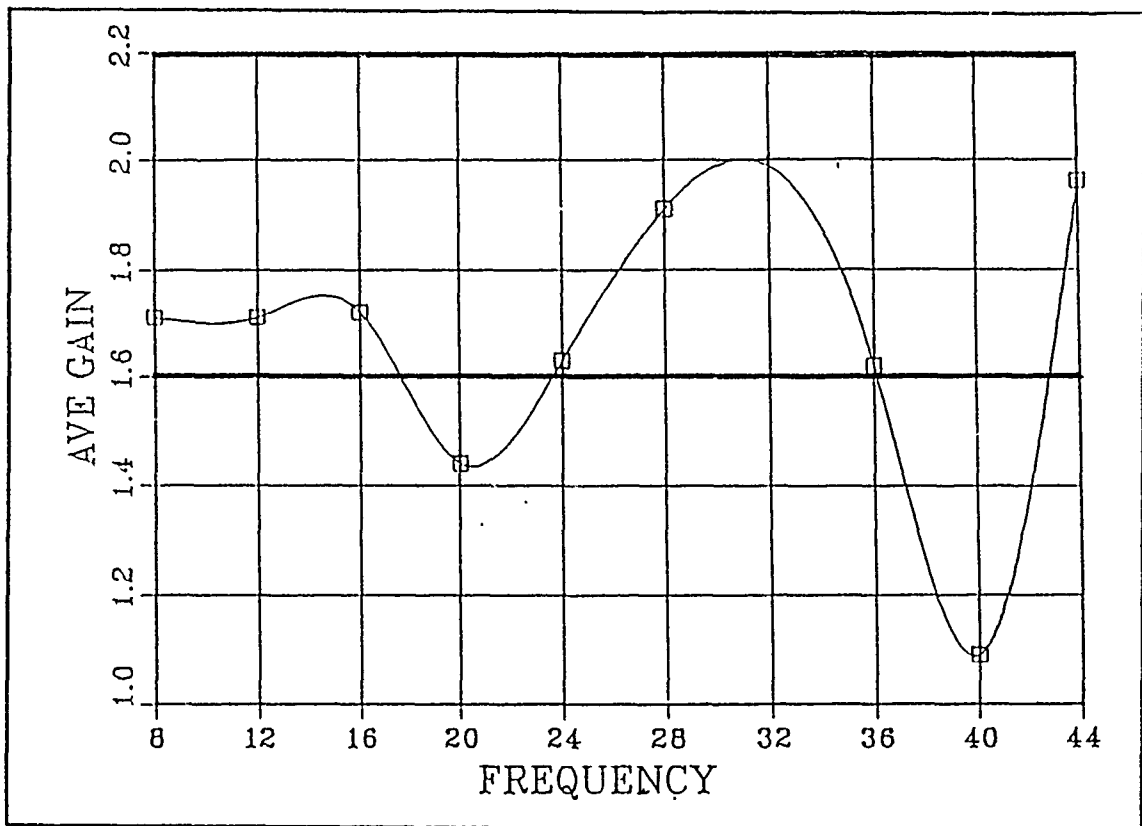


Figure 4.5 Average Power Gain for inverted cone 0.4 m above the wire grid box connected to it with four vertical wires, and wire radius 0.01 m.

From Figures 4.4 and 4.5, it is seen that the average gain values for the two models are not as close to a value of two, as they were for perfect ground, i.e. in the range 1.6-2.4. The presence of the wire grid box has affected the results, but the average gain values are still mostly acceptable.

2. Input Impedance

Figures 4.6 and 4.7 show the calculated input impedance for the two inverted cone antenna models, as a function of frequency. The results are indicated on two different curves, one for resistance (R) and the other for reactance (jX).

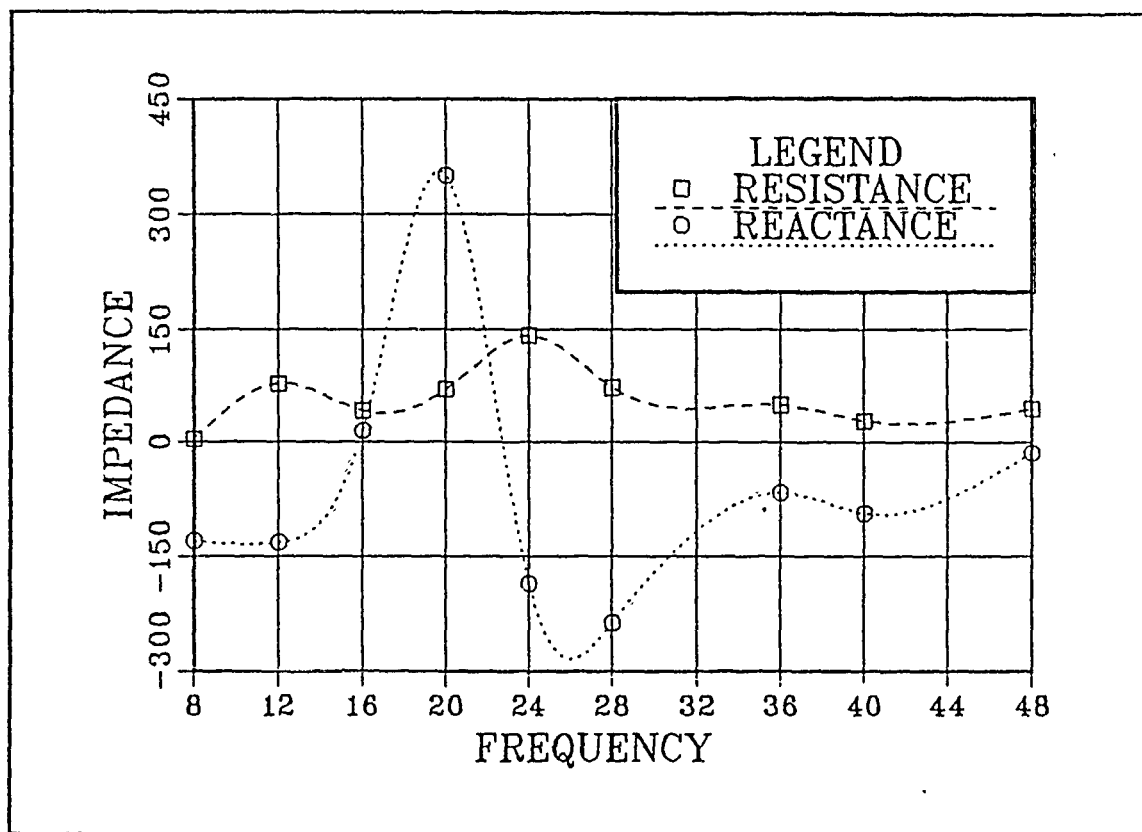


Figure 4.6 Input Impedance for inverted cone mounted on the wire grid box, with 12 feed points, one connection point and wire radius 0.01 m.

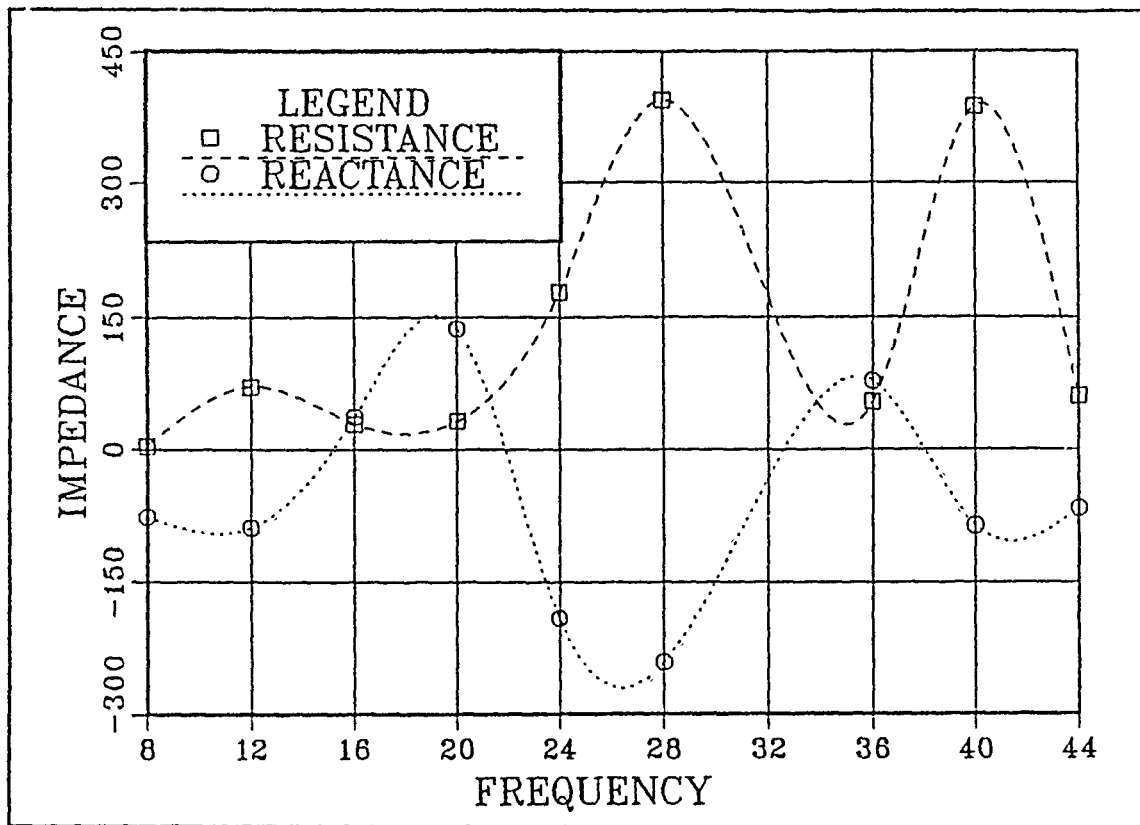


Figure 4.7 Input Impedance for inverted cone 0.4 m above the wire grid box connected to it by four vertical wires, and wire radius 0.01 m.

From the above results, it is seen that the presence of the wire grid box has affected all the computed values of the input impedance, as it did with the average gain., but there are still matchable frequency regions.

Figure 4.8 shows the Smith Chart plot for the inverted cone mounted on the wire grid box and connected to it by 12 vertical wires, using as characteristic impedance 100 Ohms (points in the frequency range 20-30 MHz are outside the 3:1 VSWR circle). The plot of the results of the inverted cone 0.4 meters above the wire grid box and connected to it by four vertical wires is shown in Figure

4.9, for a characteristic impedance 200 Ohms (points in the frequency range 28-40 MHz are outside the 3:1 VSWR circle).

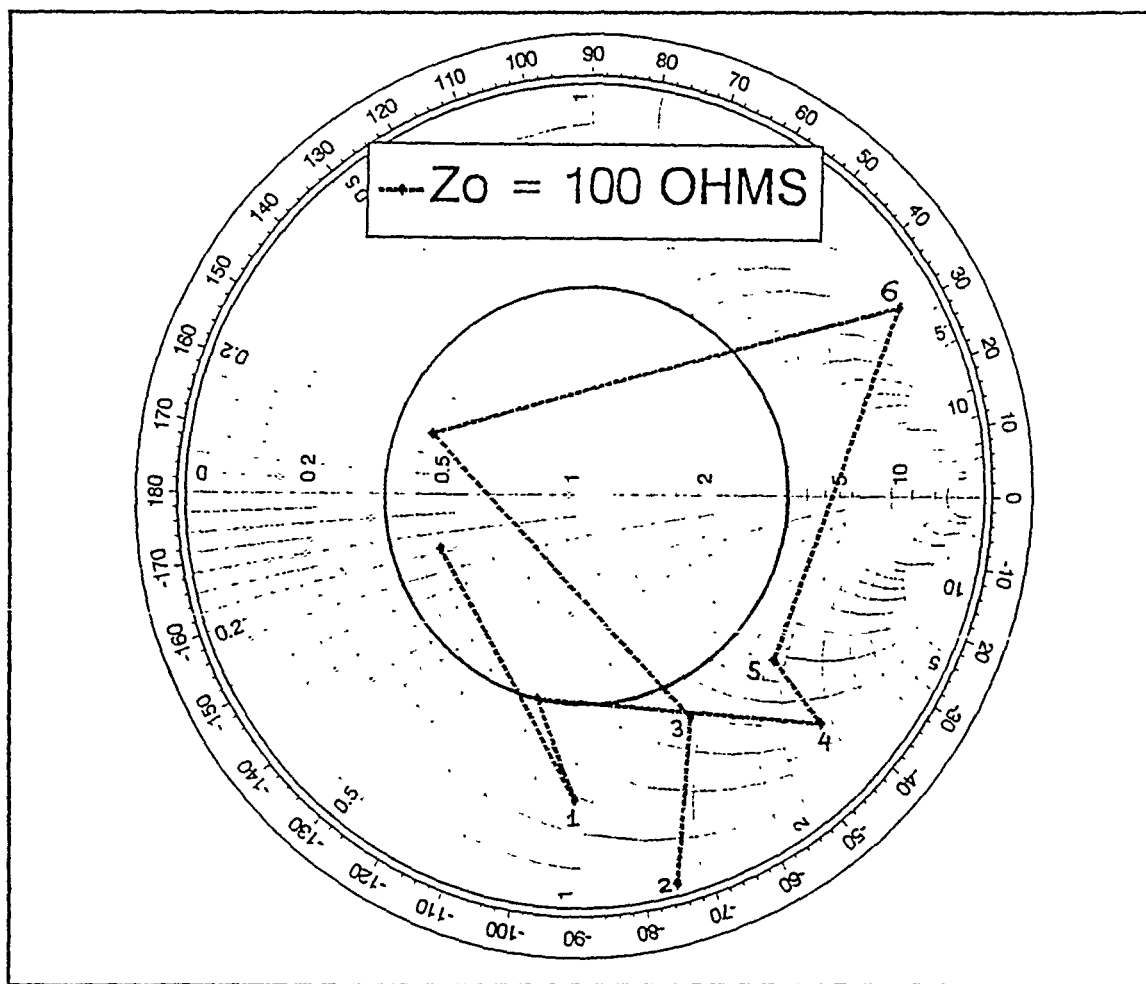


Figure 4.8 Smith Chart plot for an inverted cone antenna mounted on the wire grid box with 12 feed points, one connection point and wire radius 0.01 m, in the frequency range 8-48 MHz.

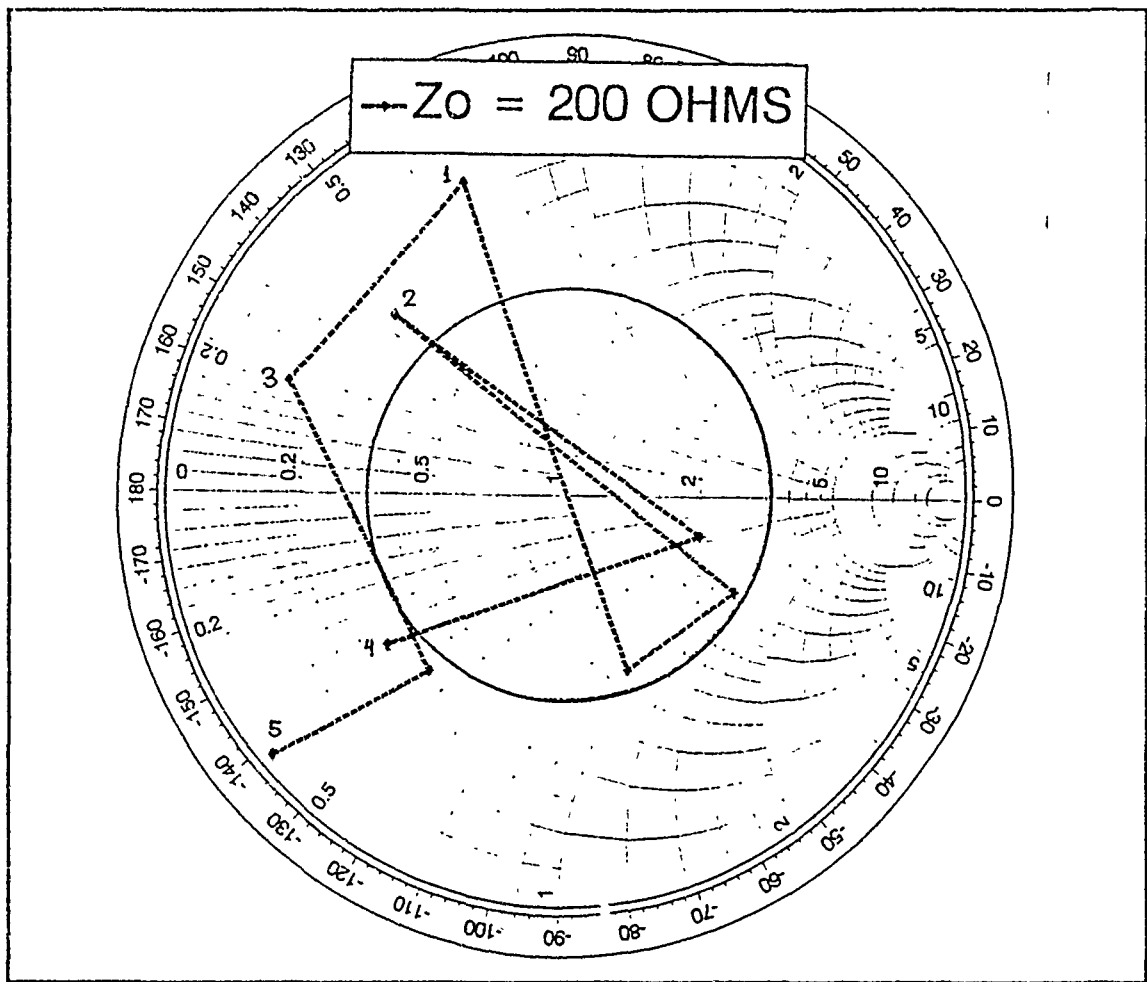


Figure 4.9 Smith Chart plot for inverted cone antenna 0.4 m above the wire grid box connected to it by four vertical wires and wire radius 0.01 m, in the frequency range 8-44 MHz.

3. Radiation Patterns

Figures 4.10 - 4.12 show the elevation patterns for the configuration of an inverted cone antenna mounted on the wire grid box with 12 feed points, one connection point and wire radius 0.01 meters, at 20 MHz.

Figures 4.13 - 4.15 show the elevation patterns for the configuration of an inverted cone antenna 0.4 meter above the wire grid box connected to it by four vertical wires, wire radius 0.01 meter, at 20 MHz.

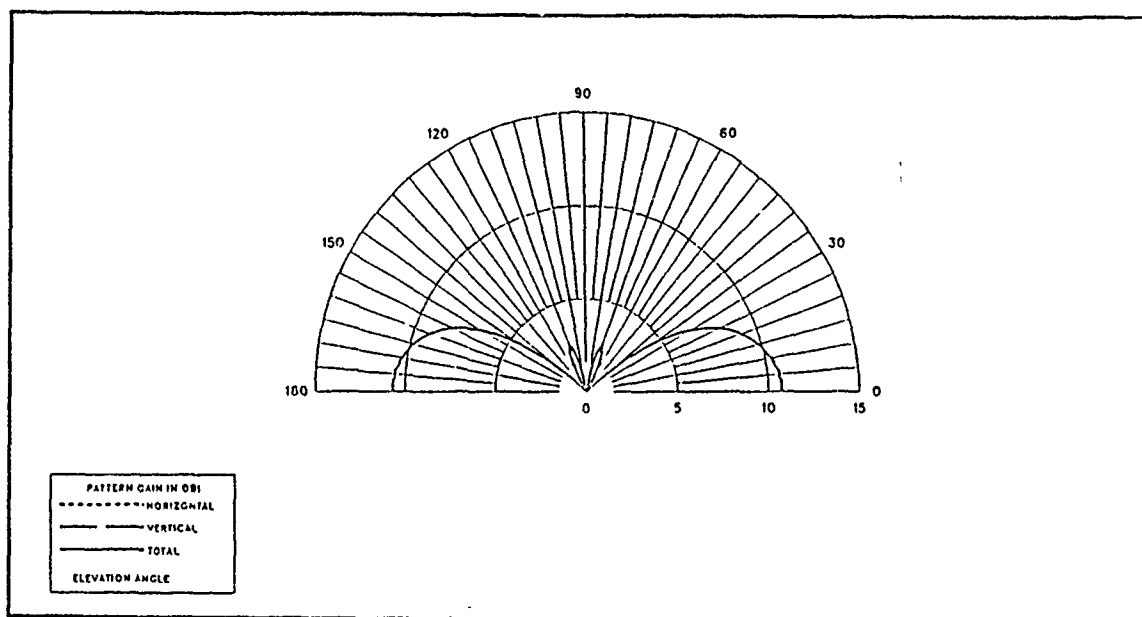


Figure 4.10 E-Field Elevation Pattern for an inverted cone antenna mounted on the wire grid box with 12 feed points, one connection point and wire radius 0.01 m, at 20 MHz, $\phi = 0$ degrees.

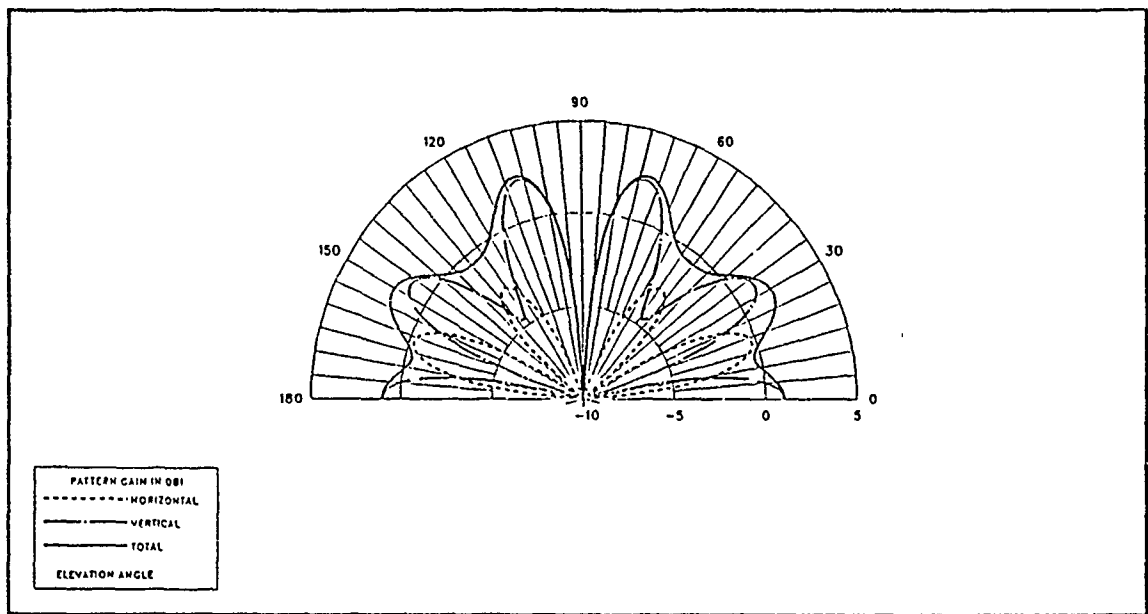


Figure 4.11 E-Field Elevation Pattern for an inverted cone antenna mounted on the wire grid box with 12 feed points, one connection point and wire radius 0.01 m, at 20 MHz, $\phi = 63.47$ degrees.

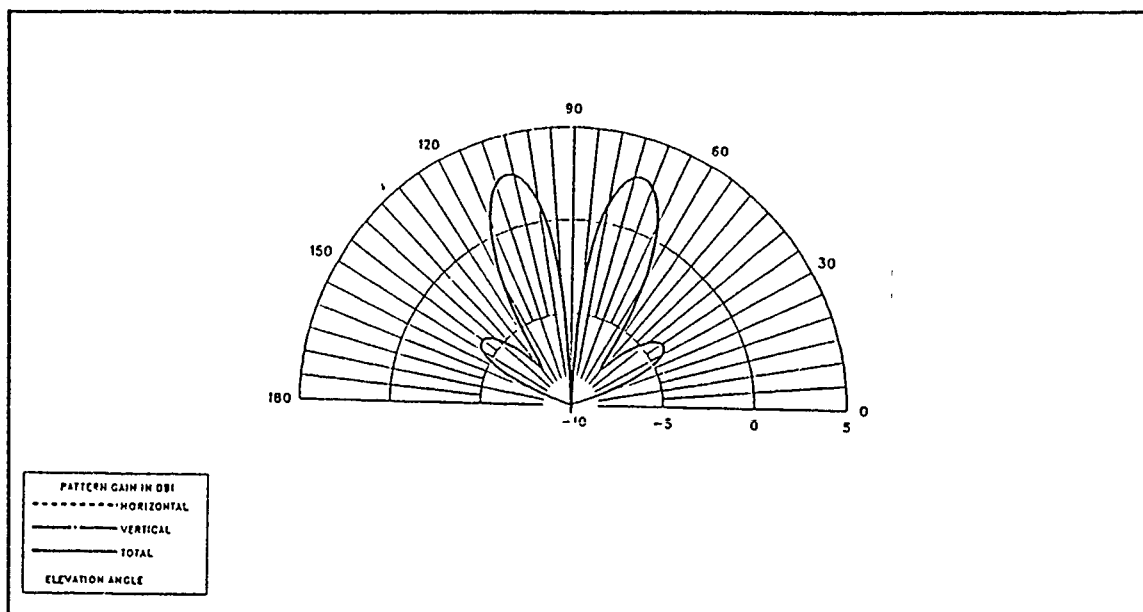


Figure 4.12 E-Field Elevation Pattern for an inverted cone antenna with 12 feed points, one connection point and wire radius 0.01 m, at 20 MHz, $\phi = 90$ degrees.

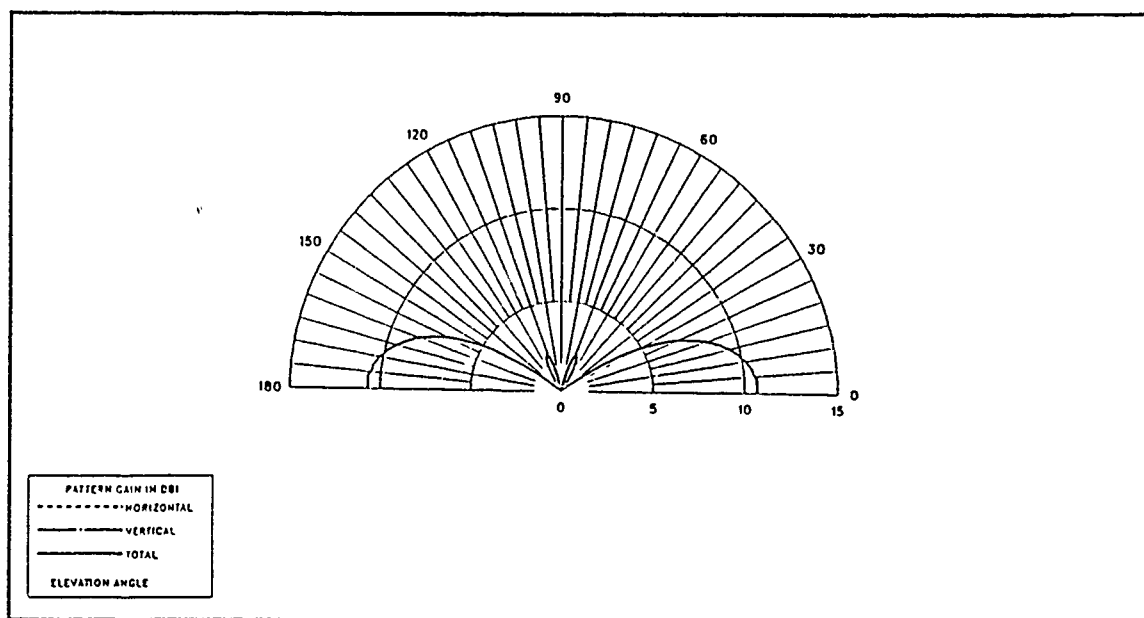


Figure 4.13 E-Field Elevation Pattern for an inverted cone antenna 0.4 m above the wire grid box connected to it by four vertical wires and wire radius 0.01 m, at 20 MHz, $\phi = 0$ degrees.

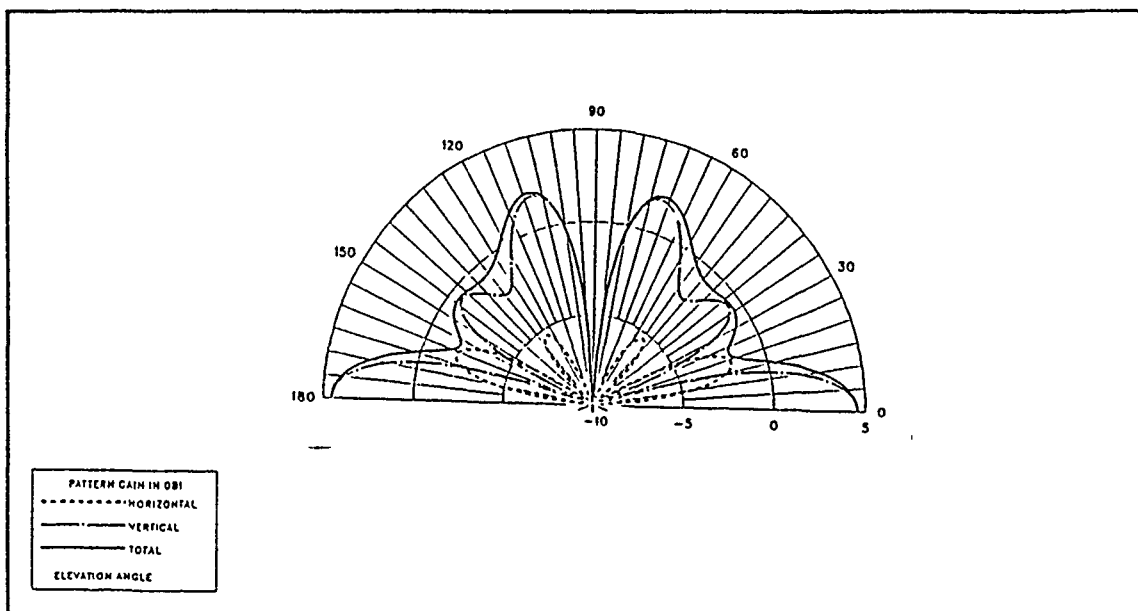


Figure 4.14 E-Field Elevation Pattern for an inverted cone antenna 0.4 m above the wire grid box connected to it by four vertical wires and wire radius 0.01 m, at 20 MHz, $\phi = 63.47$ degrees.

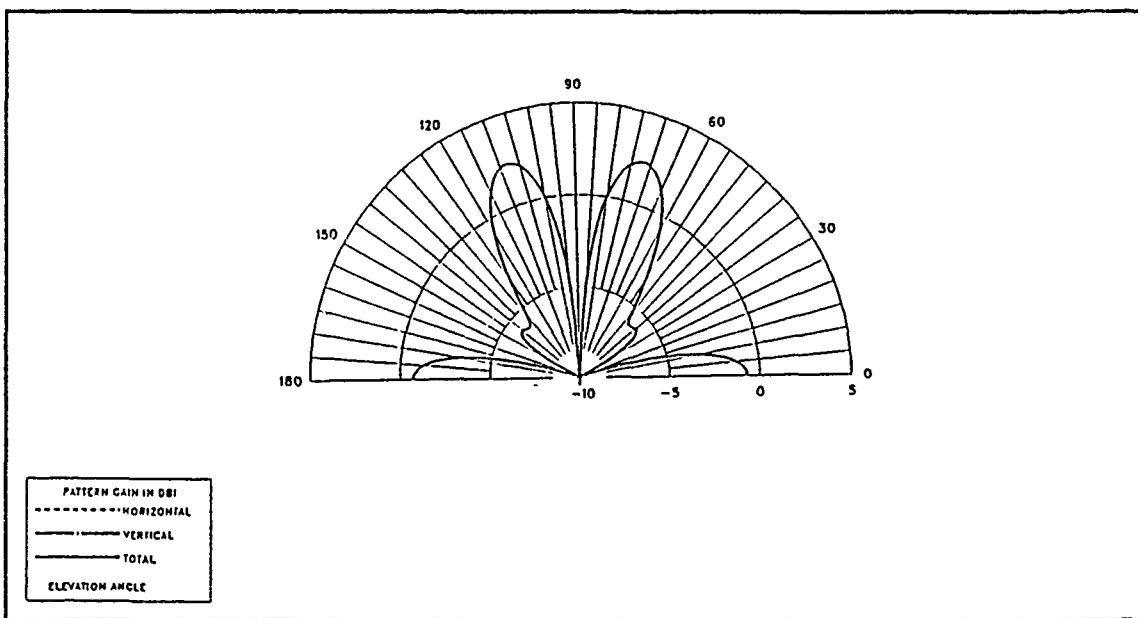


Figure 4.15 E-Field Elevation Pattern for an inverted cone antenna 0.4 m above the wire grid box connected to it by four vertical wires and wire radius 0.01 m, at 20 MHz, $\phi = 90$ degrees.

Elevation patterns of the two models seem to be similar to each other for the same value of angle ϕ , but because of the asymmetry of the whole configuration (inverted cone antenna plus wire grid box), for each value of angle ϕ there is a completely different pattern. Azimuth patterns of the two models are shown in Appendix G.

V. CONCLUSIONS AND RECOMMENDATIONS

In this thesis two different computer models were discussed; the "multi-wire" whip antenna and the inverted cone antenna. Average power gain was computed for both models, but only the results for the inverted cone were acceptable, i.e. close to two (1.6-2.4). Input impedance was computed for the inverted cone model, first over a perfect ground plane and then over a wire grid box, with acceptable results, i.e. showing the existence of matchable frequency regions. Finally, the elevation patterns are presented for two inverted cone models, one 0.4 meters above the wire grid box connected to it by four vertical wires and the other mounted on the wire grid box with 12 feed points and one connection point. The patterns change dramatically, with respect to the angle ϕ , but they seem to be similar for the two models.

A. CONCLUSIONS

The purpose of this thesis was the investigation of possible ways to reduce the number of communication antennas on a ship. A solution to this problem can be the construction of antennas performing in HF, VHF and UHF bands, in acceptable limits. For this reason, the frequency range of this study was 4-300 MHz.

The "multi-wire" whip antenna computer model was run over a perfect ground plane. The computed results for the average power gain were acceptable only in the frequency range 4-28 MHz, although many different geometry schemes were tested. For this reason, the investigation on the "multi-wire" whip antenna computer model was not extended any further.

The inverted cone computer model was run also over a perfect ground plane. The values of the the computed average power gain were close to two in the

frequency range of 4-152 MHz. In addition, the results of the computed input impedance show that matchable frequency regions exist for this antenna model, especially for two geometry configurations; the inverted cone with 12 feed points mounted on the ground plane and the inverted cone with 4 feed points and 0.4 meter distance from the ground plane. These two specific models were mounted over a wire grid box, used as a ship's shape approximation, and were run again. The values of the computed gain were different, but they were still acceptable, close enough to the value of two (1.6-2.4), in the frequency range of 8-48 MHz. In this range, there were matchable regions of the computed input impedance (considering a 3:1 VSWR as an acceptable ratio for broadband shipboard antennas). This is the reason why the inverted cone antenna model is considered valid. Further investigation may yield improvements in performance.

2. RECOMMENDATIONS

There are several aspects of this study which warrant further investigation, considering the acceptable results of the inverted cone antenna models tested over a perfect ground plane and over a wire grid box:

- Compute the average power gain, the input impedance, and the radiation patterns of the two inverted cone antenna models on the wire grid box at higher frequencies.
- Vary the number of feed positions of the inverted cone antenna on the wire grid box.
- Vary the distance between the inverted cone antenna and the wire grid box because the results for the computed average power gain and input impedance

were totally different for the three cases of this study; inverted cone mounted on the wire grid box, inverted cone 0.2 meters above the wire grid box and inverted cone 0.4 meters above the wire grid box.

- Try more geometry schemes for the inverted cone antenna, i.e. vary the number and the length of the wires to improve the frequency bandwidth of acceptable results.

APPENDIX A

Contained in this appendix are NEC data sets for the computer antenna models used in this thesis.

a. Two "multi-wire" whip antennas.

```
CE TWO "MULTI-WIRE" WHIP ANTENNAS
GW1,7,.05,0.,0.,0.,0.,10.,.01,
GW2,7,-.05,0.,0.,0.,0.,10.,.01,
GW3,7,0.,.05,0.,0.,0.,10.,.01,
GW4,7,0.,-.05,0.,0.,0.,10.,.01,
GW5,7,0.05,5.,0.,0.,5.,10.,.01,
GW6,7,-.05,5.,0.,0.,5.,10.,.01,
GW7,7,0.,5.05,0.,0.,5.,10.,.01,
GW8,7,0.,4.95,0.,0.,5.,10.,.01,
GW9,7,0.,0.,0.,0.,0.,10.,.01,
GW10,7,0.,5.,0.,0.,5.,10.,.01,
GE1,0,0.,
FR0,5,0,0,4.,4.,
EK0,
EX0,1,2,00,1.,0.,
EX0,2,2,00,1.,0.,
EX0,3,2,00,1.,0.,
EX0,4,2,00,1.,0.,
EX0,5,2,00,1.,0.,
EX0,6,2,00,1.,0.,
EX0,7,2,00,1.,0.,
EX0,8,2,00,1.,0.,
EX0,9,2,00,1.,0.,
EX0,10,2,00,1.,0.,
GN1,
RP0,91,2,1001,0.,0.,1.,90.,0.,0.,
EN
```


b. Three "multi-wire" whip antennas in triangular form.

CE THREE "MULTI-WIRE" WHIP ANTENNAS IN TRIANGULAR FORM

GW1,5,2.05,2.,0.,2.,2.,10.,.01,
 GW2,5,1.95,2.,0.,2.,2.,10.,.01,
 GW3,5,2.,2.05,0.,2.,2.,10.,.01;
 GW4,5,2.,1.55,0.,2.,2.,10.,.01,
 GW5,5,-1.95,2.,0.,-2.,2.,10.,.01,
 GW6,5,-2.05,2.,0.,-2.,2.,10.,.01,
 GW7,5,-2.,2.05,0.,-2.,2.,10.,.01,
 GW8,5,-2.,1.95,0.,-2.,2.,10.,.01,
 GW9,5,.05,-2.,0.,0.,-2.,10.,.01,
 GW10,5,-.05,-2.,0.,0.,-2.,10.,.01,
 GW11,5,0.,-2.05,0.,0.,-2.,10.,.01,
 GW12,5,0.,-1.95,0.,0.,-2.,10.,.01,
 GE1,0,0.,

c. Inverted cone antenna mounted on the ground.

CE INVERTED CONE ANTENNA CONNECTED TO THE GROUND

GW1,3,.675,0.,6.9,.5845,.3375,6.9,.01,
 GW2,3,1.5,0.,8.9,1.299,.75,8.9,.01,
 GW3,2,1.5,0.,8.9,1.5,0.,9.1,.01,
 GW4,2,1.5,0.,9.1,1.6,0.,9.1,.01,
 GW5,5,.5845,.3375,6.9,1.299,.75,8.9,.01,
 GW6,3,.5845,.3375,6.9,.3375,.5845,6.9,.01,
 GW7,3,1.299,.75,8.9,.75,1.299,8.9,.01,
 GW8,2,1.299,.75,8.9,1.299,.75,9.1,.01,
 GW9,2,1.299,.75,9.1,1.386,.8,9.1,.01,
 GW10,5,.3375,.5845,6.9,.75,1.299,8.9,.01,
 GW11,3,.3375,.5845,6.9,0.,.675,8.9,.01,
 GW12,3,.75,1.299,8.9,0.,1.5,8.9,.01,
 GW13,2,.75,1.299,8.9,.75,1.299,9.1,.01,
 GW14,2,.75,1.299,9.1,.8,1.386,9.1,.01,
 GW15,5,0.,.675,6.9,0.,1.5,8.9,.01,
 GW16,3,.675,0.,6.9,.675,0.,6.5,.01,
 GR1,4,
 GE1,0,0.,
 FR0,1,0,0,12.,0.,0.,
 EK0,
 GNI,
 EN

d. Inverted cone antenna mounted on a wire grid box.

CE INVERTED CONE ANTENNA MOUNTED ON A WIRE GRID BOX

GW1,18,6.5,0.,6.5,6.5,13.,6.5,.001,
GW2,9,6.5,13.,6.5,0.,13.,6.5,.001,
GW3,18,3.25,0.,6.5,3.25,13.,6.5,.001,
GW4,9,6.5,6.5,6.5,0.,6.5,6.5,.001,
GW5,5,3.25,3.25,6.5,0.,3.25,6.5,.001,
GW6,9,1.625,0.,6.5,1.625,6.5,6.5,.001,
GW7,9,6.5,13.,6.5,6.5,13.,0.,.001,
GX10,110,
GW81,3,1.5,0.,8.5,1.299,.75,8.5,.01,
GW82,2,1.5,0.,8.5,1.5,0.,8.7,.01,
GW83,2,1.5,0.,8.7,1.6,0.,8.7,.01,
GW84,5,1.299,.75,8.5,.5845,.3375,6.5,.01,
GW85,3,0.,0.,6.5,.5845,.3375,6.5,.01,
GM100,11,0.,0.,30.,0.,0.,0.,81.85,
GW2001,5,1.625,0.,6.5,0.675,0.,6.5,.01,
GW2002,5,-.675,0.,6.5,-1.625,0.,6.5,.01,
GW2003,5,0.,-3.25,6.5,0.,-.675,6.5,.01,
GW2004,5,0.,3.25,6.5,0.,.675,6.5,.01,
GW2005,5,1.625,0.,6.5,3.25,0.,6.5,.01,
GW2006,5,3.25,0.,6.5,6.5,0.,6.5,.01,
GW2007,5,-1.625,0.,6.5,-3.25,0.,6.5,.01,
GW2008,5,-3.25,0.,6.5,-6.5,0.,6.5,.01,
GW2009,5,0.,3.25,6.5,0.,6.5,6.5,.01,
GW2010,5,0.,6.5,6.5,0.,13.,6.5,.01,
GW2011,5,0.,-3.25,6.5,0.,-6.5,6.5,.01,
GW2012,5,0.,-6.5,6.5,0.,-13.,6.5,.01,
GW2013,5,6.5,0.,6.5,6.5,0.,0.,.01,
GW2014,5,-6.5,0.,6.5,-6.5,0.,0.,.01,
GW2015,5,0.,-13.,6.5,0.,-13.,0.,.01,
GW2016,5,0.,13.,6.5,0.,13.,0.,.01,
GE1,0,0.,
FR0,1,0,0,4.,0.,
EKO,
EX0,0,155,00,1.,0.,
EX0,0,203,00,1.,0.,
EX0,0,251,00,1.,0.,
EX0,0,299,00,1.,0.,
GN1,
RP0,91,2,1001,0.,0.,1.,90.,0.,0.,
EN

e. Inverted cone antenna 0.4 meter above a wire grid box, connected

to it by four vertical wires.

CE INVERTED CONE ANTENNA 0.4 M ABOVE THE BOX

GW1,5,6.5,0.,3.25,6.5,13.,3.25,.01,
GW2,5,6.5,13.,3.25,0.,13.,3.25,.01,
GW3,5,6.5,13.,0.,6.5,13.,3.25,.01,
GX10,111,
GW81,3,.675,0.,3.65,.5845,.3375,3.65,.01,
GW82,3,1.5,0.,5.65,1.299,.75,5.65,.01,
GW83,2,1.5,0.,5.65,1.5,0.,5.85,.01,
GW84,2,1.5,0.,5.85,1.6,0.,5.85,.01,
GW85,5,.5845,.3375,3.65,1.299,.75,5.65,.01,
GW86,3,.5845,.3375,3.65,.3375,.5845,3.65,.01,
GW87,3,1.299,.75,5.65,.75,1.299,5.65,.01,
GW88,2,1.299,.75,5.65,1.299,.75,5.85,.01,
GW89,2,1.299,.75,5.85,1.386,.8,5.85,.01,
GW90,5,.3375,.5845,3.65,.75,1.299,5.65,.01,
GW91,3,.3375,.5845,3.65,0.,.675,3.65,.01,
GW92,3,.75,1.299,5.65,0.,1.5,5.65,.01,
GW93,2,.75,1.299,5.65,.75,1.299,5.85,.01,
GW94,2,.75,1.299,5.85,.8,1.386,5.85,.01,
GW95,5,0.,.675,3.65,0.,1.5,5.65,.01,
GW96,3,.675,0.,3.65,.675,0.,3.25,.01,
GM100,3,0.,0.,90.,0.,0.,0.,81.96,
GW401,5,0.,-13.,3.25,0.,13.,3.25,.1,
GW402,5,-3.25,-13.,3.25,-3.25,13.,3.25,.1,
GW403,5,3.25,-13.,3.25,3.25,13.,3.25,.1,
GW404,5,6.5,0.,3.25,-6.5,0.,3.25,.1,
GW405,5,6.5,6.5,3.25,-6.5,6.5,3.25,.1,
GW406,5,6.5,-6.5,3.25,-6.5,-6.5,3.25,.1,
GW407,5,3.25,-3.25,3.25,-3.25,-3.25,3.25,.1,
GW408,5,3.25,3.25,3.25,-3.25,3.25,3.25,.1,
GW409,5,-1.625,-6.5,3.25,-1.625,6.5,3.25,.1,
GW410,5,1.625,-6.5,3.25,1.625,6.5,3.25,.1,
GW411,5,6.5,-6.5,3.25,6.5,-6.5,-3.25,.1,
GW412,5,6.5,6.5,3.25,6.5,6.5,-3.25,.1,
GW413,5,6.5,0.,3.25,6.5,0.,-3.25,.1,
GW414,5,-6.5,-6.5,3.25,-6.5,-6.5,-3.25,.1,
GW415,5,-6.5,6.5,3.25,-6.5,6.5,-3.25,.1,
GW416,5,-6.5,0.,3.25,-6.5,0.,-3.25,.1,
GW417,5,3.25,13.,3.25,3.25,13.,-3.25,.1,
GW418,5,0.,13.,3.25,0.,13.,-3.25,.1,
GW419,5,-3.25,13.,3.25,-3.25,13.,-3.25,.1,
GW420,5,3.25,-13.,3.25,3.25,-13.,-3.25,.1,
GW421,5,0.,-13.,3.25,0.,-13.,-3.25,.1,
GW422,5,-3.25,-13.,3.25,-3.25,-13.,-3.25,.1,
GW423,5,6.5,-13.,0.,6.5,13.,0.,.1,
GW424,5,6.5,13.,0.,-6.5,13.,0.,.1,
GW425,5,-6.5,13.,0.,-6.5,-13.,0.,.1,
GW426,5,-6.5,-13.,0.,6.5,-13.,0.,.1,
GE1,0,0.,

APPENDIX B

Contained in this appendix are average power gain values generated by the NEC computer analysis for the "multi-wire" whip antennas.

TABLE B1 Average Power Gain for 4 "multi-wire" whip antennas with antenna height 10 m and base width 0.10 m.

Frequency in MHz	Spacing between antennas 2 M		Spacing between antennas 3 M	
	Wire radius 0.01 M	Wire radius 0.02 M	Wire radius 0.01 M	Wire radius 0.02 M
4	1.99	1.99	1.99	1.77
8	2.00	2.00	2.02	0.82
12	2.01	2.01	2.05	1.24
16	2.03	2.03	2.16	1.44
20	2.07	2.07	2.40	1.69
24	2.15	2.15	2.66	1.50
28	2.32	2.32	3.21	1.76
32	2.50	2.49	3.64	1.79
36	2.45	2.47	3.33	1.75
40	2.49	2.49	3.26	1.76

TABLE B2 **Average Power Gain for 3 "multi-wire" whip antennas in triangular form with antenna height 10 m, base width 0.1 m and 6 m spacing between them.**

Frequency in MHz	3 segments		5 segments	
	Wire radius 0.01 M	Wire radius 0.02 M	Wire radius 0.01 M	Wire radius 0.02 M
4	1.93	1.94	1.93	1.92
8	2.26	2.20	2.24	2.19
12	2.01	2.00	2.01	2.01
16	1.96	1.96	1.98	1.97
20	1.85	1.86	1.97	1.99
24	1.96	1.92	2.44	2.40
28	2.18	2.13	2.98	2.95
32	2.90	2.87	3.30	3.26
36	2.34	1.99	2.78	2.70
40	2.17	0.69	2.62	2.59

TABLE B3 **Average Power Gain for 2 "multi-wire" whip antennas with a 5 m spacing between them and antenna height 10 m.**

Frequency in MHz	Base width 0.10 M		Base width 0.03 M
	Wire radius 0.01 M	Wire radius 0.02 M	Wire radius 0.03 M
4	1.99	1.99	1.99
12	2.01	2.01	2.01
20	2.09	2.09	2.08
28	2.38	2.41	2.39
36	2.71	2.74	2.72
44	4.03	4.03	4.03
52	2.85	2.86	2.87
60	3.49	3.49	3.49
68	2.93	2.93	2.94
76	3.18	3.16	3.15
84	2.98	2.97	2.98
92	3.14	3.11	3.08
100	3.19	3.18	3.18

TABLE B4 **Average Power Gain for 2 "multi-wire" whip antennas with antenna height 10 m and base width 0.10 m.**

Frequency in MHz	Antenna spacing		Antenna spacing
	3 M		4 M
	3 segments	5 segments	5 segments
4	1.99	1.99	1.99
8	1.99	2.00	2.01
12	2.01	2.01	2.04
16	2.04	2.04	2.14
20	2.07	2.10	2.36
30	2.40	2.57	3.41
40	2.34	2.58	3.09
50	9.81	3.02	3.55

TABLE B5 Average Power Gain for 3 "multi-wire" whip antennas in triangular form with antenna height 10 m, base width 0.16 m and 6 m spacing between them.

Frequency in MHz	5 segments		3 segments	
	Wire radius 0.02 M	Wire radius 0.03 M	Wire radius 0.02 M	Wire radius 0.03 M
4	0.68	1.92	1.94	1.95
8	0.93	2.21	2.26	2.22
12	1.51	2.02	2.01	2.00
16	2.46	1.98	1.96	1.96
20	2.67	1.99	1.88	1.89
24	3.32	2.34	1.97	1.95
28	3.54	2.91	2.17	2.12
32	4.09	3.27	2.89	2.87
36	2.98	2.70	2.28	1.98
40	3.73	2.59	2.16	1.88

TABLE B6 Average Power Gain for 3 "multi-wire" whip antennas in triangular form with antenna height 5 m, base width 0.16 m and 6 m spacing between them.

Frequency in MHz	3 segments		5 segments	
	Wire radius 0.02 M	Wire radius 0.03 M	Wire radius 0.02 M	Wire radius 0.03 M
4	1.71	1.86	1.83	1.84
8	1.93	1.87	1.86	1.85
12	1.85	1.77	1.77	1.75
16	2.18	2.14	2.18	2.15
20	1.96	1.95	1.97	1.96
24	1.98	1.99	2.00	1.99
28	2.37	2.56	2.55	2.55
32	2.81	3.46	3.46	3.46
36	2.07	3.28	3.12	3.25
40	2.21	2.65	2.79	2.64

Tables B7-B14 list the calculated average power gain for two "multi-wire" whip antennas in a 5 meter spacing between them.

TABLE B7 **Average Power Gain for two "multi-wire" whip antennas with antenna height 5 m.**

Base width 0.10 M		Base width 0.16 M		Base width 0.10 M		Base width 0.16 M	
Frequency in MHz	Wire radius 0.01 M	Wire radius 0.03 M	Frequency in MHz	Wire radius 0.01 M	Wire radius 0.03 M	Wire radius 0.01 M	Wire radius 0.03 M
80	2.54	2.54	140	2.81	2.78		
84	2.40	2.40	144	2.65	2.63		
88	2.35	2.36	148	2.57	2.56		
92	2.42	2.42	152	2.62	2.62		
96	2.64	2.65	156	2.84	2.83		
100	3.02	3.00	160	3.03	2.97		
104	3.20	2.99	164	2.94	2.90		
108	3.25	3.19	168	2.87	2.86		
112	3.26	3.39	172	2.90	2.91		
116	3.21	3.50	176	3.01	3.02		
120	3.09	3.47	180	3.15	3.15		
124	3.19	3.18	184	3.26	3.23		
128	3.14	3.15	188	3.23	3.13		
132	3.16	3.14	192	2.98	2.90		
136	3.02	2.98	200	2.85	2.86		

TABLE B8 **Average Power Gain for two "multi-wire" whip antennas, antenna height 3 m, base width 0.10 m and wire radius 0.01 m.**

Frequency in MHz	AVE GAIN	Frequency in MHz	AVE GAIN	Frequency in MHz	AVE GAIN
100	2.88	160	2.72	218	2.82
104	3.09	164	2.87	220	2.89
108	3.30	168	2.93	224	2.99
112	3.41	172	2.93	228	3.05
116	3.37	176	2.97	232	3.08
120	3.27	180	3.06	236	3.09
124	2.55	184	3.14	244	3.09
128	2.44	188	3.16	248	3.05
132	2.40	192	3.11	256	2.95
136	2.48	196	2.99	260	2.92
140	2.65	200	2.86	268	2.92
144	3.46	204	2.73	284	2.92
148	3.35	208	2.66	288	2.98
152	3.15	212	2.67	292	3.05
156	2.93	216	2.76	300	3.14

TABLE B9 **Average Power Gain for two "multi-wire" antennas**
with antenna height 10 m.

Frequency in MHz	Base width 0.14 M		Base width 0.16 M	
	Wire radius 0.03 M	Wire radius 0.04 M	Wire radius 0.03 M	Wire radius 0.04 M
4	2.01	1.99	1.99	1.99
8	2.01	1.99	2.00	2.00
12	2.02	2.01	2.01	2.01
16	2.04	2.04	2.04	2.04
20	2.09	2.08	2.09	2.08
24	2.13	2.13	2.13	2.13
28	2.39	2.39	2.39	2.39
32	2.78	2.78	2.78	2.78
36	2.73	2.74	2.74	2.75

TABLE B10 Average Power Gain for two "multi-wire" whip antennas with antenna height 10 m.

	Base width 0.16 M	Base width 0.24 M	Base width 0.40 M	Base width 0.80 M
Frequency in MHz	Wire radius 0.05 M	Wire radius 0.04 M	Wire radius 0.06 M	Wire radius 0.08 M
4	1.99	1.99	1.99	2.00
8	1.99	2.00	2.00	2.00
12	2.01	2.01	2.01	2.01
16	2.04	2.04	2.04	2.04
20	2.08	2.09	2.08	2.09
24	2.13	2.14	2.15	2.16
28	2.39	2.39	2.40	2.41
32	2.78	2.78	2.78	2.77
36	2.76	2.78	2.85	2.94

TABLE B11 Average Power Gain for two "multi-wire" whip antennas with antenna height 5 m.

	Base width 0.14 M	Base width 0.16 M	Base width 0.40 M	Base width 0.80 M
Frequency in MHz	Wire radius 0.03 M	Wire radius 0.04 M	Wire radius 0.06 M	Wire radius 0.80 M
4	1.99	1.99	2.00	6.13
8	1.99	1.99	2.00	7.87
12	2.01	2.01	2.01	23.9
16	2.03	2.03	2.04	-6.18
20	2.09	2.09	2.09	-4.96
24	2.22	2.22	2.23	1.83
28	2.48	2.48	2.48	2.34
32	2.92	2.91	2.91	2.89
36	3.45	3.44	3.43	3.56

TABLE B12 Average Power Gain for two "multi-wire" whip antennas.

	Antenna height 3 M		Antenna height 2 M
	Base width	Base width	Base width
	0.40 M	0.80 M	0.10 M
Frequency in MHz	Wire radius 0.06 M	Wire radius 0.06 M	Wire radius 0.01 M
4	2.68	2.01	2.00
8	2.84	2.12	2.00
12	3.51	2.24	2.01
16	3.88	2.83	2.03
20	1.80	1.86	2.09
24	2.34	2.52	2.20
28	2.56	2.59	2.40
32	2.92	2.87	2.72
36	3.42	3.28	3.13

TABLE B13 Average Power Gain for two "multi-wire" whip antennas with antenna height 2 m.

Frequency in MHz	Base width 0.14 M		Base width 0.40 M		Base width 0.80 M
	Wire radius 0.03 M	Wire radius 0.04 M	Wire radius 0.06 M	Wire radius 0.08 M	Wire radius 0.08 M
4	1.99	1.99	2.00	1.99	
8	1.99	1.99	2.00	2.00	
12	2.01	2.01	2.01	2.01	
16	2.03	2.03	2.03	2.03	
20	2.09	2.08	2.09	2.09	
24	2.20	2.19	2.20	2.20	
28	2.40	2.40	2.40	2.40	
32	2.72	2.71	2.72	2.71	
36	3.13	3.13	3.13	3.11	

TABLE B14 Average Power Gain for two "multi-wire" whip antennas with antenna height 1 m.

	Base width 0.16 M	Base width 0.24 M	Base width 0.40 M	Base width 0.80 M
Frequency in MHz	Wire radius 0.05 M	Wire radius 0.04 M	Wire radius 0.06 M	Wire radius 0.08 M
4	1.98	1.99	1.99	1.99
8	1.99	1.99	1.99	1.99
12	1.99	2.01	1.99	2.00
16	2.02	2.03	2.02	2.02
20	2.07	2.08	2.07	2.08
24	2.18	2.19	2.18	2.18
28	2.37	2.39	2.37	2.38
32	2.67	2.69	2.67	2.67
36	3.06	3.08	3.06	3.06

APPENDIX C

Elevation patterns for the "multi-wire" whip antenna computer model were obtained for the configuration of two antennas with a 5 meter spacing between them, wire radius 0.01 meters, base width 0.10 meters, and antenna height 10 meters, in the frequency range 4-100 MHz..

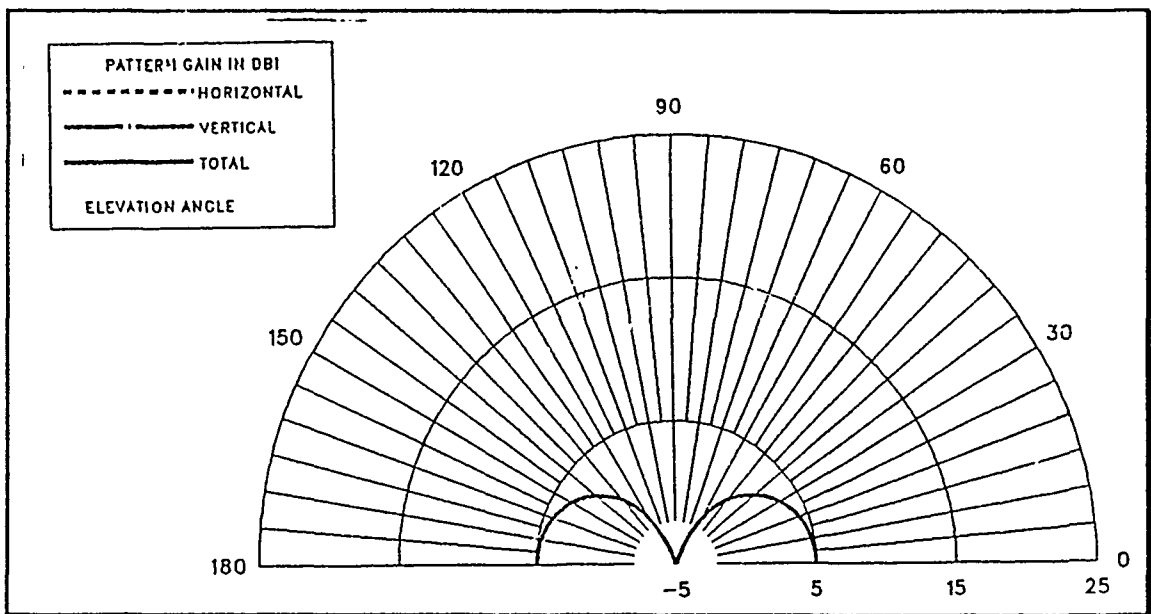


Figure C.1 E-Field Elevation Pattern for two "multi-wire" whip antennas, with a 5 m spacing between them, base width 0.10 m, antenna height 10 m, at 4 MHz, $\phi = 0$ degrees.

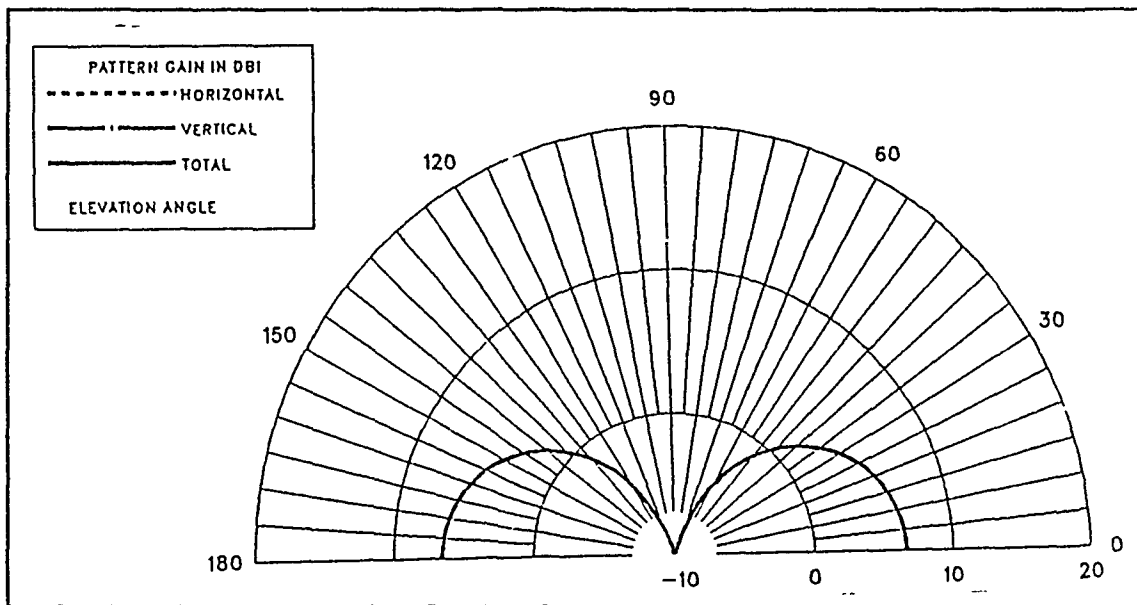


Figure C.2 E-Field Elevation Pattern for two "multi-wire" whip antennas, with a 5 m spacing between them, wire radius 0.10 m, antenna height 10 m, at 12 MHz, $\phi = 0$ degrees.

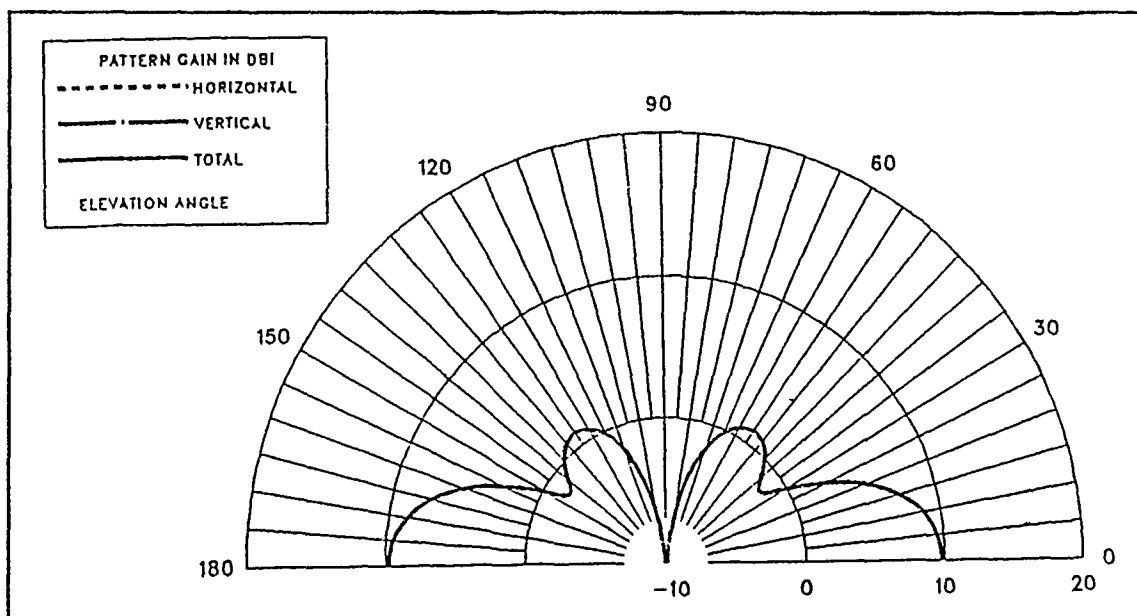


Figure C.3 E-Field Elevation Pattern for two "multi-wire" whip antennas, with a 5 m spacing between them, wire radius 0.10 m, antenna height 10 m, at 20 MHz, $\phi = 0$ degrees.

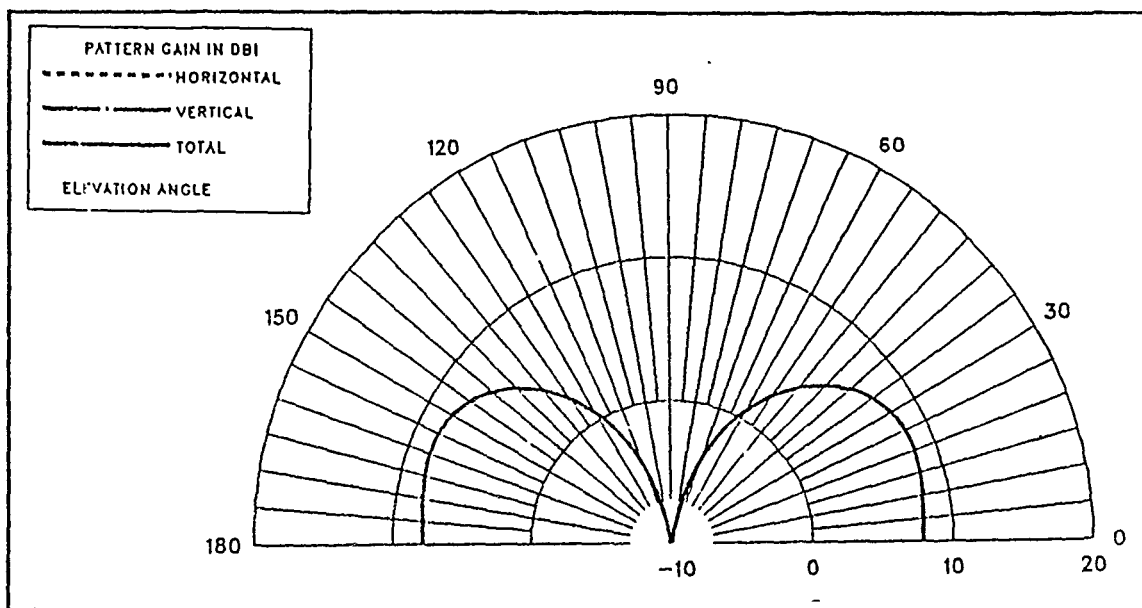


Figure C.4 E-Field Elevation Pattern for two "multi-wire" whip antennas, with a 5 m spacing between them, wire radius 0.10 m, antenna height 10 m, at 30 MHz, $\phi = 0$ degrees.

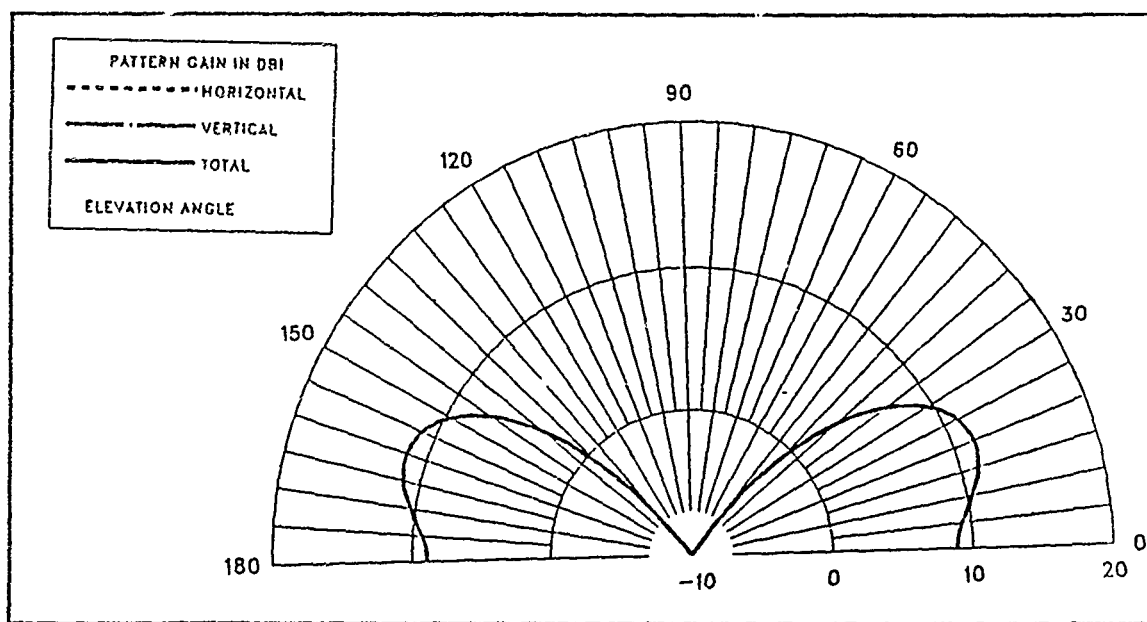


Figure C.5 E-Field Elevation Pattern for two "multi-wire" whip antennas, with a 5 m spacing between them, wire radius 0.10 m, antenna height 10 m, at 40 MHz, $\phi = 0$ degrees.

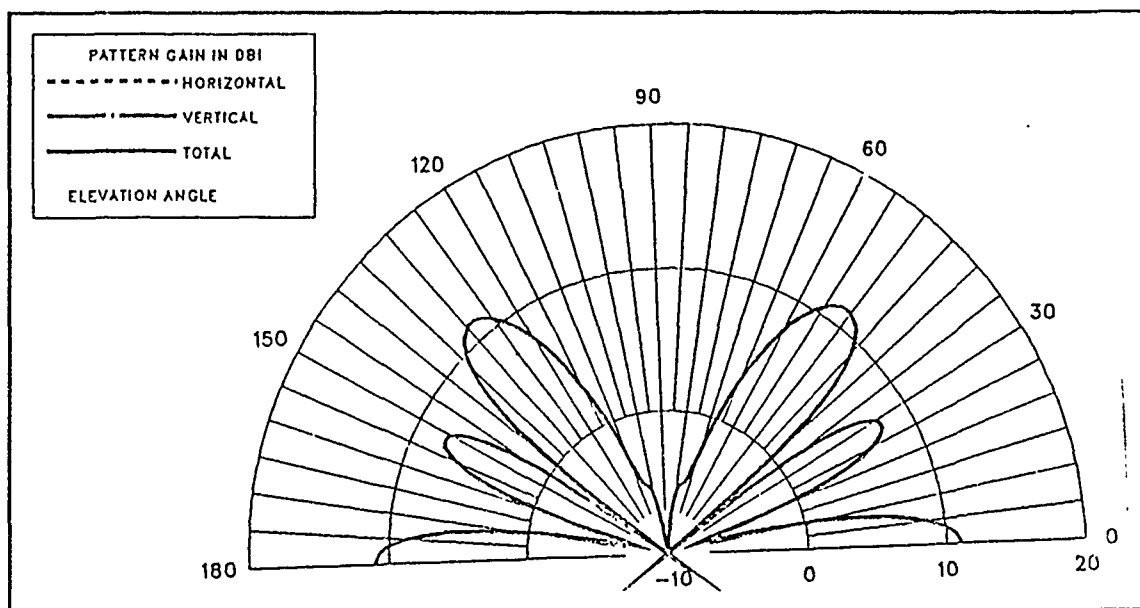


Figure C.6 E-Field Elevation Pattern for two "multi-wire" whip antennas, with a 5 m spacing between them, wire radius 0.10 m, antenna height 10 m, at 60 MHz, $\phi = 0$ degrees.

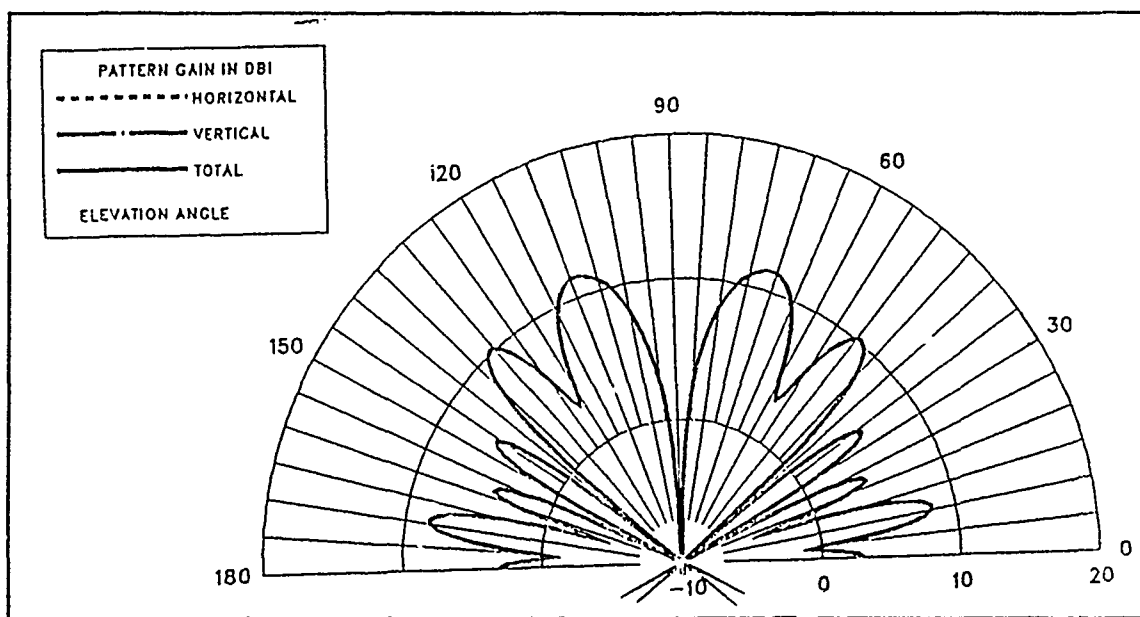


Figure C.7 E-Field Elevation Pattern for two "multi-wire" whip antennas, with a 5 m spacing between them, wire radius 0.10 m, antenna height 10 m, at 80 MHz, $\phi = 0$ degrees.

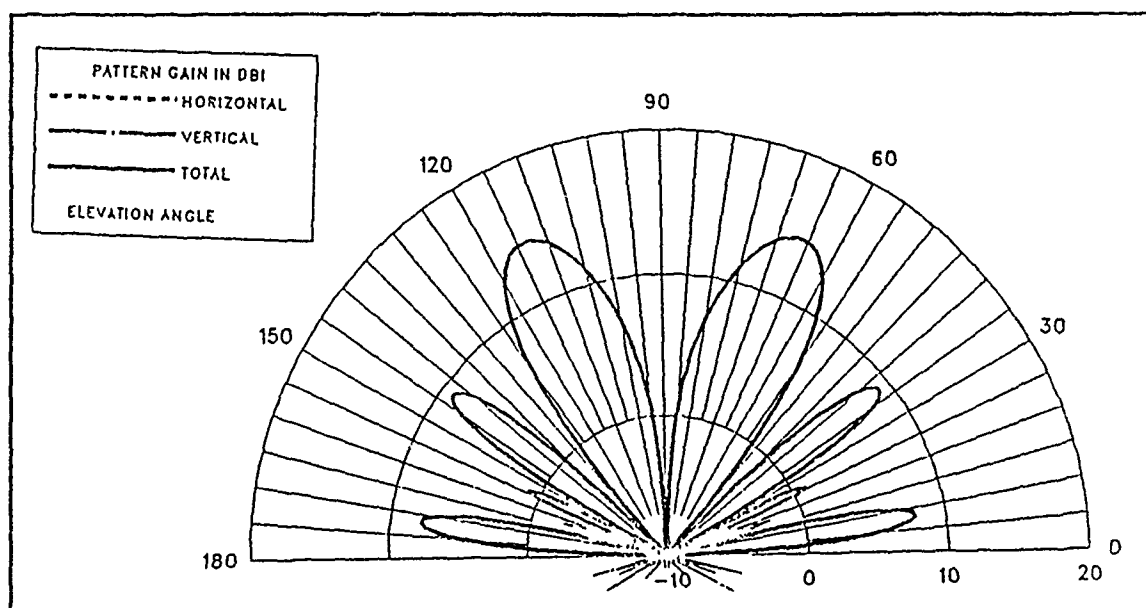


Figure C.8 E-Field Elevation Pattern for two "multi-wire" whip antennas, with a 5 m spacing between them, wire radius 0.10 m, antenna height 10 m, at 100 MHz, $\phi = 0$ degrees.

APPENDIX D

Contained in this appendix are average power gain values generated by the NEC computer analysis for inverted cone antenna models.

TABLE D1 Average Power Gain for inverted cone mounted on the ground with 4 feed points and wire radius 0.01 m.

Frequency in MHz	AVE GAIN	Frequency in MHz	AVE GAIN
4	2.01	64	1.58
8	2.01	68	1.60
12	2.01	72	1.71
16	2.01	76	1.81
20	2.02	80	1.87
24	2.03	84	1.92
28	2.04	88	2.11
32	2.07	92	2.05
36	2.10	96	2.07
40	2.15	100	2.15
44	2.22	104	2.24
48	2.32	108	2.30
52	2.48	112	2.33
56	2.76	116	2.32
60	2.54	120	2.28

TABLE D2 **Average Power Gain for inverted cone mounted on the ground with 2 feed points.**

Frequency in MHz	Wire radius 0.01 M	Wire radius 0.05 M	Wire radius 0.10 M
4	2.57	2.67	1.89
16	2.01	1.99	1.60
28	2.01	1.99	1.62
40	2.05	2.02	1.88
52	2.67	2.52	1.67
64	2.19	2.40	1.48
76	2.10	2.20	1.42
88	1.85	1.88	1.55
100	1.72	1.64	1.45
112	2.28	1.94	1.43
124	1.94	2.05	2.13
136	1.81	1.36	2.73
148	1.81	1.29	2.74
162	1.78	1.56	2.27
174	1.65	1.88	2.33

TABLE D3 **Average Power Gain for inverted cone 0.4 m above the ground with 2 feed points and wire radius 0.01 m.**

Frequency in MHz	AVE GAIN	Frequency in MHz	AVE GAIN
4	1.93	76	2.12
8	1.93	80	2.24
12	1.93	84	2.26
16	1.93	88	2.26
20	1.93	92	2.36
24	1.93	96	2.47
28	1.93	100	2.60
32	1.94	104	2.77
36	1.94	108	2.94
40	1.95	112	3.05
44	1.96	116	3.27
48	1.85	120	3.46
52	1.74	124	3.66
56	1.90	128	3.63
60	1.96	132	3.57
64	1.82	136	3.39
68	1.95	140	3.26
72	2.02	144	3.19

TABLE D4 **Average Power Gain for inverted cone 0.2 m above the ground with 2 feed points.**

Frequency in MHz	Wire radius 0.01 M	Wire radius 0.05 M	Wire radius 0.10 M
8	1.99	1.70	1.64
20	1.48	1.48	1.55
32	1.83	1.77	1.82
44	2.34	2.26	2.04
56	2.49	2.63	1.71
68	2.24	2.46	1.42
80	1.87	2.10	1.42
92	1.48	1.58	1.10
104	1.25	1.31	1.31
116	1.41	1.34	1.29
128	1.34	1.44	1.52
140	1.70	1.83	1.67
152	1.70	1.51	1.15
164	1.40	1.43	1.05
182	1.46	1.44	1.08

APPENDIX E

Tables E1 and E2 list the calculated input impedance for the two different inverted cone antenna models used in this thesis.

TABLE E1 Input Impedance for inverted cone mounted on the ground with 12 feed points, one connection point and wire radius 0.01 m.

Frequency in MHz	Resistance (R)	Reactance (jX)	Frequency in MHz	Resistance (R)	Reactance (jX)
4	8.05	-2,664	80	389.7	-223.4
8	32.9	-1,192	84	338.1	-216.2
12	76.2	-643.4	88	196.4	-46.7
16	140.6	-330.5	92	325.4	-59.9
20	227.6	-123.0	96	321.8	-89.8
24	335.7	15.4	100	308.4	-92.6
28	457.2	94.1	104	295.6	-86.5
32	577.7	116.4	108	283.7	-76.0
36	679.1	90.9	112	272.2	-62.7
40	747.9	33.6	116	260.9	-46.4
44	780.4	-35.7	120	249.8	-26.5
48	782.4	-101.2	124	224.1	-10.4
52	763.8	-154.3	128	221.0	20.3
56	586.3	-241.4	132	226.8	65.4
60	545.9	-251.0	136	266.5	138.6

64	509.0	-251.6	140	473.1	197.9
68	476.1	-246.7	144	512.8	-200.6
72	446.9	-238.9	148	269.5	-184.9
76	419.5	-230.4	152	196.8	-112.1

TABLE E2 **Input Impedance for inverted cone 0.4 m above the ground with 4 feed points.**

Frequency in MHz	Wire radius 0.01 M		Wire radius 0.10 M	
	Resistance (R)	Reactance (jX)	Resistance (R)	Reactance (jX)
4	2.73	-741.7	3.5	-468
12	29.9	-147.4	46.1	-66.4
20	114.5	22.9	176	-6.0
28	247.7	24.4	180	-110
36	246.8	-75.7	115	-119
44	176.1	-95.4	81.7	-98.0
52	126.6	-70.2	66.3	-75.0
60	98.9	-27.3	66.7	-54.0
68	86.6	-98.8	72.8	-44.4
75	75.9	40.3	75.9	-52.2
84	124.1	97.6	67.8	-56.5
92	127.4	34.6	52.8	-54.7
100	95.9	56.9	40.8	-41.0
108	85.1	86.7	40.4	-27.3
116	83.2	96.2	43.0	-19.9

120	74.2	110.5	43.8	-18.1
-----	------	-------	------	-------

APPENDIX F

Contained in this appendix are radiation patterns generated by the NEC computer analysis for the following configurations of an inverted cone:

- a. Antenna mounted on the ground with 12 feed points and wire radius 0.01 m (Figures F.1-F.6).
- b. Antenna 0.4 m above the ground with 4 feed points and wire radius 0.01 m (Figures F.7-F.14).

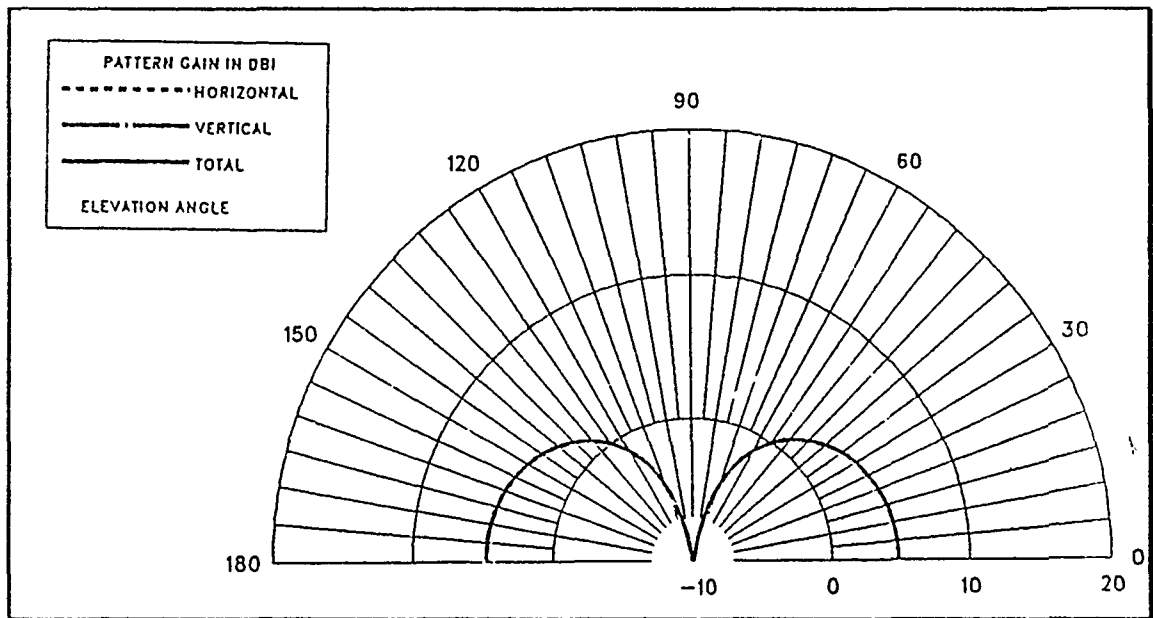


Figure F.1 E-Field Elevation Pattern for inverted cone mounted on the ground with 12 feed points, wire radius 0.01 m, at 8 MHz, $\phi = 0$ degrees.

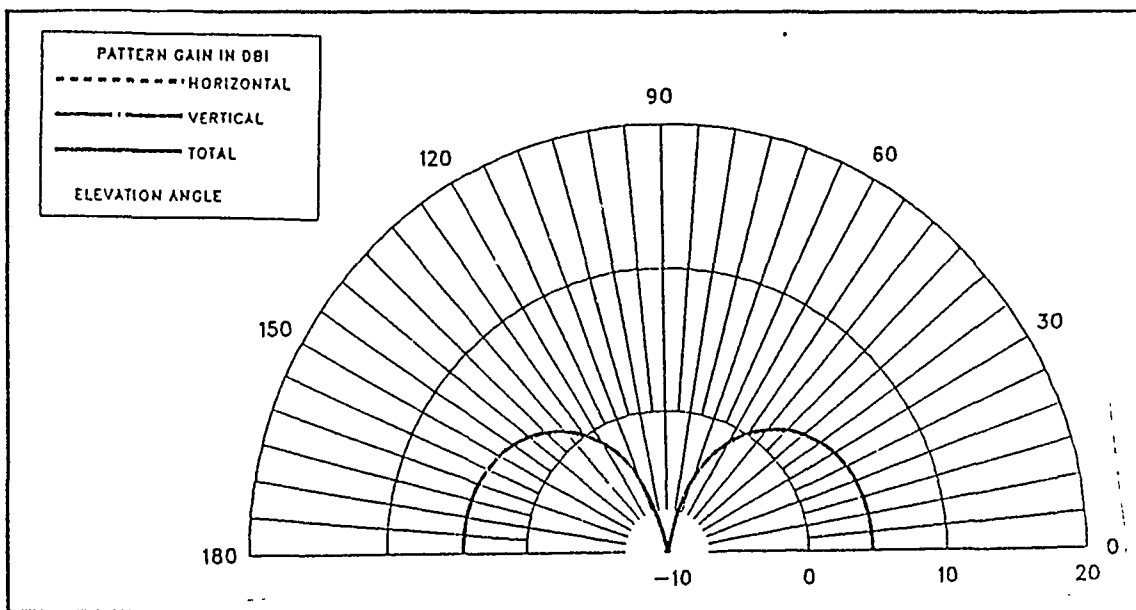


Figure F.2 E-Field Elevation Pattern for inverted cone mounted on the ground with 12 feed points, wire radius 0.01 m, at 60 MHz, $\phi = 0$ degrees.

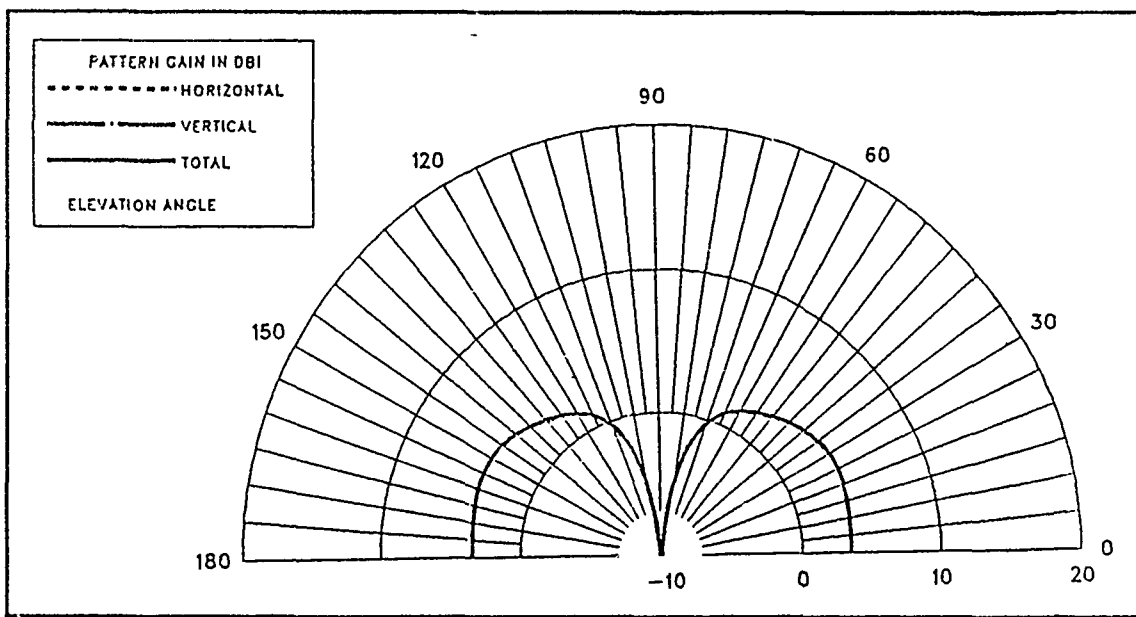


Figure F.3 E-Field Elevation Pattern for inverted cone mounted on the ground with 12 feed points, wire radius 0.01 m, at 80 MHz, $\phi = 0$ degrees.

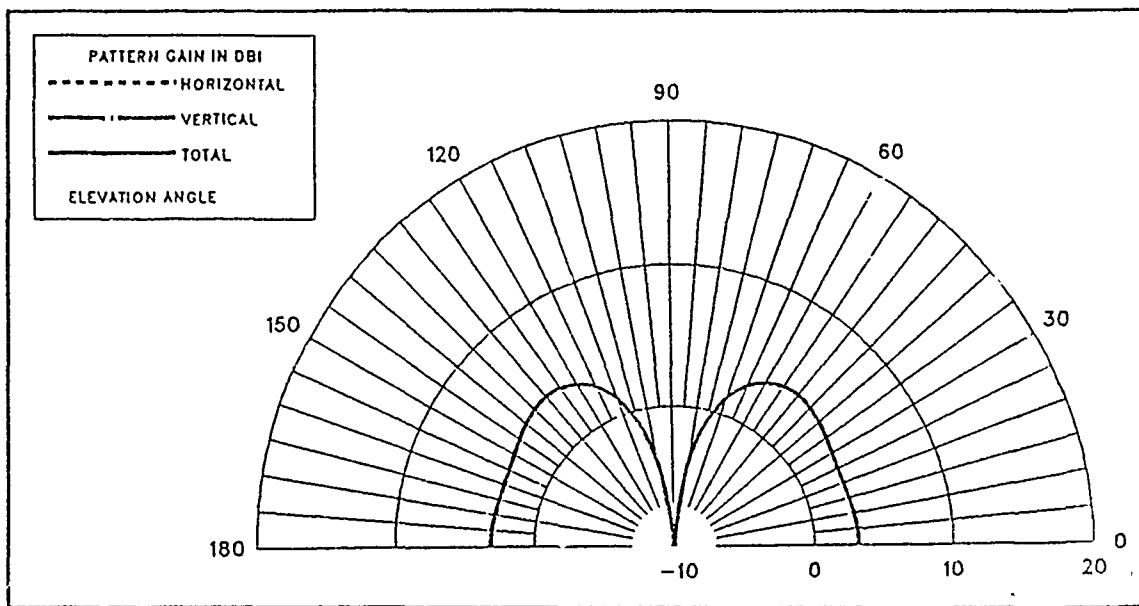


Figure F.4 E-Field Elevation Pattern for inverted cone mounted on the ground with 12 feed points, wire radius 0.01 m, at 100 MHz, $\phi = 0$ degrees.

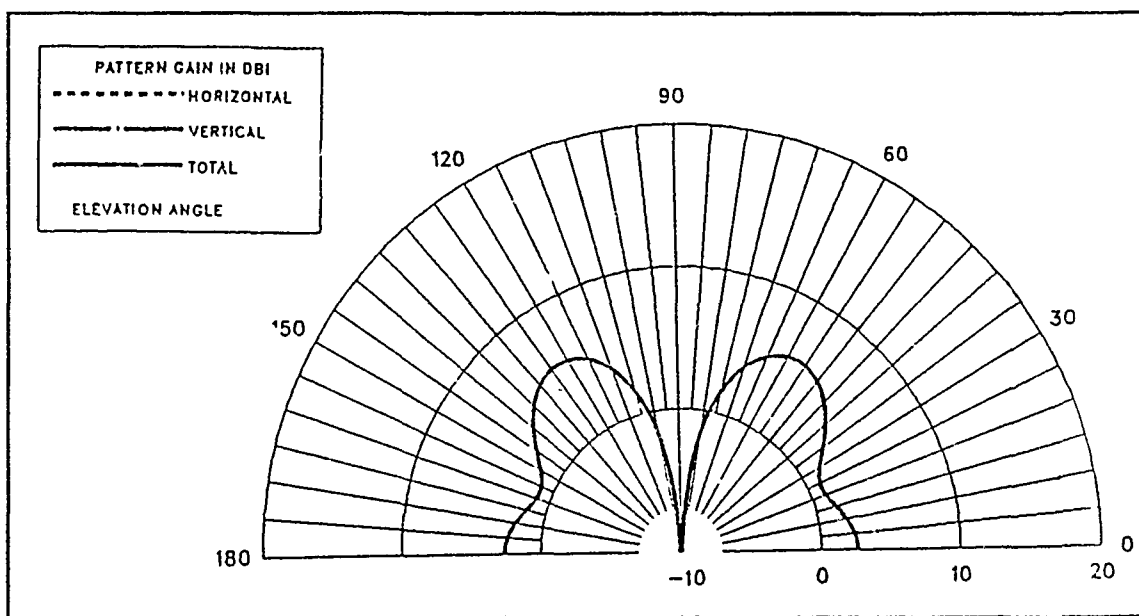


Figure F.5 E-Field Elevation Pattern for inverted cone mounted on the ground with 12 feed points, wire radius 0.01 m, at 120 MHz, $\phi = 0$ degrees.

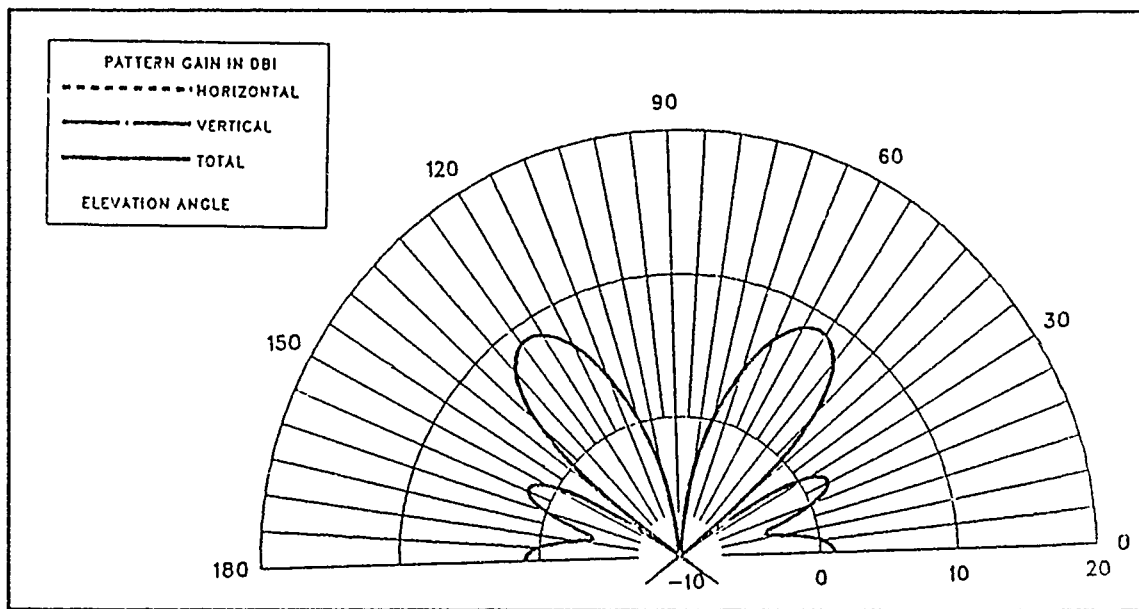


Figure F.6 E-Field Elevation Pattern for inverted cone mounted on the ground with 12 feed points, wire radius 0.01 m, at 140 MHz, $\phi = 0$ degrees.

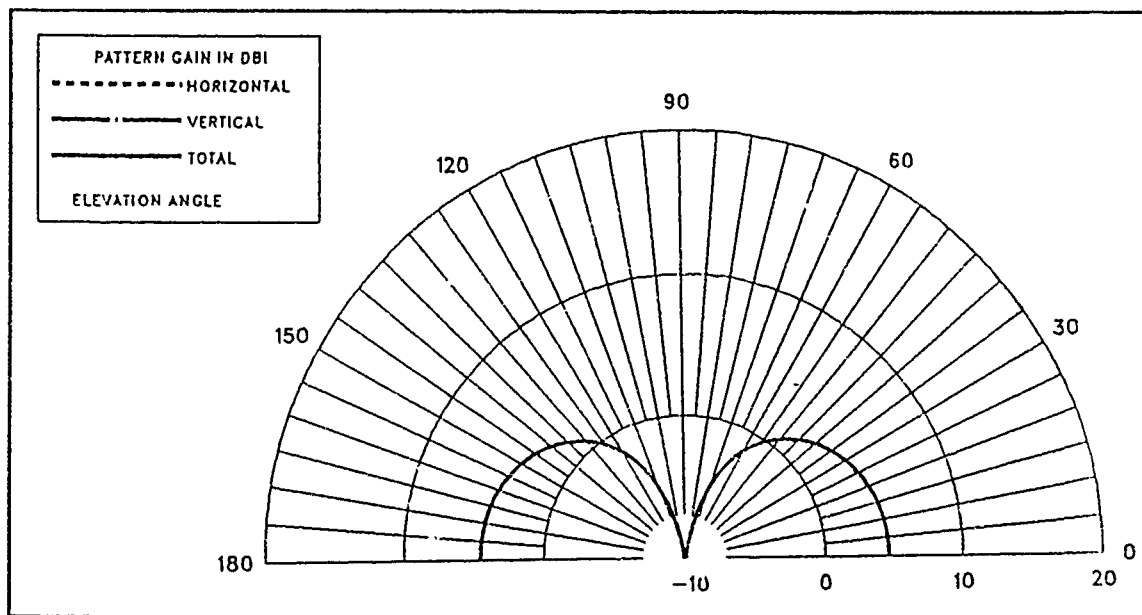


Figure F.7 E-Field Elevation Pattern for inverted cone 0.4 m above the ground with 4 feed points, wire radius 0.01 m, at 8 MHz, $\phi = 0$ degrees.

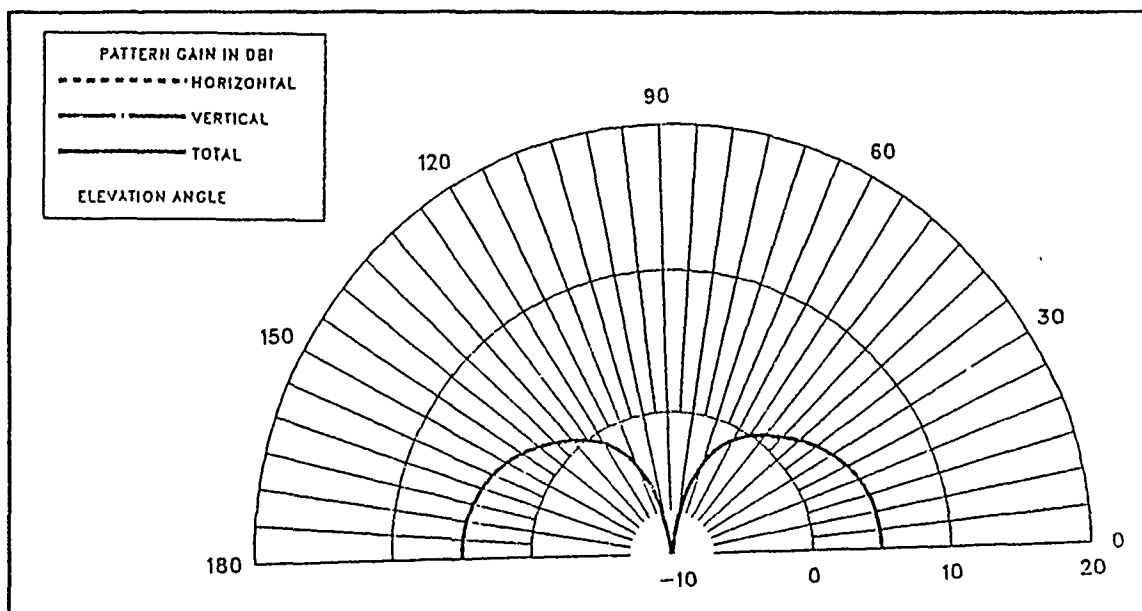


Figure F.8 E-Field Elevation Pattern for inverted cone 0.4 m, above the ground with 4 feed points, wire radius 0.01 m, at 60 MHz, $\phi = 0$ degrees.

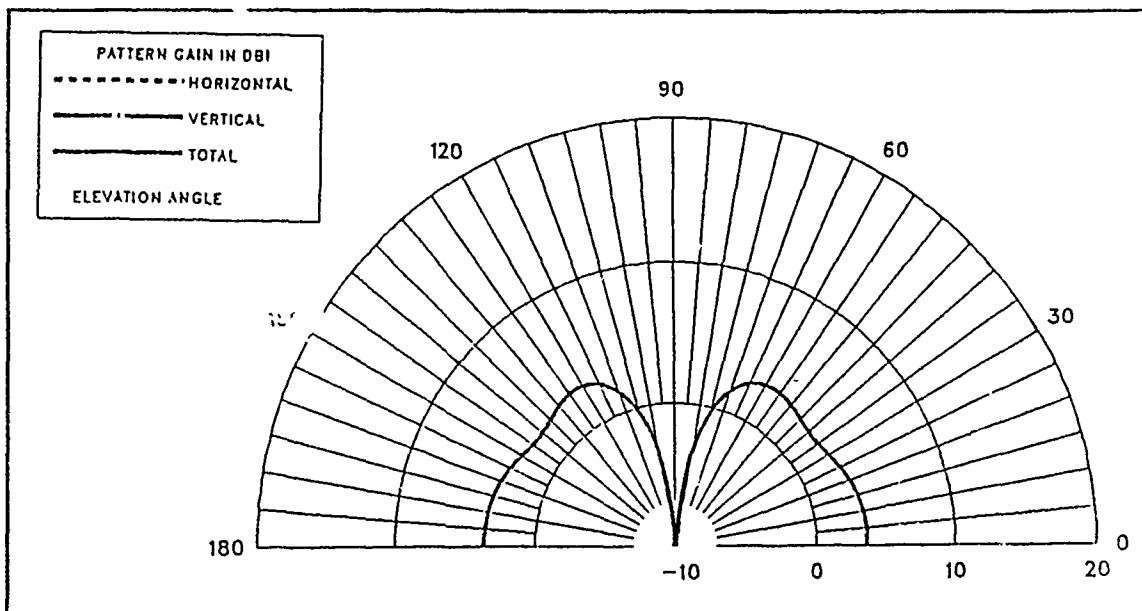


Figure F.9 E-Field Elevation Pattern for inverted cone 0.4 m above the wire grid box with 4 feed points, wire radius 0.01 m, at 70 MHz, $\phi = 0$ degrees.

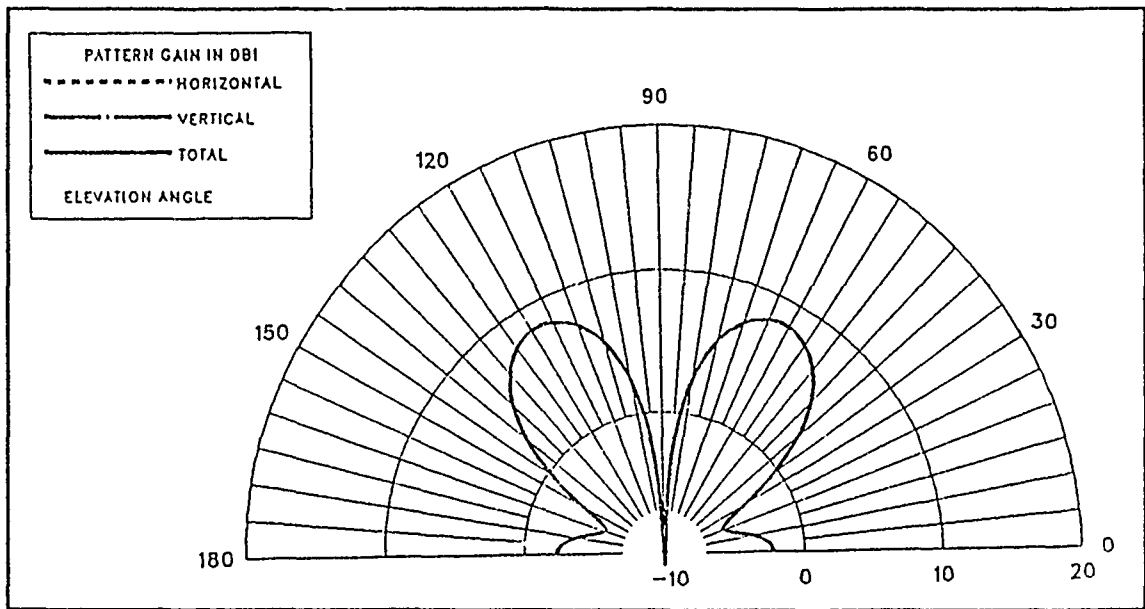


Figure F.10 E-Field Elevation Pattern for inverted cone 0.4 m above the wire grid box with 4 feed points, wire radius 0.01 m, at 80 MHz, $\phi = 0$ degrees.

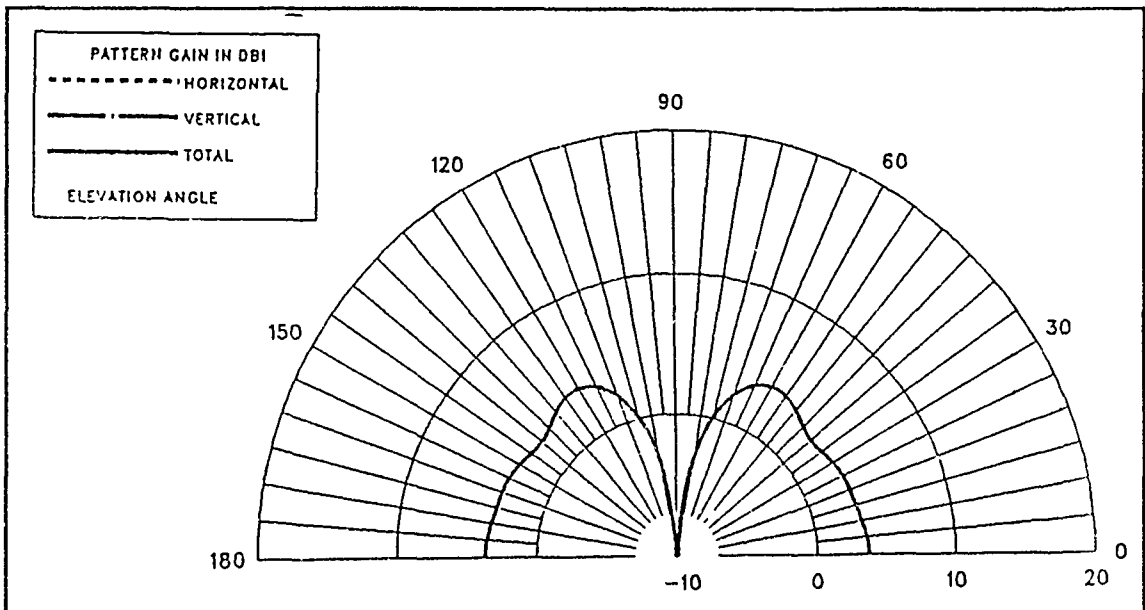


Figure F.11 E-Field Elevation Pattern for inverted cone 0.4 m above the wire grid box with 4 feed points, wire radius 0.01 m, at 90 MHz, $\phi = 0$ degrees.

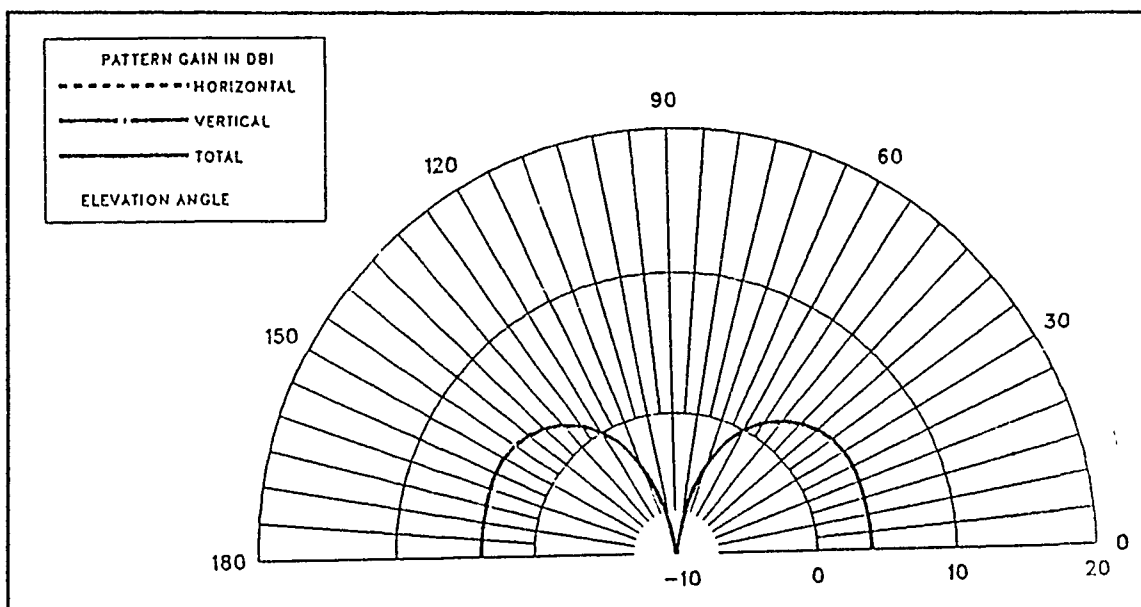


Figure F.12 E-Field Elevation Pattern for inverted cone 0.4 m above the wire grid box with 4 feed points, wire radius 0.01 m, at 100 MHz, $\phi = 0$ degrees.

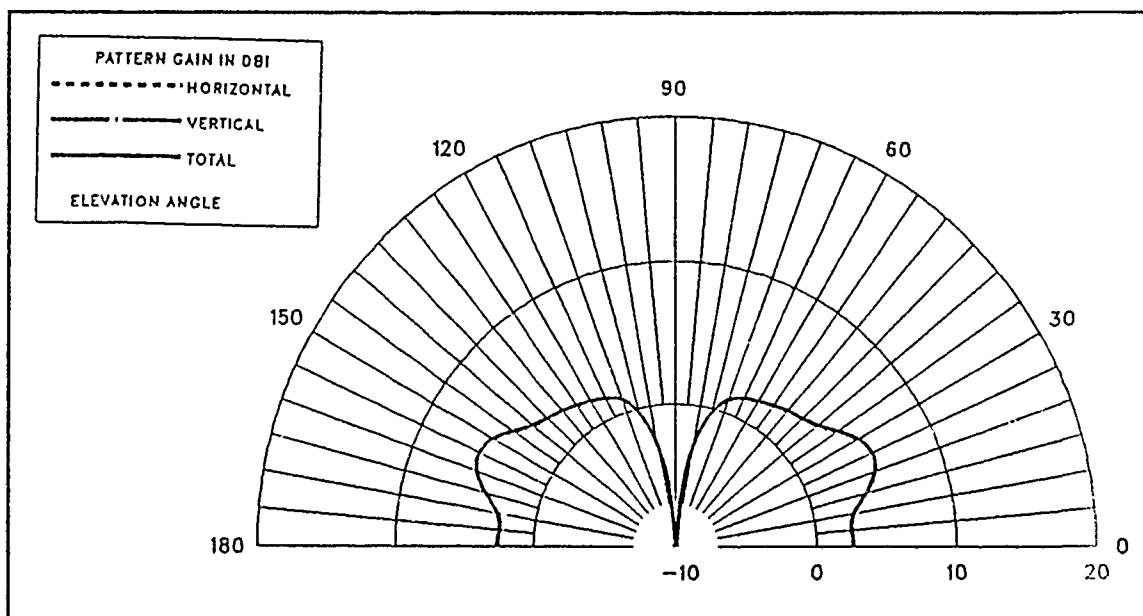


Figure F.13 E-Field Elevation Pattern for inverted cone 0.4 m above the wire grid box with 4 feed points, wire radius 0.01 m, at 120 MHz, $\phi = 0$ degrees.

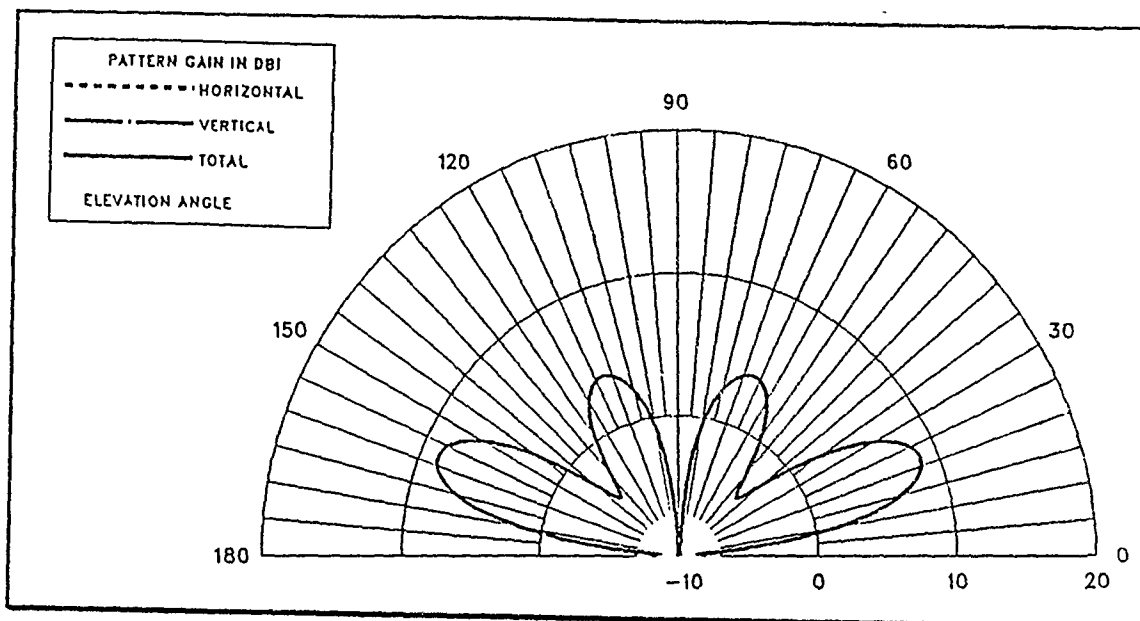


Figure F.14 E-Field Elevation Pattern for inverted cone 0.4 m above the wire grid box with 4 feed points, wire radius 0.01 m, at 140 MHz, $\phi = 0$ degrees.

APPENDIX G

Contained in this appendix are azimuth patterns for the inverted cone antenna models above the wire grid box.

Figures G.1-G.5 show the azimuth patterns for the inverted cone mounted on the wire grid box with 12 feed points, one connection point, wire radius 0.01 meters, at 20 MHz.

Figures G.6-G.10 show the azimuth patterns for the inverted cone 0.4 meters above the wire grid box connected to it by four vertical wires, wire radius 0.01 meters, at 20 MHz.

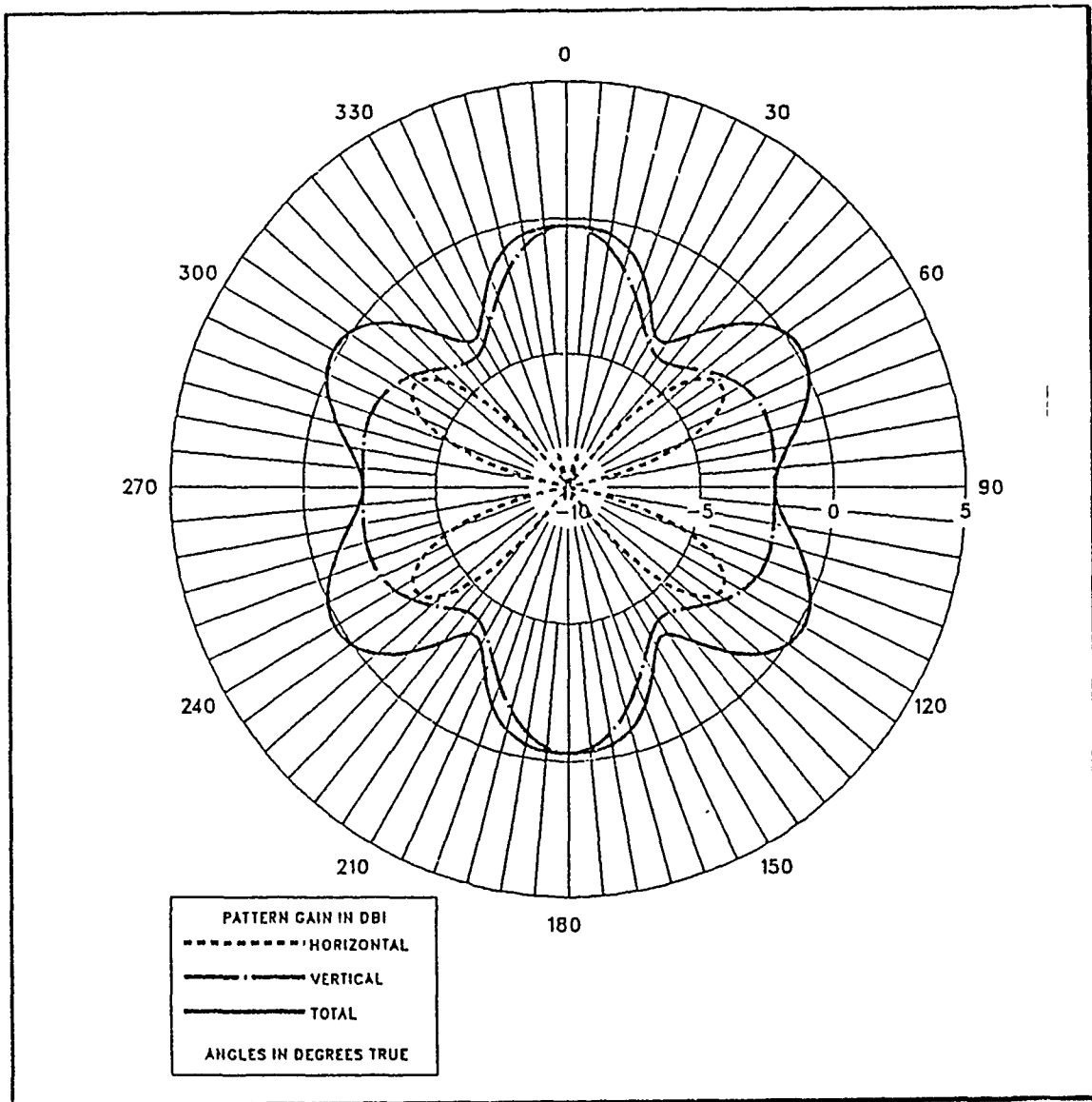


Figure G.1 E-Field Azimuth Pattern for inverted cone mounted on the wire grid box with 12 feed points and one connection point, at 20 MHz, $\theta = 30$ degrees.

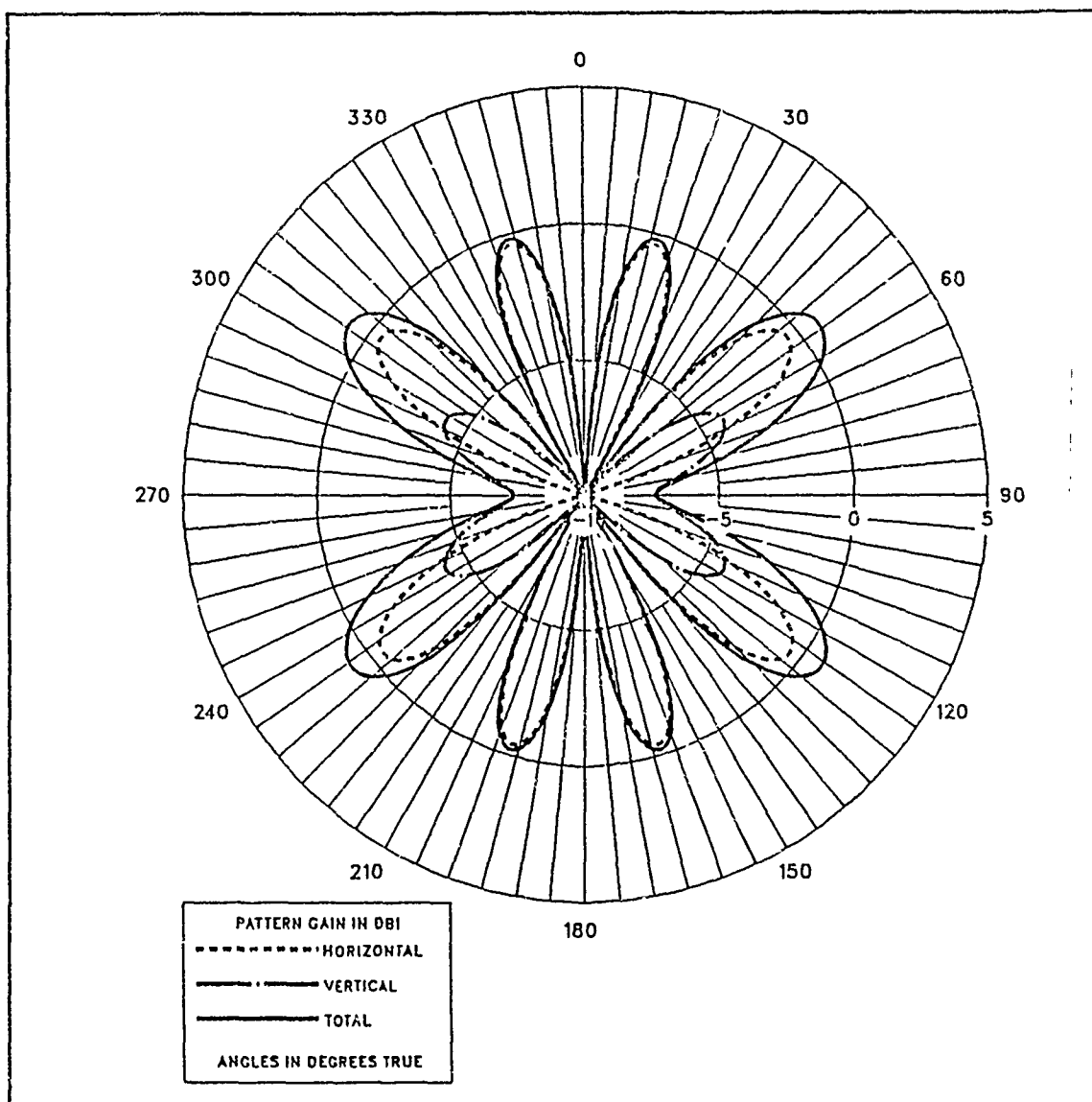


Figure G.2 E-Field Azimuth Pattern for inverted cone mounted on the wire grid box with 12 feed points, one connection point, at 20 MHz, $\theta = 40$ degrees.

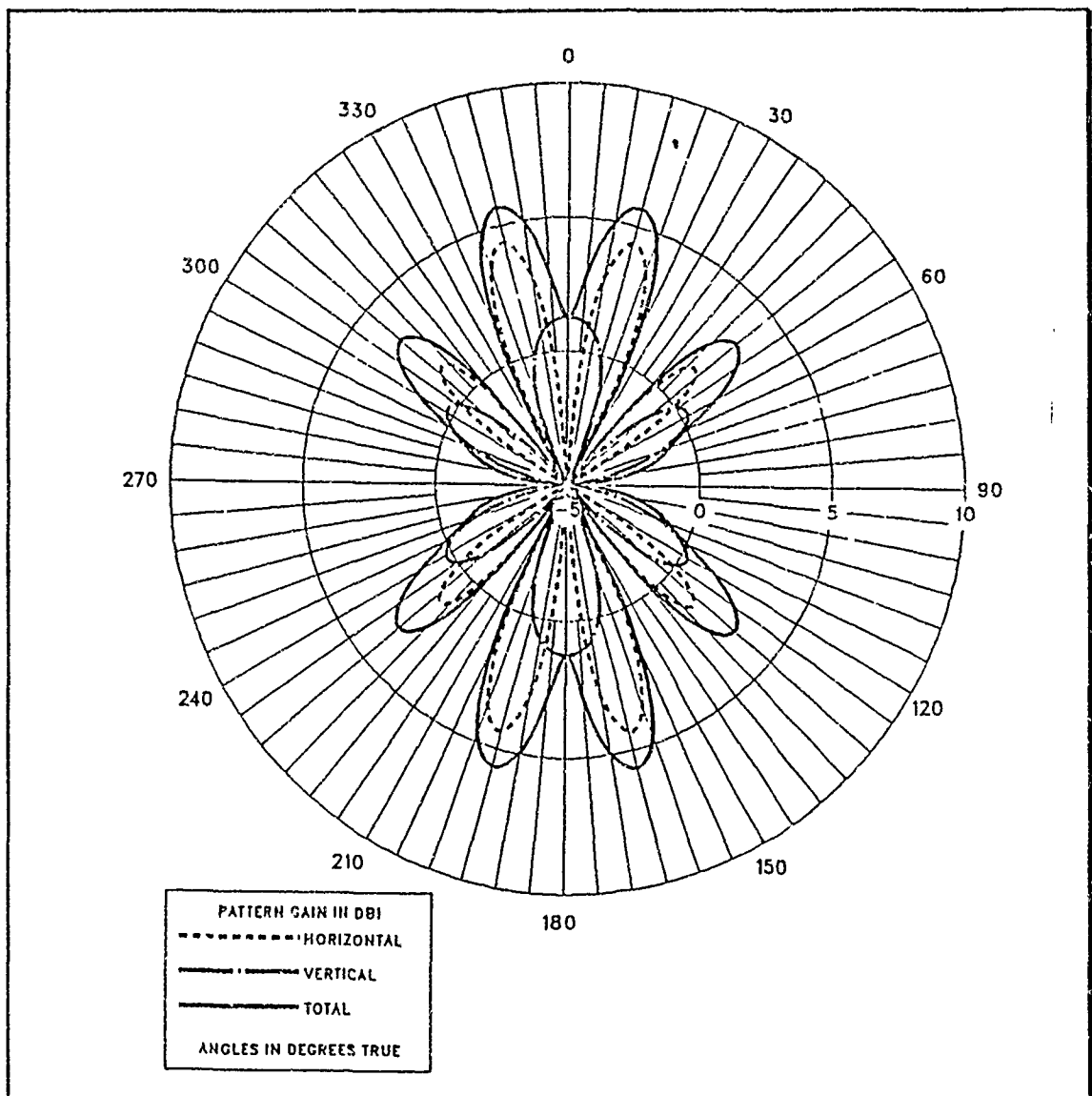


Figure G.3 E-Field Azimuth Pattern for inverted cone mounted on the wire grid box with 12 feed points, one connection point, at 20 MHz, $\theta = 50$ degrees.

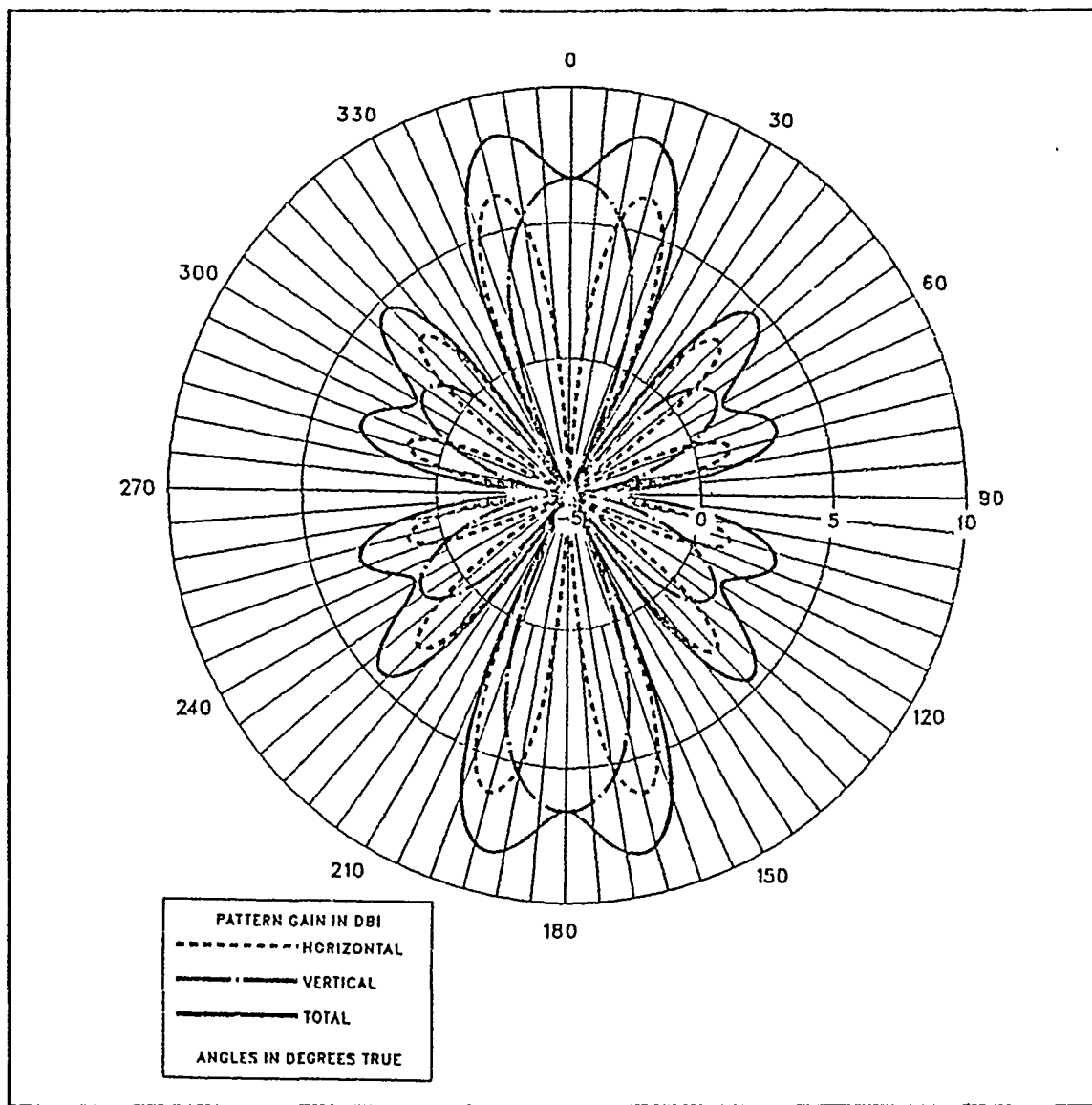


Figure G.4 E-Field Azimuth Pattern for inverted cone mounted on the wire grid box with 12 feed points, one connection point, at 20 MHz, $\theta = 60$ degrees.

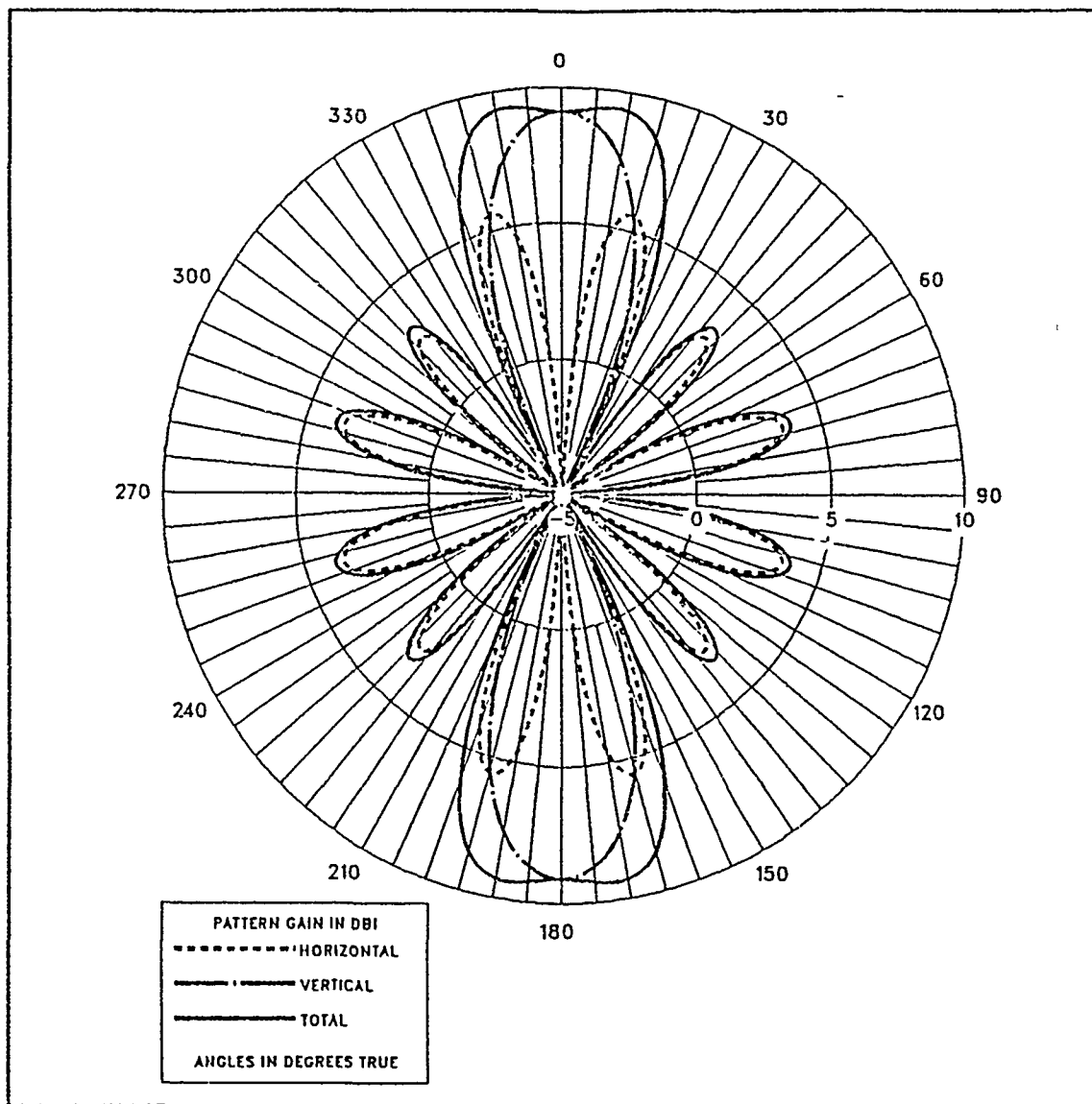


Figure G.5 E-Field Azimuth Pattern for inverted cone mounted on the wire grid box with 12 feed points, one connection point, at 20 MHz, $\theta = 70$ degrees.

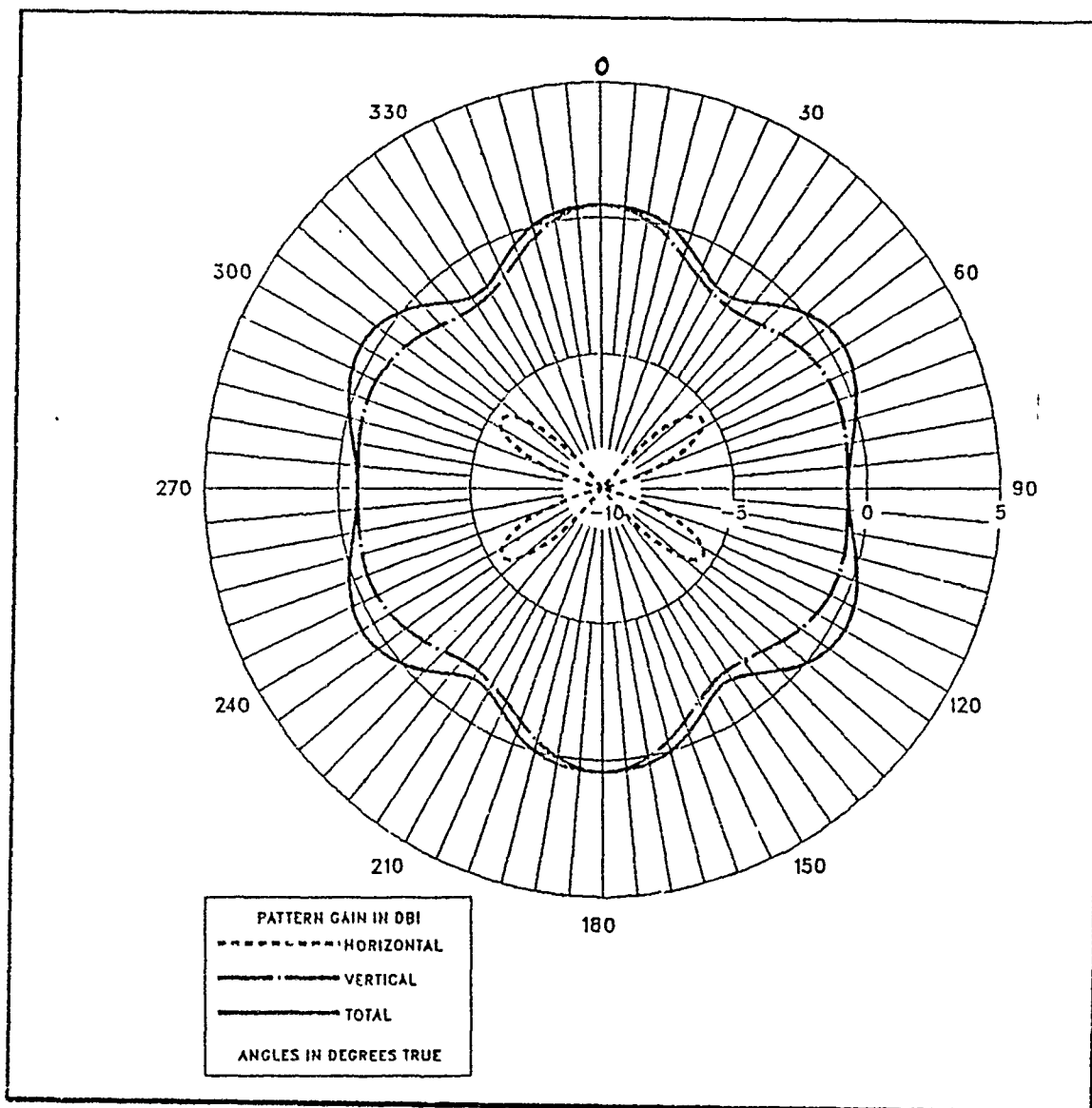


Figure G.6 E-Field Azimuth Pattern for inverted cone 0.4 m above the wire grid box connected to it by four vertical wires, at 20 MHz, $\theta = 30$ degrees.

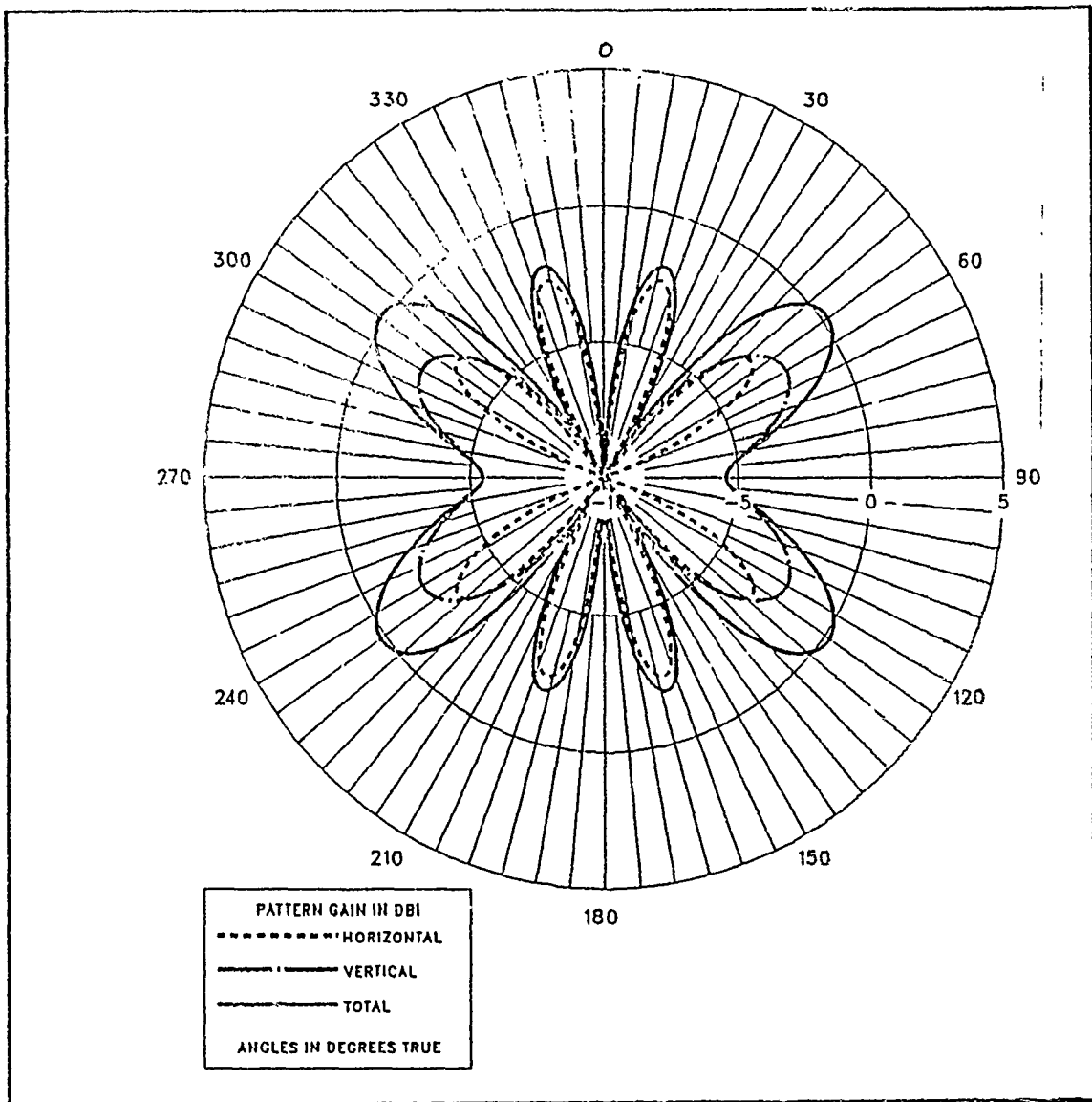


Figure G.7 E-Field Azimuth Pattern for inverted cone 0.4 m above the wire grid box connected to it by four vertical wires, at 20 MHz, $\theta = 40$ degrees.

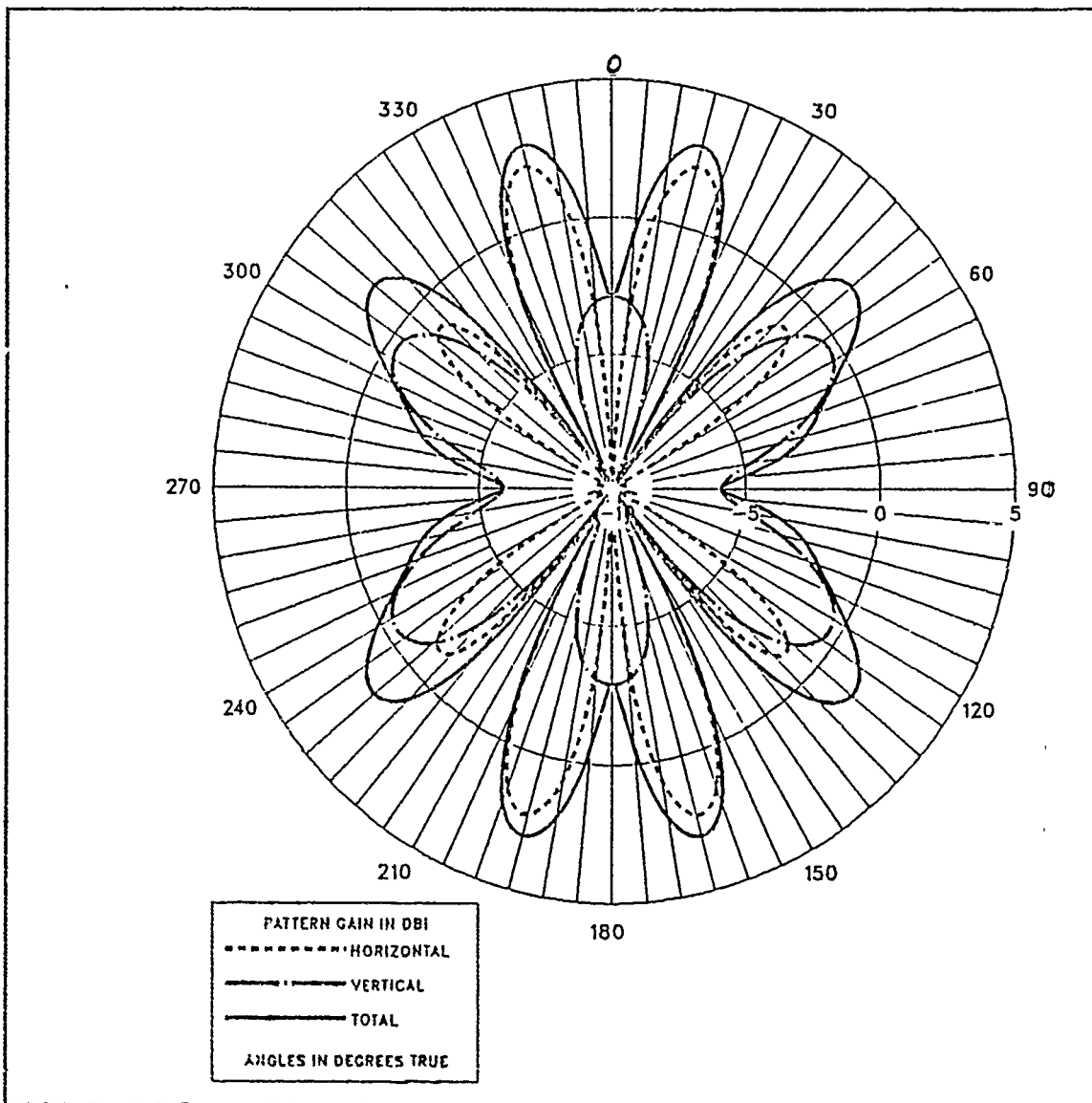


Figure G.8 E-Field Azimuth Pattern for inverted cone 0.4 m above the wire grid box connected to it by four vertical wires, at 20 MHz, $\theta = 50$ degrees.

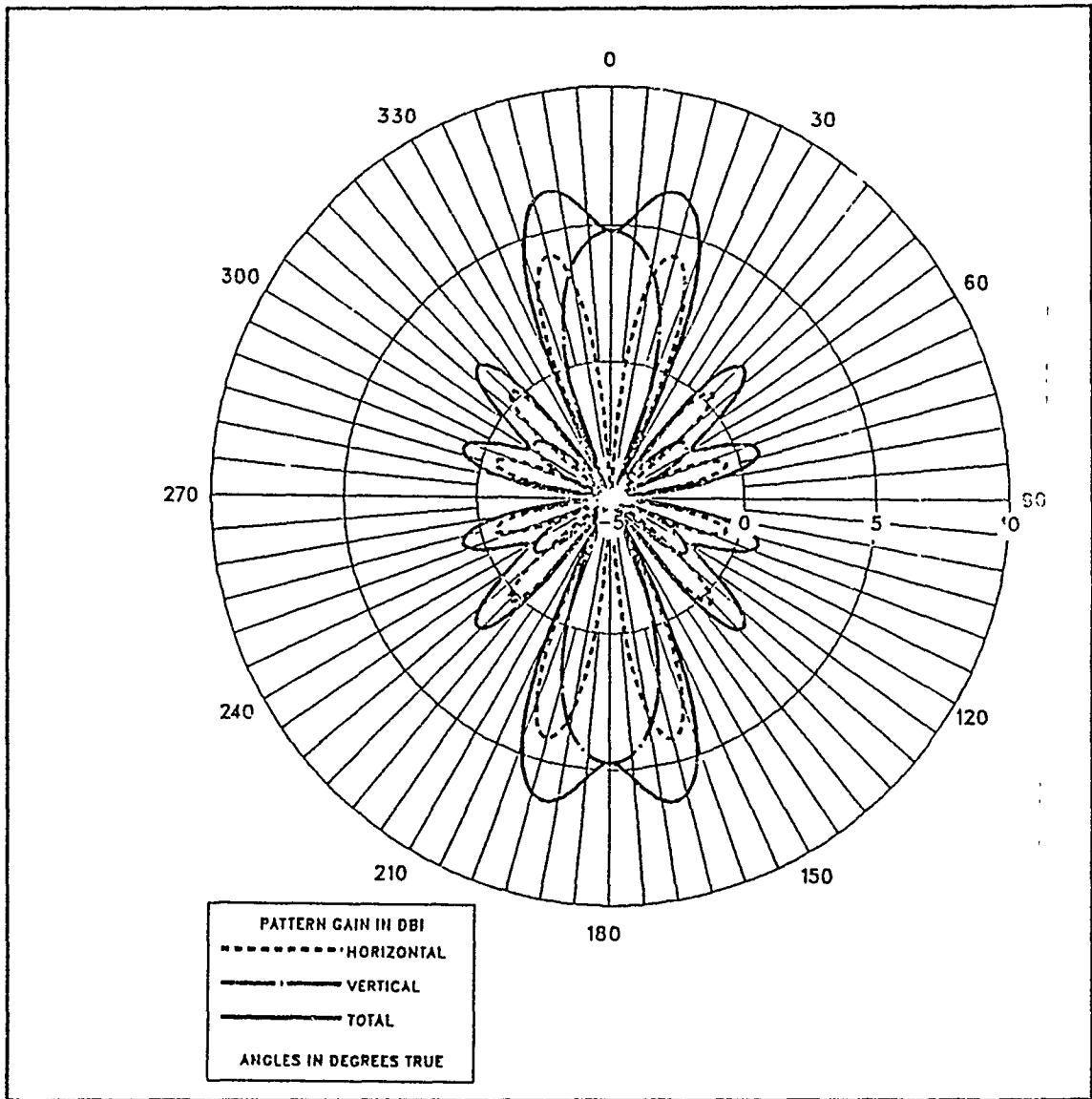


Figure G.9 E-Field Azimuth Pattern for inverted cone 0.4 m above the wire grid box connected to it by four vertical wires, at 20 MHz, $\theta = 60$ degrees.

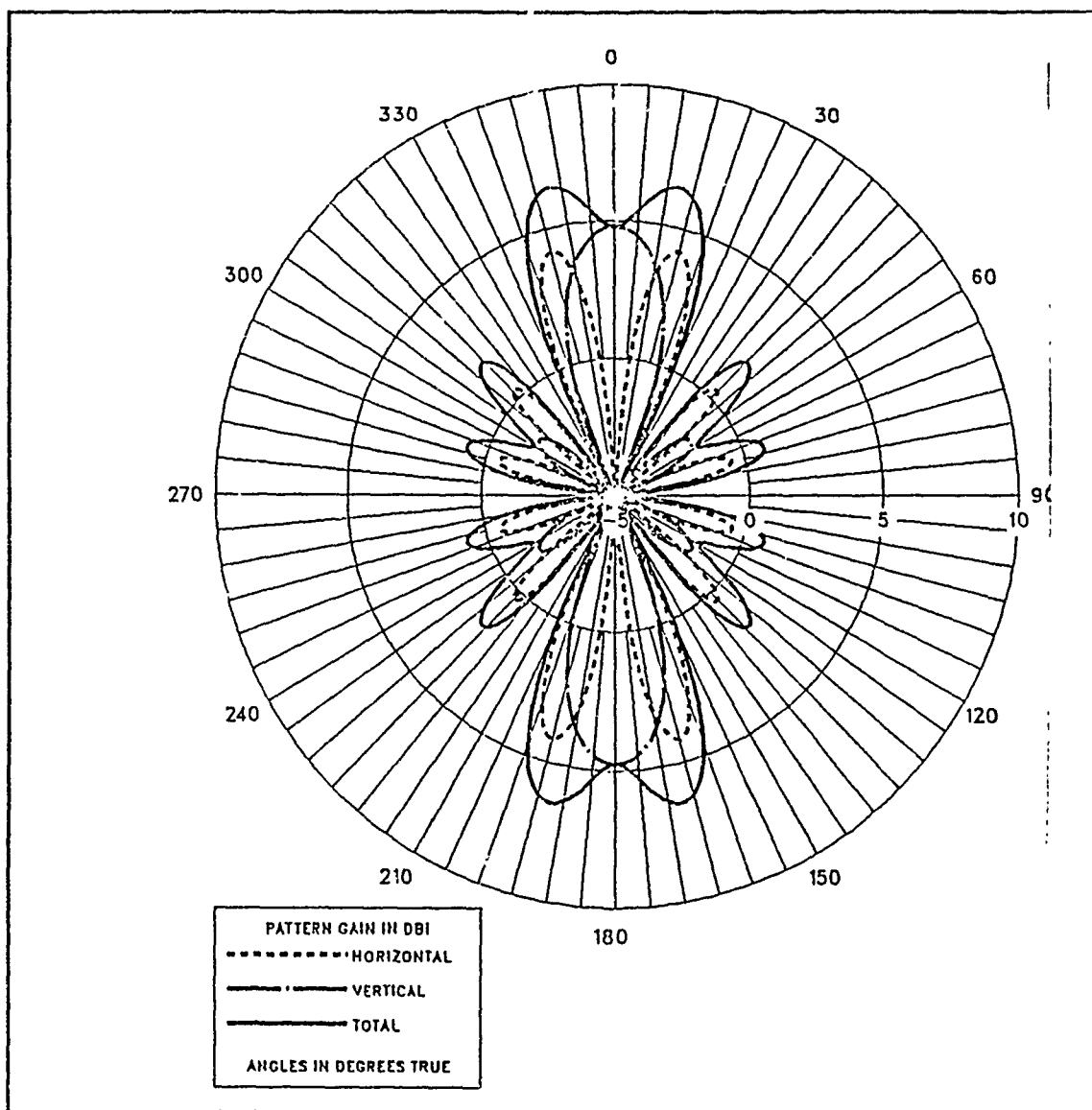


Figure G.10 E-Field Azimuth Pattern for inverted cone 0.4 m above the wire grid box connected to it by four vertical wires, at 20 MHz, $\theta = 70$ degrees.

LIST OF REFERENCES

1. Numerical Electromagnetics Code (NEC-1), Part I: *NEC Program Description-Theory*, Lawrence Livermore Laboratory, Livermore, CA, 1981.

BIBLIOGRAPHY

1. Law, E. Preston, *Shipboard Antennas*, 1983.
2. Rudge, A.W. and Milne, K., *The Handbook of Antenna Design*, Volume 2, London, UK, 1983.
3. Naval Ocean Systems Center Technical Document 116, Volume 2, *Numerical Electromagnetics Code (NEC)-Method of Moments*, G.J. Burke and A.J. Poggio, Lawrence Livermore Laboratory, January 1981.
4. Logan, J.C. and Rockway, J.W., *Ship EM Design Technology*, Naval Engineers Journal, May 1988.
5. Logan, J.C. and Li, S.T., *A Role Model for Electromagnetic System Design*, IEEE, December 1988.
6. Choi, Il Yong, *Design of Survivable Shipboard HF Mast Antenna Models Using the Numerical Electromagnetics Code*, M.S.E.E. Thesis, Naval Postgraduate School, Monterey, California, September 1987.
7. Vorrias Ioannis G., *Shipboard Combat Survivable HF Antenna Designs*, M.S.E.E. Thesis, Naval Postgraduate School, Monterey, California, December 1986.
8. Theofanopoulos Constantinous, *Performance Evaluation of a Half-Wave Resonant Slot Antenna over Perfect Ground Using Numerical Electromagnetics Code*, M.S.E.E. Thesis, Naval Postgraduate School, Monterey, California, March 1987.

INITIAL DISTRIBUTION LIST

	No. Copies
1. Defense Technical Information Center Cameron Station Alexandria, VA 22304-6145	2
2. Library, Code 52 Naval Postgraduate School Monterey, CA 93943-5100	2
3. Chairman, Code EC Naval Postgraduate School Department of Electrical and Computer Engineering Monterey, CA 93943-5000	1
4. Alfred Resnick, Capital Cities Comm. ABC Radio 1345 Ave. of Americas 26th Floor New York, NY 10105	1
5. Professor Richard W. Adler, Code EC/Ab Department of Electrical and Computer Engineering Naval Postgraduate School Monterey, CA 93943-5000	2
6. Naval Sea Systems Command, Code 06D4 Attention: Captain Horback NC2 Rm 7S18 Washington, D.C. 20362	1
7. John Rockway, NOSC Code 825 271 Catalina Blvd. San Diego, CA 92151	1
8. James C. Logan University of South Carolina Electrical Engineering Department Columbia, SC 29208	1
9. Yiannis Fragoulis Androu 15 Kypseli 11257 Athens Greece	2